MODELLING THE IMPACT OF COASTAL URBANIZATION ON THE WEST AFRICAN SUMMER MONSOON CLIMATE

BY

FAYE, AISSATOU

Bsc, Msc (MET/15/5740)

A THESIS IN THE DEPARTMENT OF METEOROLOGY AND CLIMATE SCIENCE, SCHOOL OF EARTH AND MINERAL SCIENCES, IN PARTNERSHIP WITH THE WEST AFRICAN SCIENCE SERVICE CENTER ON CLIMATE CHANGE AND ADAPTED LAND USE (WASCAL), SUBMITTED TO THE SCHOOL OF POSTGRADUATE STUDIES IN PARTIAL FULFILMENT OF THE REQUIREMENTS FOR THE AWARD OF DOCTOR OF PHILOSOPHY IN METEOROLOGY AND CLIMATE SCIENCE OF THE FEDERAL UNIVERSITY OF TECHNOLOGY AKURE, NIGERIA.

October, 2019

DECLARATION

I hereby declare that this Thesis was written by me and is a correct record of my own research work. It has not been presented in any previous application for any degree of this or any other University. All citations and sources of information are clearly acknowledged by means of references.

Candidate's Name: FAYE, AISSATOU

Signature: 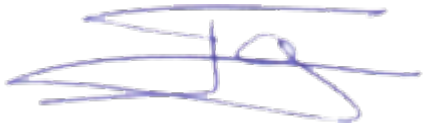 **Date:** 29/10/2019

CERTIFICATION

We certify that this Thesis entitled "Modelling the Impact of Coastal Urbanization on the West African Summer Monsoon Climate" is the outcome of the research carried out by FAYE, Aissatou in the Department of Meteorology and Climate Science, the Federal University of Technology, Akure. Nigeria, in partnership with the West African Science Service Center on Climate Change and Adapted Land Use (WASCAL).

Major Supervisor's Name: Prof. Amadou Thierno Gaye

Signature: ..... **Date:** 24/10/2019

Co-Supervisor's name: Dr. Ayo Oluleye

Signature: ..... **Date:** 29-10-2019

Co-Supervisor's name: Dr. Mouhamadou Bamba Sylla

Signature: ..... **Date:** 29/10/2019

ACKNOWLEDGEMENTS

My sincere appreciation goes to the Bundesministerium für Bildung und Forschung (BMBF), which is the Federal Ministry of Education and Research of Germany, through the West African Science Service Center on Climate Change and Adapted Land Use (WASCAL) for providing the scholarship and financial support for this programme.

I also appreciate thank the Executive Director and the staff of WASCAL Head office, Accra, Ghana.

This doctorate programme thesis was co-funded by the Intergovernmental Panel on Climate Change (IPCC) Scholarship Programme through the financial support of the Cuomo Foundation. Many thanks for their financial support. Special thanks to Mxolisi Shongwe.

I am also grateful to the Director of WASCAL-GRP-WACS, Prof. K.O. Ogunjobi, for his support, encouragement, and understanding.

My profound appreciation goes to the Staff of WASCAL-GRP-WACS, and the entire staff of the Department of Meteorology and Climate Science, FUTA for their great support and cooperation throughout during these three years.

I am grateful to my major supervisor Prof. Amadou Thierno Gaye from the Laboratoire de Physique de l'Atmosphére et de l'Océan Simeon Fongang (LPAO-SF) of the Cheikh Anta Diop University of Dakar (UCAD).

I am also deeply grateful to my FUTA co-supervisor Dr. Ayo Oluleye for his guidance, encouragement and co-operation throughout the course of this programme.

I appreciate the effort of my co-supervisor, Dr. Mouhamdaou Bamba Sylla, acting Director of WASCAL Competence Center. This work would not have been possible without his scientific orientation, support, motivation, and encouragement. Thanks a lot, Bamba.

I would like to thank my external examiner for accepting to examine this work and for his valuable comments which contribute to improving this work.

Many thanks to the Earth System Physics (ESP) section of the Abdus Salam International Centre for Theoretical Physics (ICTP) for their financial support and the computational facilities. I am deeply grateful to Filippo Giorgi, head of the ESP section for his scientific support and guidance. My warm thanks to Graziano Giuliani for introducing me to the RegCM4 modelling. I thank him for his guidance and for providing meaningful insights into this thesis during my stay in Trieste. Special thank you to all the members of ESP team: Erika Coppola, Marco Stefanelli, Pandora Malchose, Suzane, Rita….

I acknowledge all my colleagues from the WASCAL-WACS. Special thanks to Alima for their friendship and for being there to listen when I needed an ear.

I am also thankful to all my colleagues from LPAO-SF/UCAD.

I also wish to appreciate the WASCAL Competence Center in Burkina Faso and all the good people I met in Ouagadougou. Special thanks to Mrs. Aoua Traorè Sawadogo.

I must express my heartfelt gratitude to the members of my family especially my mother, my father, my sisters and my brothers for their prayers and encouragements.

DEDICATION

This work is dedicated to my lovely family.

ABSTRACT

A lot of research has been done to understand and improve the relationship between land use and land cover modification vis-a-vis their interaction with the West African climate variability and climate change. However, the urbanization influence on the West African climate is not yet an elaborately researched subject of studies. In this context, this thesis examines the impact of coastal urbanization on the West African summer climate, by using the Regional Climate Model version 4 (RegCM4) coupled with the Community Land Surface Model version 4.5 (CLM4.5). A series of experiments were performed, in the present-day climate (1984-2005) and the RCP8.5 far future (2079-2100), at 25 Km of horizontal resolution over the West African domain. Two types of simulations were performed with and without modification of the natural vegetation land cover with the urban parameterization (CLMU). Results from the model evaluation show the good performance of RegCM4 to simulate the main climatic variables and atmospheric circulation over West Africa during the June-September (JJAS) summer months. Arguably, RegCM4 reproduces well the spatio-temporal pattern of rainfall and temperature over West Africa in comparison with observations datasets. Again, the model's capability to reproduce the West African atmospheric circulation drives and atmospheric variables compared to reanalyses was examined. RegCM4 gives a good representation of atmospheric circulation from the lower to the upper troposphere.

The projected changes in West African climate under RCP8.5 and both RCP8.5 and urbanization were evaluated. For all the simulations, a significant warming is expected over the whole West Africa and will be more pronounced in the Sahel-Sahara at the end of the 21st century. A significant increase in temperature is also expected along the West African coastal region which corresponded to the 'perturbed' region. In the precipitation

simulations, all the different simulations projected drier conditions in visually the entire West African region. However, the expected change is less significant in the combined urban expansion and RCP8.5 simulations. Evaluation of contribution due to urbanization alone shows that the change in the land cover gave a response of an average increase in temperature of approximately 3ºC over the urbanized region. The results imply that urban effects can reach the same magnitude as global warming. This warming could be a result of the urban heat island processes. Precipitation in the urbanized region and their sub-urban regions shows an increase of at least ~10%. This means that urbanization has both local and regional effects on the precipitation in West Africa. Furthermore, the results show that the characteristics of some atmospheric circulation such as AEJ and AEWs would change in the future climate. For example, a southward displacement of the AEJ position was observed which can explain the projected drier conditions in the region, especially in the Sahel part. Moreover, it should be noted that urbanization influences the atmospheric circulation drivers through the AEJ and AEWs. More convective activities are found under urban conditions and the sensitivity of the AWEs to the land surface conditions is noticed.

RESUME

De nombreuses recherches ont été menées pour comprendre et améliorer la relation entre la modification de l'utilisation et l'occupation des terres et la variabilité et le changement climatique en Afrique de l'Ouest. Toutefois, l'influence de l'urbanisation sur le climat Ouest Africain n'est pas encore étudiée de manière approfondie. C'est dans ce contexte que cette thèse examine l'impact de l'urbanisation côtière sur le climat de l'Afrique de l'Ouest, en utilisant le modèle régional de climat RegCM4 couplé avec le modèle de surface CLM4.5. Une série d'expériences a été réalisée, pour le climat actuel (1984-2005) et pour le futur lointain (2079-2100) sous le scénario d'émission RCP8.5, avec une résolution horizontale de 25 km couvrant le domaine Ouest Africain. RegCM4 a été forcé à ses frontières latérales and initiales par le modèle global de circulation MPI-ESM-MR. Deux types de simulations ont été réalisées : avec et sans modification de la couverture végétale naturelle et avec la paramétrisation urbaine (CLMU).

Dans un premier temps, la capacité du RegCM4 á reproduire le climat actuel (1986-2005) pendant la saison des pluies (Juin-Septembre) a été évaluée et inter-comparée en les confrontant avec diffèrent types d'observations (CRU, CPC, UDEL) and rèanalyses (NCEP et ERA5). Les résultats montrent une bonne performance de RegCM4 à simuler les principales variables climatiques et la circulation atmosphérique en Afrique de l'Ouest pendant la saison des pluies. En effet, RegCM4 reproduit bien la configuration spatio-temporelle des précipitations et de la température en Afrique de l'Ouest par rapport aux ensembles de données d'observations. Une fois encore, la capacité du modèle à reproduire la circulation atmosphérique et les variables atmosphériques par rapport aux réanalyses a été examinée. RegCM4 donne une bonne représentation de la circulation atmosphérique de la surface à la haute troposphère.

Dans un deuxième temps, nous avons estimé un possible impact de la modification de la couverture végétale naturelle au niveau de la bande côtière sur la moyenne and la variabilité du climat au niveau de la région. Pour cela, nous avons calculé le futur changement relatif au climat présent sous le scénario RCP8.5 seul et sous le scenario RCP8.5 plus urbanisation combinés. Les résultats montrent que, à la fin du 21ème siècle, un réchauffement significatif est attendu sur l'ensemble du domaine de l'Afrique de l'Ouest et ce réchauffement sera plus prononcé sur la bande Sahélo-Saharienne. Une augmentation significative de la température est également prévue le long de la région côtière ouest africaine qui correspond à la région « perturbée ». Pour les précipitations, toutes les différentes simulations prévoient une importante réduction pratiquement sur toute la région. Cependant, cette sècheresse est moins importante dans les simulations combinées RCP8.5 and expansion urbaine comparé à la simulation RCP8.5 seule. L'évaluation de la contribution due à l'urbanisation à elle seule montre que l'évolution de la couverture terrestre a provoqué une augmentation moyenne de la température de 3ºC environ dans la région « urbanisée ». Les résultats suggèrent aussi que les effets urbains peuvent atteindre la même ampleur que le réchauffement climatique. Ce réchauffement pourrait être dû aux processus d'îlots de chaleur urbaine. Pour les précipitations, on note une augmentation d'au moins 10% environ dans la région « urbanisée » et leurs régions suburbaines. Cela signifie que l'urbanisation influence les précipitations à l'échelle locale et régionale.

Enfin, la dernière partie de cette thèse a consisté à étudier l'impact de l'urbanisation sur la dynamique de la mousson Ouest Africaine. Les résultats montrent que les caractéristiques de certaines circulations atmosphériques telles que le JEA et les OEA changeraient dans le climat futur. Par exemple, une migration vers le sud du JEA a été observé, qui peut expliquer la sècheresse prévue dans la région, en particulier sur la

partie sahélienne. En outre, il convient de noter que l'urbanisation influence le JEA et les OEA. Une activité convective plus importante est trouvée sous les conditions urbaines et la sensibilité des OEA aux conditions de la surface du sol a été notée.

TABLE OF CONTENTS

LIST OF TABLES

Table **Page**

LIST OF FIGURES

Figure **Page**

LIST OF ACRONYMS

AEJ	African Easterly Jet
AEWs	African Easterly Waves
AMMA	African Monsoon Multidisciplinary Analyses
BATS	Bio-sphere Atmosphere Transfer scheme
CAM4.0	Community Atmosphere version 4.0
CAM5.0	Community Atmosphere version 5.0
CLM4.5	Community Land Model version 4.5
CLMU	Community Land Model Urban
CMIP5	Coupled Model Intercomparison Project Phase 5
CORDEX	COordinated Regional climate Downscaling Experiment
CPC	Climate Prediction Center
CRU	Climate Research Unit
ECHAM6	European Centre Hamburg Model
ECMWF	European Centre for Medium-Range Weather Forecasts
EOF	Empirical Orthogonal Function
ERA5	European Centre for Medium-Range Weather Forecasts version 5
GCMs	Global Climate Models
HD	High Density
IPCC	Intergovernmental Panel on Climate Change
ITCP	International Centre for Theoretical Physics
ITCZ	Inter-Tropical Convergence Zone
ITD	Inter-Tropical Discontinuity

JJAS	June-July-August-September
LD	Low Density
LSMs	Land Surface Models
LULC	Land Use Land Cover
MCS	Mesoscale Convective Systems
MD	Medium Density
MM5	Mesoscale Model version 5
MPI-ESM-MR	Max-Planck-Institute Earth System Model Medium Resolution
NCAR	National Center for Atmospheric Research
NCEP	National Center for Environmental Predictions
PC	Principal Components
PFTs	Plants Functional Types
RCMs	Regional Climate Models
RCP8.5	Representative Concentration Pathways 8.5
RegCM3	Regional Climate Model version 3
RegCM4	Regional Climate Model version 4
SHL	Sahara Heat Low
SUBEX	Subgrid Explicit Moisture Scheme
TBD	Tall Building District
TEJ	Tropical Easterly Jet
UCM	Urban Canopy Model
UDEL	University of Delaware
UHI	Urban Heat Island
WAM	West African Monsoon

WASMC	West African Summer Monsoon Climate
WRF	Weather Research and Forecasting

CHAPTER ONE

INTRODUCTION

1.1 Background to the study

Currently, a picture of the World's population shows that more than 55% of the population lives in urban areas and this is expected to increase up to 68% by 2050 (UN Department of Economic and Social Affairs, 2018). African, especially West African, cities are no exception, with as much as more of half the population expected to live in urban areas by 2050 (World Bank, 2016; UN Department of Economic and Social Affairs, 2018). Urbanization is a result of population migration from rural areas in addition to natural urban demographic growth. Urbanization, which exponentially increases with industrialization, is usually induced by humans and affects the social and environmental landscape, produces an important quantity of greenhouse gases and particles in the atmosphere, which directly influences the climate.

The increases in population in urban areas is associated with change and modification of the natural environment (Dorning *et al.,* 2015) while the impact on the atmospheric environment is considered as the most far-reaching (Seto and Reenberg, 2014). For instance, the higher demand of housing in urban areas brings changes in land use where vegetation areas are transformed to high rise buildings and roads, which alters the energy balance (Seto *et al*., 2011; Bai *et al.*, 2014).

Moreover, Sensible heat flux, which refers to the amount of energy transferred to the environment by the modified urban surface and the incoming solar radiation, can alter the energy balance and, eventually, the temperature of cities. This can produce an urban heat island (UHI) effect in cities. All of these phenomena are causing noticeable changes

in meteorological conditions, and climates of cities and nearby areas thereby creating a new local climate called the urban climate (Landsberg, 1981; Oke, 1981).

Urban climates are distinguished from those of less built-up areas by differences of air temperature, humidity, wind speed and direction, and amount of precipitation. These differences are attributable in large part to the altering of the natural terrain through the construction of artificial structures and surfaces. For example, tall buildings, paved streets, and parking lots affect wind flow, precipitation runoff, and the energy balance of a locale.

The elevation in temperatures is most generally explained in terms of the basic surface energy balance processes of shortwave and longwave radiation exchange, latent, sensible, and conductive heat flows (Oke, 1987). The regional albedo of cities is significantly lower than natural surfaces due to the preponderance of dark asphalt roadways, rooftops, and urban canyon light trapping.

It is mostly of note that attention has been, recently, paid to urbanization questions relative to climate by the scientific community.

However, to better understand the urban-atmosphere interactions and the contributions of urbanization of the climate change, a range of approaches and techniques, such as the geographic information system (GIS), Remote Sensing (Liaqut *et al.,* 2019), satellites (Sun *et al.,* 2019; Paranunzio *et al.*, 2019) and numerous modeling studies (Jackson *et al.*, 2010; Martilli *et al.,* 2002; McCarthy *et al.*, 2010; Oleson *et al.*, 2010 ; 2015; Daniel *et al*., 2019), have been used. Due to the complexity of the urban-climate interactions, the use of regional climate models (RCMs) coupled with land surface models (LSMs) remains one of the best tools to assess the impacts of urbanization on climate at local and regional scales (Oleson *et al*., 2015; Daniel *et al*., 2019; Huszar *et al.*, 2019). Also,

modeling studies have the advantage of allowing interactions between complex systems of urban-atmosphere-climate. Recently too, urban canopy models have been developed using more explicit representations of the urban morphology and parametrizations of the associated processes (Oleson *et al.,* 2010; Shepherd *et al.,* 2010). Several numerical studies have demonstrated the strong correlation between rapid growth and changing climate. For example, studies such as Lamptey e*t al.* (2005); Miao *et al.* (2015), Wang *et al.* (2013) and Yang *et al.* (2014) have shown that urbanization impacts on climate are complex and vary between regions at different scales throughout the world.

Firstly, urbanization influences temperature significantly. Since Oke (1981) found that urbanization leads to increase in the near-surface temperature at the local scale. One of the most urban climate features called "Urban Heat Island" (UHI) effect in the literature is defined by the temperature difference between urban and its surrounding rural areas and can amplify the local and regional temperature patterns (Martilli *et al.*, 2002; Shepherd e*t al.,* 2010; Jackson *et al.,* 2010; McCarthy *et al*., 2010; Oleson *et al.*, 2011). More recently, findings have demonstrated that urbanization is a considerable contributor to the urban warming through UHI both in the present (Cao *et al.*, 2016; Laux *et al.*, 2017) and the future (Hamdi *et al*., 2014; Argüeso *et al.*, 2014; 2015). It has also been shown that more than 40% of global warming was induced by rapid urbanization development since the late 1970s (Yang *et al.*, 2011).

Secondly, precipitation response to urban modification has also been assessed. Unlike the UHI effect, the effects of urbanization on precipitation remain complex and unclear since results varied from different modeling studies. For instance, Zhang *et al.* (2009); Feng *et al.* (2015), using the Weather Research and Forecasting (WRF) model with an urban canopy model (UCM), found that urban conditions lead to precipitations decrease in urban areas in Beijing during the summer period. At the same time, Shao *et al.* (2013),

using the Regional Climate Model version 3 (RegCM3) over East Asia, found that change of land use due to urbanization, contributes to the East Asian monsoon weakening during the last decade. However, Mote *et al.* (2007), Zhang *et al.* (2009), Li *et al.* (2011), Wang *et al.* (2013) and Yang *et al.* (2014) using the WRF coupled with UCM, have found that urbanization may lead to precipitation increasing over and downwind of cities due to atmospheric convective activities favored by urban land use. Yet, the links between urbanization and increased incidence of extreme climate events have also been an attractive topic among the scientific community during the recent decades. Studies have revealed that urbanization is known to be associated with the more frequent and intense occurrence of extreme climate events (Fischer *et al.,* 2012). More severe droughts (Liang *et al.*, 2019), floods (Zope *et al*., 2016; Devi *et al.*, 2019), heat waves (Grimmond, 2007; Zhang *et al.*, 2009), heat stress (Fischer and Schär, 2010; Fischer *et al.*, 2012) will place increasing pressure on the livability of cities as well. For instance, Miao *et al.* (2011); Chen *et al.* (2015); Li *et al.* (2019) have found that urban areas play an important role in the increase of extreme rainfall. These authors found a strong correlation between extreme heavy rainfall, heat waves, and heat stress in urban areas during the urbanization period.

Besides their impacts on local climate and climate change, urbanization is another important factor affecting the greenhouse gases, particles, and other pollutant emissions. So far, cities are responsible for the majority of greenhouse gases emissions (>70% of global greenhouses gases emissions) (Kumar *et al.*, 2017; Gulia *et al.*, 2018) due to industrialization, transportation, energy consumption leading to bad air quality and health problems (Balogun *et al*., 2010; Revi *et al.* 2014; Knippertz *et al.*, 2015). Several experimental studies have shown that the most polluted regions, especially in terms of high concentration of particulate matter (PM) and carbon monoxide are located in urban

conglomerations (Revi *et al.*, 2014). It is known that these emissions can have impact on the climate by the way they affect radiation and clouds (Giorgi and Meleux, 2007; Martin *et al.,* 2017). This could modify the regional climate response to local and regional climate change (Boucher *et al.*, 2013; Bony *et al.,* 2015).

All of the studies have demonstrated that during this 21st century, besides the climate change causes and impacts, the impact of urbanization on climate have been one of the biggest issues for the scientific community. For example, it appears challenging to understand, quantify and qualify the climate response to anthropogenic LULC changes and/or climate change scenarios especially in West Africa, which is one the most vulnerable regions to climate change impacts and its consequences (Niang *et al*., 2014; Diallo *et al*., 2016). Over this region, the climate is dominated by a climatic system known as West African Monsoon (WAM). Interactions LULC changes and WAM have been investigated by several studies such as Charney (1975); Zheng and Eltahir (1997), Abiodun *et al.* (2008), (2012), Paeth *et al.* (2009), Taylor *et al.* (2011), Sylla *et al.* (2016a), Bamba *et al.* (2018). Most of them showed the strong sensitivity of the WAM to land surface changes at a range of time and space scales. Charney (1975), in a pioneering work, demonstrated positive feedback between rainfall and albedo via local vegetation modification and land surface processes to explain the drought that occurred in the Sahel. Also, Abiodun *et al.* (2008), using RegCM3, linked the droughts conditions observed during these last decades in the Sahel region to the desertification and deforestation over this region. Again, Fontaine *et al.* (1999), Taylor *et al.* (2011), Boone *et al*. (2016), Wang *et al.* (2016), and Sylla *et al.* (2016a) using regional climate models, have showed that changes in LULC affect the atmospheric circulation features leading to a strong inter-annual and inter-decadal variability causing a shift in precipitation pattern. According to these studies, it is obvious that the land surface changes play an

important role in the climate variability over this region. Despite, the efforts to link land cover changes and climate variability and/or climate change in this region, there are still a lot of open questions such as what is the contribution of urbanization in climate variability? What is the contribution of urbanization to climate change, especially with the current rapid West Africa's urbanization rate? How can the West African climate and its uncertain climate projections be characterized in the context of its urbanization? Many of the studies focusing on the impact of LULC changes on the West African climate have not yet treated the question of urbanization.

In order to elucidate the question of rapid urbanization, especially the consequence urban expansion consequences on the West African climate, the purpose of this thesis is to qualify and quantify the effects on urbanization on regional climate.

1.2 Statement of the research problem

The WAM is a primordial climate component in West Africa which defines the hydrological cycle, run-off, agriculture, and the socio-economic sector. During the past two decades, the WAM has been known to have a strong variability which affects the lives of the people. For example, the drought in the 1970s and 1980s has several consequences like famine and water scarcity. Several studies were carried out to understand this strong variability (Fontaine and Janicot, 1998; Nicholson, 2001; Nicholson and Grist, 2001; Lebel and Ali, 2009) and to predict the future climate in West Africa (Diallo *et al.*, 2012; Sylla *et al.*, 2013; Wang *et al.*, 2016; Raj *et al.,* 2019). Most of them linked this variability to the changes in the land surface conditions and /or the climate change phenomenon. For example, previous studies (Charney, 1975; Abiodun *et al.,* 2008; Paeth *et al.,* 2009; Sylla *et al.,* 2016a) linked the West African climate variability and change observed during the last years to the LULC changes.

According to the fifth report of the International Panel on Climate Change (AR5 IPCC, 2014), after the greenhouse gases effects, urbanization which is an extreme form of LULC change, is the most recognized man-made factor that influences the changing and/or variability of climate locally and regionally (Revi *et al.*, 2014; Hassan *et al.*, 2016). For instance, several investigations (Miao *et al*., 2011; Zope *et al*., 2016; Li *et al*., 2019) especially based on the Asian and Chinese region, have been carried out, focusing on the sensitivity of the regional climate to the rapid urban land cover changes. Results from these studies show that urbanization is an important aspect that can explain the climate variability observed during the last 30 years (Kaufmann *et al.,* 2007; Zhang e*t al.,* 2009, Cao *et al.,* 2016). In addition, increasing megacities in West Africa especially along the coast is unprecedented and these cities through their emissions are major contributors to climate change (Field, 2014). For example, the last IPCC (2014) report revealed that 70% of greenhouse-gas emissions come from cities, and their location along the coastal region remains one of the greatest challenges due to the vulnerability to sea level rising and high flooding risk (Seto *et al.*, 2011). However, till date, the influence of urbanization or the expansion of built-up areas on West Africa climate using a regional climate model (RCM) has not yet been investigated.

Furthermore, most models have not yet included gridded urbanization, and for those that have, treatment of land use was inconsistent and incomplete. There were also particular difficulties stemming from the need to reconcile the interface of past land-use reconstructions and future projections (McCarthy *et al.*, 2010; Revi *et al.*, 2014; Abiodun *et al.*, 2017).

In response to all of these, this study investigates the effects of urbanization on the West African climate during the monsoon months using a regional climate model.

1.3 Research Justification

In the most recent years, urbanization has posed great challenges all over West Africa. This is because it is one of the world's fastest growing regions with the urban rate jumping from 8.3 % in 1950 to almost 50% in 2015 (African Development Bank, OECD, and United Nations Development Programme, 2016) and with the greatest percentage of the population concentrating in the coastal areas (Seto et al., 2011; Dobigny et al., 2018). As a consequence, the natural land cover has been modified. This is believed to be affecting directly and/or indirectly the regional climate. Over West Africa, it is arguable that the sensitivity of the climate to the land surface conditions changes. For instance, Charney (1975) demonstrated that the droughts conditions between 1960 and 1970 are due to the deforestation and desertification observed in the region, especially, in the Sahel region. Also, Abiodun et al. (2008) and Sylla et al. (2016a) revealed that the changes in vegetation can cause substantial reductions in rainfall over West Africa.

However, the question bordering on the impact of urbanization on the West African climate sensitivity has not fully been investigated. This study, therefore, investigates the potential impact of urbanization on the West African climate. Understanding the effect on rapid urban expansion on the West African climate presupposes an urgent need for a better knowledge of the WAM sensitivity and variability, and a better projection of future climate patterns in the region.

1.4 Aim and Objectives

This thesis aims to assess the impact of coastal urbanization on the West African summer climate, using the Regional Climate Model version 4 (RegCM4).

The specific objectives of this work are to :

(i) assess the capability of RegCM4 to capture the main characteristics of the West African summer climate;

(ii) evaluate the impacts of coastal urbanization on the mean and variability of the West African summer climate; and

(iii) evaluate the physical process by which urbanization influences the main West African climate features i.e. the dynamics of the West African summer climate.

1.5 Thesis Structure

This PhD thesis is organized as follows: Chapter One contains the introduction. This is succeeded by Chapter Two which presents a review of related literature on the West African summer climate and the associated urban influence on climate. In Chapter Three, the model used, the experiment design and the model setup, as well as the processes used to implement an urban expansion in RegCM4 and the different experimental designs are described. Results from the previous chapter are used to establish the effect of urbanization on the West African summer climate in Chapter Four. Chapter Five summarizes and discusses the results of the work. It also gives suggestions and recommendations for future studies.

CHAPTER TWO

LITERATURE REVIEW

Across West Africa, it has been proven well that climate is impacted by interaction between land and atmosphere (Charney, 1975; Wang and Eltahir, 2000; Koster *et al*., 2004; Xue *et al*., 2016, Wang *et al.*, 2016). Thus, changes in the LULC have a great impact on the regional climate (Taylor *et al.,* 2002; Sultan *et al.,* 2005; Sylla *et al.,* 2016a). However, the way LULC change index; such as urbanization and its associated processes, affects as forcing on West Africa's climate is currently being poorly investigated and understood. This chapter presents a review of available literature on the knowledge about West African climate system and the various forcing, mechanisms involved. It also considers a focus on LULC change interactions with regional climate. To establish the theoretical basis for this research, this chapter presents a review of studies on the West African Summer Monsoon Climate (WASMC), as well as the urbanization influence on climate. Thus, it contains two major parts: the first section gives an overview of the WASMC, which determines the climate of the region and its sensitivity on LULC modification, the second part provides the reason for the nature of urbanization at global scale and the consequences of urbanization on climate at local and regional scales.

2.1 West African Climate

2.1.1 West African Monsoon dynamics

West Africa's climate is dominated by a system called the West African Monsoon (WAM) also known as the West African Summer Monsoon Climate (WASMC), a large scale circulation associated with seasonal reversing wind due to land-sea temperature

contrast between the Gulf of Guinea in the tropical Atlantic and the Western part of African continent, covering from the Sahara desert to the Gulf of Guinea coast (Eltahir and Gong, 1996; Afiesimama *et al.*, 2006; Sylla *et al.*, 2013) during the summer monsoon season. The WAM is principally characterized by the migration of zonally banded rainfall from the Guinea coast to the Sahel. It follows the movement of the Intertropical Convergence Zone (ITCZ) which in turn is driven by two continental trade winds from the (1) Atlantic Ocean and (2) Sahara desert. It provides most of the rainfall for West African countries especially over Sahel (Omotosho, 1985; Sultan *et al*., 2005) during the boreal summer period from June to September.

So far, the WAM is a coupled and complexed system which interacts with some components of the Earth's system (Sultan and Janicot, 2003; Hall and Peyrillé, 2006; Lafore *et al*., 2010). It is the resultant effect of several forcings such as atmosphere (Jenkins *et al.,* 2005), ocean (Fontaine *et al.,* 2010; Rodríguez-Fonseca e*t al.,* 2011), and land surfaces feedbacks (Abiodun *et al.*, 2008; Paeth *et al.*, 2009; Sylla *et al.*, 2016a; Yu *et al.*, 2016). It is also influenced by natural climate processes (teleconnections) that occur over a range of temporal and spatial scales also called the multi-decadal variability (Sultan and Janicot, 2003; Hall and Peyrillé, 2006) such as El Niño/ENSO, the Quasi Binary Oscillation (QBO), the North Atlantic Oscillation (NAO), Atlantic Multi-decadal Oscillation (AMO) and Madden-Julian Oscillation (MJO). These often help to explain the climate variations in West Africa (Maynard *et al.*, 2002). Previous studies have demonstrated that many atmospheric processes also modulate the WAM variability and sensitivity like squall lines (Fink, 2003; Gaye e*t al.*, 2005), African Easterly Jet (AEJ), Tropical Easterly Jet (TEJ), African Easterly Waves (AEWs) (Cook, 1999; Diedhiou *et al.*, 1999), Sahara Heat Low (SHL) (Lavaysse *et al.,* 2009). These represent

the WAM features (see Figure 2.1 and Figure 2.2). The WAM quality, i.e. rainfall amount and variability, is determined by intensity and the position of its features (Afiesimama *et al.*, 2006; Redelsperger *et al.*, 2006; Raj *et al.,* 2019).

2.1.2 West African Monsoon Features

2.1.2.1 Sahara Heat Low

The Sahara Heat Low (SHL) is defined as a thermal depression generally below 600 hPa (Figure 2.1 and Figure 2.2) observed over West Africa (Thorncroft and Blackburn, 1999). It is an intensely dry, very hot layer often overlying the cooler, more humid surface air. As it arrives from continental areas out of the ocean, it is lifted above the denser marine air causing the trade inversion layer where temperature increases with height. SHL is due to strong heating of the Sahara surface creating a low pressure system which leads to the development of a thermal low pressure near the surface during the boreal summer period (Lavaysse *et al.*, 2009). Thorncroft and Blackburn (1999) suggested that this heating, reaching 700 mb where in the AEJ region, is particularly important for AEJ maintenance and is associated with meridional gradients in potential vorticity. Moreover, Lavaysse *et al.* (2009) revealed that a northward shift of the SHL is associated with a northward movement of solar radiation maximum at the surface. They also suggested that the SHL onset (northward migration) occurs 5 days before the monsoon onset in the Sahel as previously defined by Sultan and Janicot (2003). Similar results were found by Hagos and Cook (2007) and Thorncroft *et al.* (2011) who emphasized that the WAM onset over the Sahel is determined by the SHL which plays a significant role in the monsoon jump process, an abrupt shift of the rain belt.

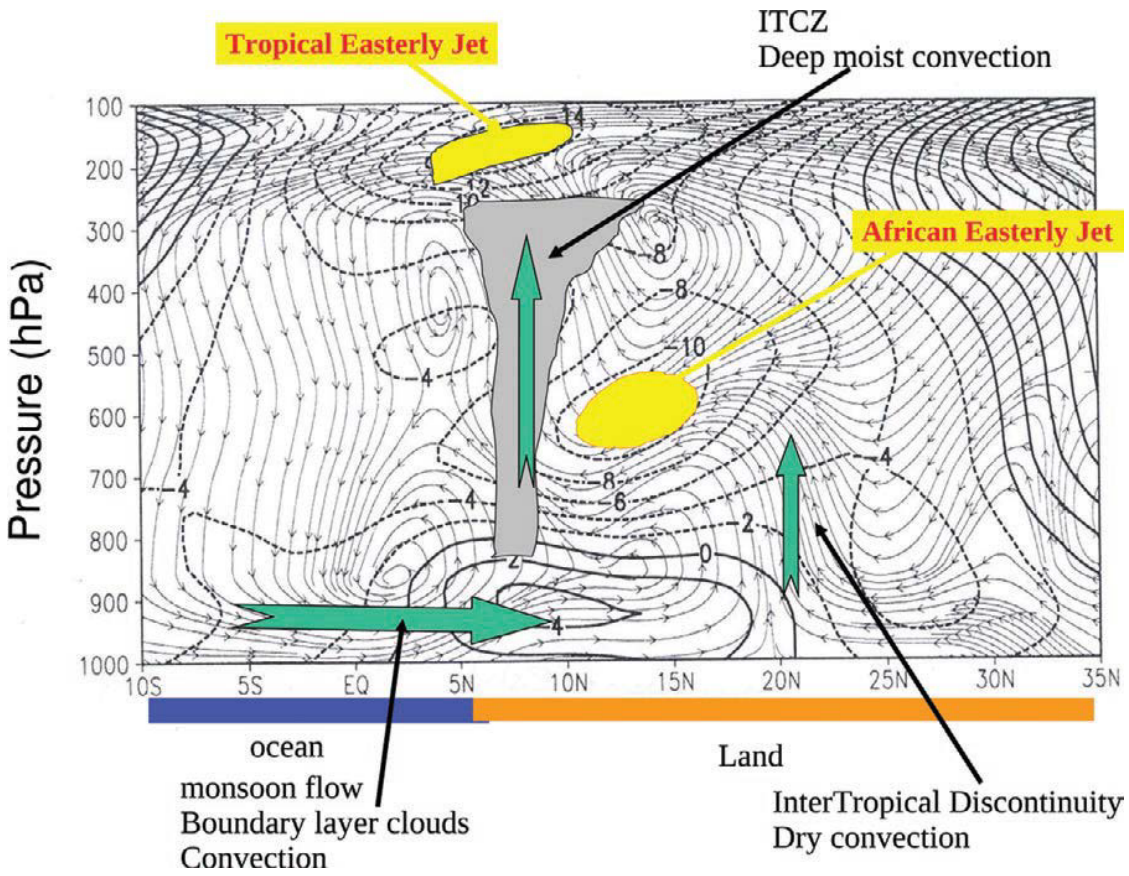

Figure 2.1: Summer mean meridional circulation and associated mean winds (ms^{-1}) over West Africa [adapted from Hourdin *et al*. (2010)].

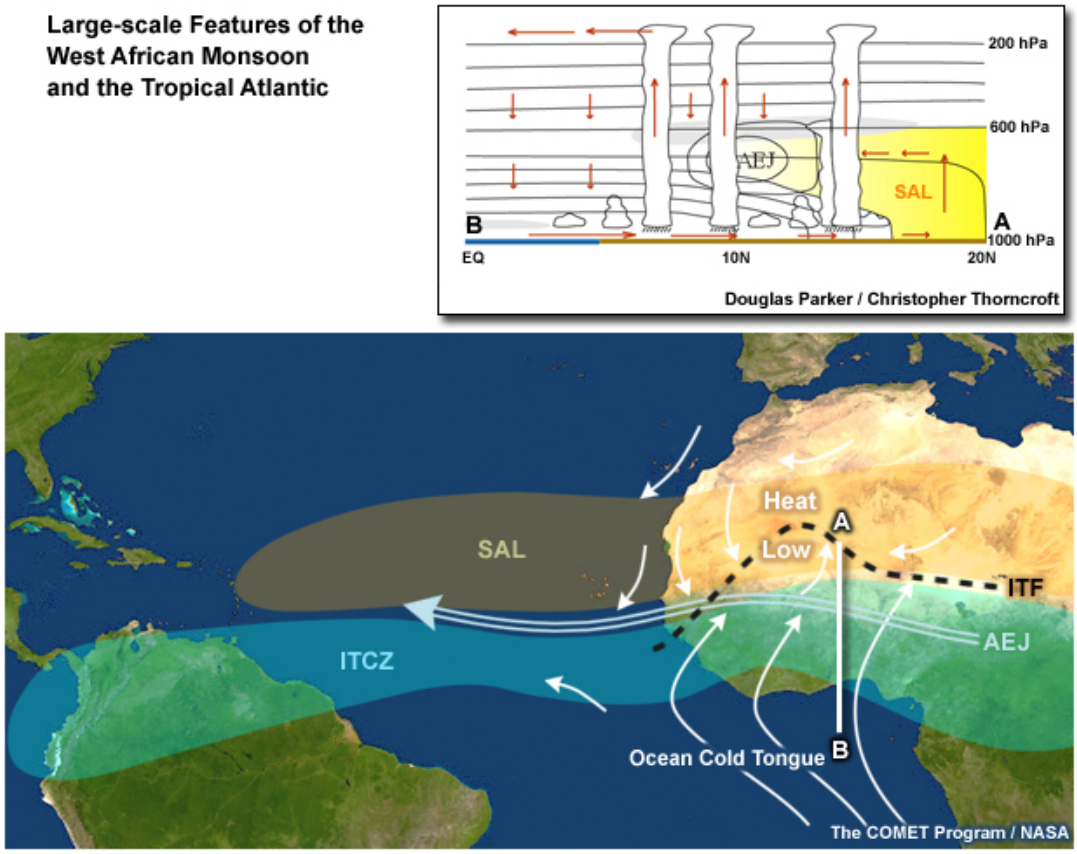

Figure 2.2: Large-scale features of the West African Monsoon and the Tropical Atlantic [adapted from Parker *et al.* (2005)].

Usually, strong SHL phases, defined by an increase of low-level atmospheric thickness, are associated with positive temperature anomalies in the low layers, a monsoon flow strengthening, the divergence flux negative anomalies, moisture advection enhancement over the central Sahel, AEJ intensification and upward vertical motions located south of ITD enhancement. These conditions appear to be favorable for the occurrence of convection over the central Sahel, since strongest and most widespread convective activity over the central and eastern Sahel occurs when the SHL intensity is the strongest (Lavaysse *et al*., 2009).

2.1.2.2 African Easterly Jet (AEJ)

The African Easterly Jet (AEJ) is one of the key features of the WAM system. It is defined as a strong zonal wind located between 600 and 700 hPa (Figure 2.1) (Cook, 1999; Thorncroft and Blackburn, 1999; Cornforth *et al*., 2009) with a speed of about 12-15 $m.s^{-1}$ (Grist et al., 2002). It occurs in the Guinea Coast (10ºN) and moves to the north part ~15ºN (Burpee, 1972; Sultan and Janicot, 2003). Burpee (1972) suggested that the AEJ is formed as the response to the existence of barotropic and baroclinic instabilities, leading to the development of the African Easterly Waves (AEWs) growing at the expense of the AEJ. This implies that the observed AEJ is a result of the combination of the diabetically forced meridional circulation maintaining it and the AEWs weakening it. Studies such as Thorncroft and Blackburn (1999), Cook (1999), and Cornforth *et al.* (2009) demonstrated the presence of the AEJ by the strong meridional soil moisture gradients between the Atlantic Ocean and the Sahara desert. Nicholson (2013) also revealed that the AEJ is maintained by the juxtaposition of moist convection from the south and dry convection from the north. Moreover, Thorncroft and Blackburn (1999) suggested that the AEJ is maintained by two diabetically forcing

meridional circulations patterns: the first is associated with dry convection in Sahara regions, and the second is linked to the deep moist convection in the ITCZ.

Several studies have shown the link between the AEJ and the WAM especially the rainfall anomalies (Cook, 1999; Nicholson, 2008; Cornforth et *al*., 2009). The latitudinal position of AEJ core can vary considerably and its characteristic is very important in rainfall variability over the northern Sahel (Nicholson, 2008). It has been demonstrated that in wet (dry) years, the AEJ tends to be weaker (stronger) and have a northward (southward or equatorward) shift (Nicholson and Grist, 2003; Jenkins *et al*., 2005; Nicholson, 2008; Sylla *et al.*, 2010). In addition, studies have explained the mechanisms by which the AEJ affects the rainfall. For instance, Cook (1999) showed that AEJ creates a divergence of moisture below the level of condensation leading to a reduction of the rainfall amount. Moreover, vertical wind shear associated with the AEJ strongly influences the formation and organization of Mesoscale Convective Systems (MCSs) responsible for about 95% of rain in Sahelian zone (Laurent *et al.,* 1998) and 50 % in Sudanian zone (Omotosho, 1985).

The AEJ, as well as the WAM, are sensitive to the meridional surface gradients of mass and energy and these gradients are in turn very sensitive to the land surfaces conditions (albedo, vegetation, deforestation, soil moisture). Fontaine *et al.* (1999), Sultan and Janicot (2003), Sylla *et al*. (2016a) and Bamba *et al.* (2018) demonstrated that small perturbations on land surface conditions can affect the AEJ structure and consequently the WASM processes.

2.1.2.3 Tropical Easterly Jet (TEJ)

The TEJ is also an important feature of the northern hemispheric summer (Cook, 1999; Cornforth *et al*., 2009). It is an upper easterly jet located around 100-200 hPa during the African monsoon period south of the ITD and north of the Equator. It corresponds to the upper branch of the Walker circulation, initialed by the Asian monsoon circulation, which is very intense due to the strong thermal contrast between the upper atmosphere above the Indian Ocean and the Tibetan plateau as well as the steep orography.

Previous studies have revealed that TEJ modulates the WAM. TEJ structure and intensity variability influence the development of deep convection, moisture convection and interannual variability of the monsoon over West Africa. Weak (strong) TEJ is often associated with weak (strong) monsoon flow (Nicholson and Grist, 2003; Nicholson, 2008). Nicholson (2008) revealed that a strong TEJ is linked to cool conditions in tropical upper atmosphere, a latitudinal temperature gradient associated with an intense monsoon rainfall and an increase rain belt. However, till now the physical mechanisms about TEJ role are still not fully elucidated.

2.1.2.4 African Easterly Waves (AEWs)

The AEWs are westward-traveling waves forming near the AEJ zonal circulation pattern over tropical North Africa during the summer rainy season (Burpee, 1972; Kiladis et al., 2006). The AEWs grow at the expense of the AEJ via combined baroclinic-barotropic energy conversion process. Early studies from Burpee (1972) and Reed et al. (1977) have demonstrated that the AEWs were formed by the barotropic-baroclinic instability (Charney and Stern, 1962). This instability requires a sign change of the meridional gradient of potential vorticity gradient or negative potential vorticity (PV) gradient coupled with a surface maximum gradient of potential temperature (Burpee, 1972;

Thorncroft and Blackburn, 1999; Diedhiou et al., 1999). The sign reversal of PV at the AEJ level is consistent with the presence of a strip of high PV on the southern flank of the AEJ, which is in turn augmented by deep convection during the active monsoon. This is illustrated by the JJAS mean of potential vorticity on the 315K potential temperature surface which generally goes through the AEJ core.

Previous studies have linked the AEWs to precipitation through the MCSs, which produce most of the rainfall during the summer monsoon in West Africa. Fortune (1980), Landsea and Gray (1992); Gaye *et al.* (2005), Reed *et al.* (1977), Fink and Reiner (2003), and Schlueter *et al.* (2019) demonstrated that these AEWs modulate the precipitation throughout the MCSs. The AEWs bring the most significant weather, where they may form MCSs, often including squall lines. These are associated with local circulations bringing convective rainfall to the African Sahel. Diedhiou *et al.* (1999) and Gaye *et al.* (2005) found that positive rainfall anomalies in and ahead of AEWs troughs. Also, others studies found that some convection occurred east of the trough, in the southerly flow. AEWs over the northern part of Sahel (17.5ºN) are more likely to have moist mesoscale convection east of troughs, while AEWs at more southerly latitudes (7.5ºN) seem to be rainy more often at and west of troughs. Fink and Reiner (2003) suggested that more than 60% of organized squall lines during summer are associated with AEWs.

2.2 Land Use and Land Cover (LULC) Changes in West Africa and their impacts

One of the main characteristics of the West African region is a strong variation at spatio-temporal scale in climate, especially the rainfall distribution, which is one of the most determinant parameters of its regional climate. The climate in West Africa has experienced significant variability on several varying from scales from intra-seasonal to

decadal along the 20th century. This variation of rainfall patterns leads to important impacts on livelihood conditions, agriculture, water availability, economic growth, and stability on the region. Little changes in rainfall patterns, when experienced over a long period of years, have a great effect on the vegetation and thus affect the populations. For example, since 1960s, most parts of West Africa, particularly the Sahel region, experienced repeated series of occurrences of disastrous events such as drought, flood, water stress, and heat waves. These disastrous events may even increase with global climate change as suggested by Diallo *et al*. (2012) and Sylla *et al.* (2016b). They, using a regional climate model (RegCM) under climate changes scenarios, found an increased risk of heavy precipitation, floods hazards, temperature and an expected regional decrease of rainfall over West Africa, in particular in the Sahel region, by the end of the 21st century. Furthermore, during the past two decades, the WAM has been the focus of considerable projects such as AMMA (Redelsperger *et al.*, 2006) which the purpose is to understand the West African climate and their variability. Several others numerous studies such as Afiesimama *et al.* (2006), Sylla *et al.* (2013) have attempted to provide a better understanding of the causes of variability and sensitivity of the WAM leading to better policies and strategies promoting sustainable food production and adequate water resources in the region.

These studies pointed out that the West African climate variability can be classified as internal and external. The internal climate variability refers to the changes of climate by itself, This means that the changes are due to natural variations of atmospheric or oceanic phenomenon such as ENSO, NAO, etc. In turn, the external climate variability means that the changes are from the anthropogenic external forcing such as the greenhouses gas concentration which is the most visible and the most important for the

region (Sylla *et al.*, 2016b; Taylor *et al.*, 2017). While the climate change has been shown to have a major impact of rainfall variability, numerous studies have also demonstrated the important role of land surface conditions changes and processes on the West African climate variability and sensitivity (Charney, 1975; Zheng and Eltahir, 1997; Abiodun *et al.*, 2012; Sylla e*t al.*, 2016a). For instance, studies have demonstrated that the changes LULC are believed to be the major anthropogenic cause of climate perturbations in West Africa, especially the Sahel region. The land surface conditions impact the West African regional climate through biogeophysical and biogeochemical processes by modifying surface albedo, carbon cycle, water cycle, and momentum exchange (Kueppers *et al.,* 2007; Hagos *et al.*, 2014; Boone *et al.*, 2016). Since Charney (1975) suggested that the drought conditions in the Sahel can be explained by the reduction of vegetation, which leads to an increase of albedo and decrease of precipitation; this study serves as the foundation for the commonly cited positive vegetation albedo feedback mechanism for the Sahel. Recent modeling studies, regarding land surface forcing, have also demonstrated the sensitivity of the West African climate to the land surfaces conditions (Xue, 1997; Wang and Eltahir, 2000; Abiodun *et al.,* 2008; Yu *et al.*, 2016; Boone *et al*., 2016; Wang *et al.,* 2016; Xue *et al.,* 2016; Diba *et al.,* 2018). For instance, Xue *et al.* (2004) showed that the vegetation degradation has a role in the drought events in the Sahel, through the increase in albedo and the reduction of evaporation, leading to reduced net radiation and inhibited convection, respectively, which in turn weaken the monsoon circulation. Abiodun *et al.* (2008) concluded that both deforestation and desertification are likely to weaken the monsoon flow over Sahel region. Quesada *et al.* (2017), using a regional climate model, found that future LULC changes significantly reduce monsoon rainfall. Bamba *et al.* (2018) simulated the effect of vegetation on WASMC by adding vegetation in two

different positions (forest or evergreen broadleaf) in RegCM4. He found a reduction of temperature and increase (or decrease) of rainfall (depending on the position and location of the greenbelt). Also, in response to reforestation scenarios, Diasso and Abiodun (2017) found a decrease in the warming pattern over Savanna and an increase of the rainfall. Sylla *et al.* (2016a) showed that conversion of forests into croplands tend to induce warmer condition in West Africa because of the potential reduction in evapotranspiration.

Despite the aforementioned studies, many challenges remain for modeling the land surface influence on the atmosphere in West Africa. Surface processes are often poorly represented or ignored like the case of urbanization. It should be emphasized that none of the experiments incorporate urbanization forcings. This is particularly important to assess urbanization influence on regional climate, especially in West Africa, which is the second-largest region on Earth and the fastest growing urban region in terms of population. To date, the relationship between urbanization changes and the WASMC using a regional climate model has not been fully investigated. Based on our knowledge, this study is the first over West African region to try to study the potential effect of urbanization on regional climate using a regional climate model. This work tries to fill this gap.

Furthermore, it is important that we understand the feedback processes associated with urban expansion changes and its influence on regional climate in order to assess the potential impact of future changes and to develop adaptation and mitigation strategies.

2.3 Regional climate modeling over West Africa

Due to the strong variability of the West African climate observed during these past years, there have been increasing numerical studies investigating the global climate, both to aid our understanding and to improve regional future projections in the context of climate change. A large volume of modeling simulations has been performed using Global Climate Models (GCMs). Results have highlighted that GCMs are valuable and sophisticated tools for better understanding the West African climate. They are also used to make projections of anticipated climate change associated with anthropogenic effects such as emissions of greenhouses gases, aerosols or LULC (Hourdin *et al.*, 2010). However, due to their coarse horizontal resolutions, GCMs cannot adequately represent some main WAM characteristics and features of the fine scale structures that significantly determined the climate over the region (Hourdin *et al.*, 2010; Sylla *et al.*, 2010). This means that the use of GCMs for regional climate understanding and projection is significantly limited (Sylla *et al.,* 2010). Therefore, different dynamical, statistical and combined approaches can be used to downscale coarse-grid data sets from GCMs to the regional and local scale in order to account for the effects of fine scale forcings, complex topography or land surface distribution (Giorgi and Mearns, 1991; Giorgi, 2006). This technique consists of using a limited area climate model, i.e. the Regional Climate Models (RCMs), over a given region of interest (more description of RCMs is available in Chapter Three).

Over the past three decades, much effort has been devoted to the use, evaluation, and application of RCMs over West Africa (Afiesimama *et al.*, 2006; Nikulin *et al.*, 2012; Sylla *et al.*, 2013). Due to the higher resolution and a more complete representation of physical processes in RCMs, this considerably has been provided as solution to the

GCM's problem and has been demonstrated to be able to improve the WAM climatology as well as the variability (Diallo *et al.*, 2012; Sylla *et al.*, 2013; Gbobaniyi *et al.,* 2014; Akinsanola *et al.*, 2015). It has also aided the understanding of the interactions between the dynamical features affecting precipitation (Browne and Sylla, 2012) and the contribution of LULC changes on monsoon circulation dynamics (Paeth *et al.,* 2009; Abiodun *et al.,* 2012).

Despite some errors or biases of RCMs outputs, it remains the best tool to study the West African climate (Diallo *et al.*, 2012; Nikulin *et al*., 2012; Gbobaniyi *et al.*, 2014). An ensemble of high-resolution regional climate model was used to assess the West African climate and to predict the future climate pattern such as WRF (Alaka and Maloney, 2017), RegCM (Browne and Sylla, 2012; Diallo e*t al.,* 2012), or from an inter-comparison projects such as Coordinated Regional Climate Downscaling Experiment (CORDEX; Nikulin *et al.*, 2012; Gbobaniyi *et al*., 2014). A range of studies has demonstrated the capability of these RCMs to properly simulate the West African climate. For example, Afiesimama *et al.* (2006), Sylla *et al.* (2010), Browne and Sylla (2012) and Sylla *et al*. (2013) have demonstrated that RegCM gives good results in simulating the WAM climatology as well as the variability and the future projection compared to other RCMs.

2.4 Context: an urbanized world

Currently, around 55% of the world's population lives in urban areas and future projections indicate that this number will have swollen to 70% by 2050 (UNDESA, 2018). The degree of urbanization, by contrast, varies considerably from continent to continent. For instance, in South America, it is generally above 50%, the proportion in Venezuela is above 90% and in Africa, it is about 30% (World Bank, 2016). However,

Africa and Asia are the fastest growing urbanizing regions in the world (Yuen and Kumssa, 2011). The urbanization process is mainly linked to economic growth, commercialization, industrialization, as well as rural-urban migration and globalization (Seto *et al.*, 2011; Burdett, 2018). Owing to the fact that most employment opportunities are within urban areas, cities attract a large part of a country's job seeking population. This is especially true in developing countries, where an increasing share of economic activities take place in the cities, and the differential between urban and rural wages is growing. The processes of urbanization have been associated with social, economic, environmental, and health transformations or issues (Grimmond *et al.*, 2011; Seto *et al.,* 2012). Additionally, urbanization is a global phenomenon that is paramount is the modification of the natural land cover. It can directly or indirectly influence the climate at the local and regional scales (Oke, 1987; Shepherd *et al.,* 2010; Revi, *et al.*, 2014). For instance, recent analyses of disaster impacts show that a high proportion of the world's population, most affected by extreme weather events is concentrated in urban areas (IFRC, 2010; Seto *et al.*, 2012; Revi *et al.*, 2014). However, the climate change adaptation in cities is among the biggest challenges because these areas face two major issues: the large-scale consequences of climate change induced by emissions of long-lived greenhouse gases, and the local and regional climate change resulting from land use change, and other environmental impacts, associated with urbanization (LULC changes, McCarthy *et al.*, 2010; Seto and Reenberg, 2014; Revi *et al.,* 2014).

2.5 Urbanization in West Africa

Currently, 50 % of West Africa's population lives in urban areas, being one of the world's fastest region in terms of urban population (UNDESA, 2018) and by 2050, it is projected that 80 % of them will be living in urban areas. West Africa has been experiencing intensive urbanization over the past 60 years and cities have fundamentally

transformed the social, economic and political geography of the region (Yuen and Kumssa, 2011). According to World Bank (2016), more than half of West Africa's population lives within 100 km of the coast, river systems, or major bodies of water and a significant percent of this growth is positioned in low-elevation coastal zones (Figure 2.3) (Alcala and Russ, 2006; Seto *et al.,* 2011; Dobigny *et al.*, 2018). This can be explained by historical and economic reasons. Coastal urbanization is also linked with colonization where newly developed centers are made to control and administer the colonized population and to exploit and export natural resources (Beauchemin and Bocquier, 2004; ADB, OECD, and UNDP, 2016). This partially explains why urban growth remains high in coastal cities such as Lagos (Nigeria), Ibadan (Nigeria), Abidjan (Côte d'Ivoire), Accra (Ghana), Dakar (Senegal) (Dobigny *et al.,* 2018) with large scale differences in the distributions of urban areas (see Figure 2.3).

The cities' locations make them important economic centers and are prone to experiencing warming and variation in weather. Their locations also make them vulnerable to sea-level rise, drought, flooding, stronger storms, erosion, salination, climate change impacts (Douglas *et al.*, 2008; Kithiia, 2011). Studies revealed that urbanization is one of the principal consequences of land use and land cover changes (Grimmond *et al.*, 2011; Seto *et al.*, 2012), leading to significant climate change and environmental issues. In summary, West Africa is a model of rapid transition from forest/agriculture land-use to urbanization and it therefore provides a leading and an ideal case where the influence of urbanization influence on climate at a regional level could be investigated.

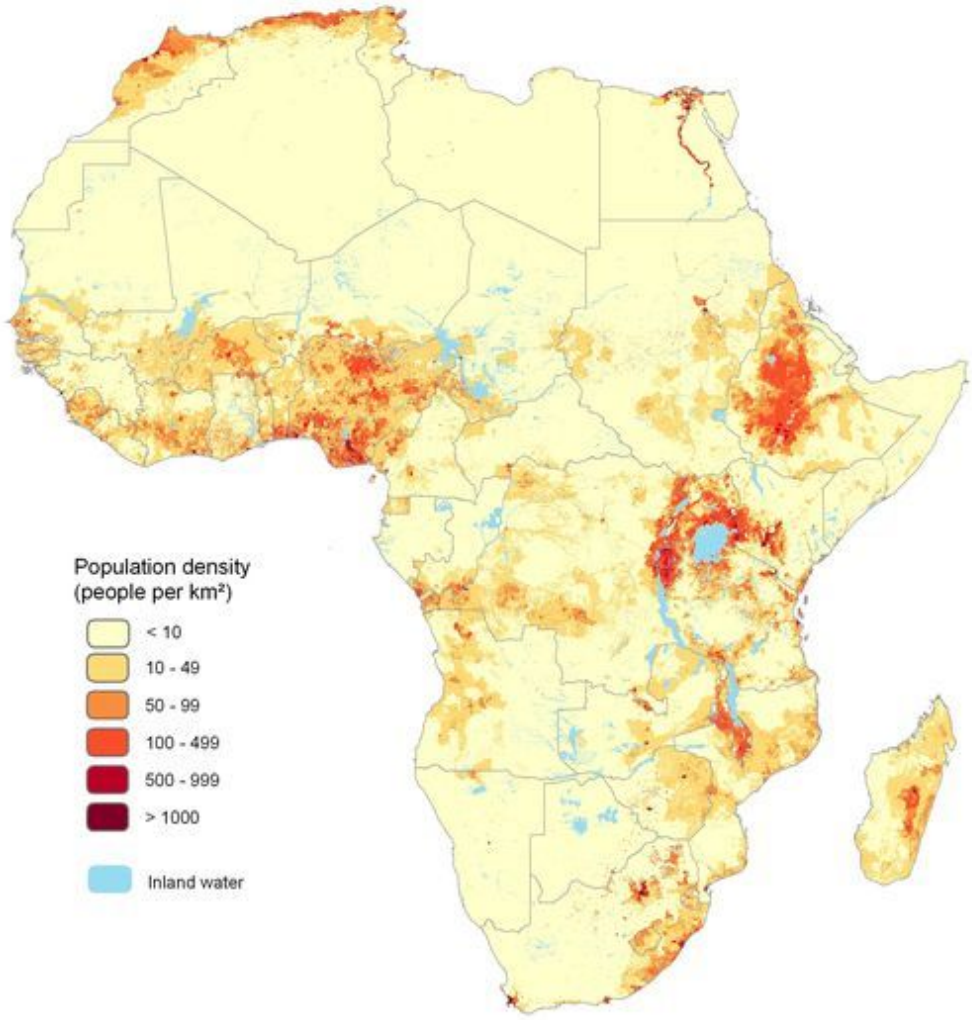

Figure 2.3: Population densities by administrative units in West Africa in 2015.

https://www.grida.no/resources/8498

2.6 Urbanization impacts on climate

Climate change and/or climate variability are caused by many factors which include oceanic processes, variation in solar radiation, the modification of land use and land cover composition and human-made activities. Moreover, over the last centuries, the earth's terrestrial surface has witnessed profound changes which, due to the human land use activities, have had great impact on the climate system. Moreover, LULC changes influence the climate through changes in surface albedo; land roughness, hydrological and thermal features. However, urbanization, which is a very extreme case of LULC changes, is the commonest cause of changing environmental change on earth in the 21st century.

According to the IPCC report (Revi *et al.*, 2014), after the important and rapid emission of greenhouse gases, land-use changes, particular urbanization, is the most important anthropogenic change that influences climate. Hence, these urban areas experience many problems such as economic, social, environmental, health, etc. (Kaufmann *et al.*, 2007; Seto *et al.,* 2011). For example, natural and agricultural land are transformed to residential, commercial, and industrial land cover which alters the land surface properties. Replacing the natural land cover with these new land cover will lead to significant changes in land surface properties. As a result, a new climate is created at local or regional scales called urban climate (Landsberg, 1981; Oke, 1987). An urban climate is a form of man-made climate which is not as conducive as the natural, and undisturbed climate (Pielke *et al.*, 2002). Urbanization modifies the physical and thermodynamic characteristics of the underlying surface and makes the land cover in urban areas very different from that of the surrounding areas. These differences create a horizontal gradient of energy budget and moisture in the surrounding environment,

impacting the boundary layer characteristics as well as the heat and water exchange (Miao *et al.,* 2009; Cao *et al.*, 2016) between the land surfaces and the atmosphere which, thereby, influence rainfall (Cao *et al.*, 2016; Laux *et al.,* 2017), temperature (Sun e*t al.*, 2018), carbon emissions and pollutants (Liao *et al.*, 2015).

2.6.1 Urban Heat Island (UHI)

Studies highlight the urban characteristics that result in urban climate modification, most often expressed as urban heat island (UHI) (Figure 2.4). UHI is defined by the difference of temperature pattern, particularly at night, between urban and rural areas (Jackson e*t al.,* 2010; Oleson *et al.*, 2011). It is first documented by Landsberg (1981) and Oke (1981) and it is an example of an extreme case of how land use can modify the climate at the local and regional scale. It is mainly caused due to the heat stored and re-radiated by massive and complex urban built structures (Oke, 1987; Grimmond, 2007; Oleson *et al.*, 2008; Fischer *et al.*, 2012). During urban expansions, the vegetation land covers are reduced and replaced by impervious construction materials and built-up area, which are of higher conductivity and capacities, and shed water more rapidly; at the same time, the city buildings have more vertical surfaces and form what is known as "urban canopy layer" (Grimmond, 2007; Miao *et al.*, 2009). As the material used in cities have higher capacity and lower albedo; they absorb a huge amount of heat during the day through solar radiations which later emit into urban canopy at nights (Rizwan *et al.*, 2008; Miao *et al.*, 2009; Lemonsu *et al.,* 2015; Sun *et al.,* 2018). As a result, the boundary layer's temperature goes higher than nearby rural areas. Also, due to the almost non-existence of vegetation, and a hyper-arid environmental matrix, a higher sensible heat flux is observed, which leads to the reduction of evaporation

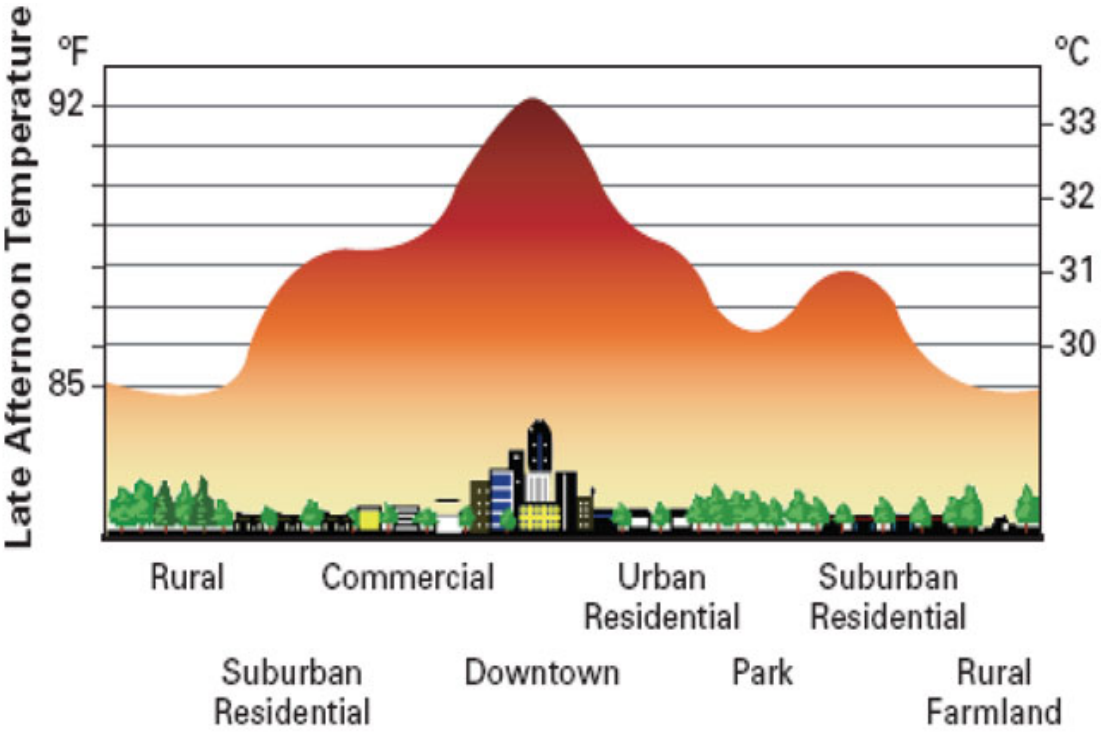

Figure 2.4: The schematic representation of the temperature profile of the urban heat island and its variation with the type of the elements in the urban area.

This figure is adapted from http://www.jandjasphalt.com/concrete-companies-affect-temperature-of-city.

(Grimmond, 2007; Mahmood *et al.,* 2014). Other anthropogenic heat source released from vehicles, air conditioners and other heat sources also contributed to the UHI.

The UHI can have many adverse effects on people and the environment (Kalnay and Cai, 2003; Hamdi *et al.,* 2014), air quality suffers, as sunlight and radiated heat quickly cook car exhaust into smog. Cities are usually experience increased daytime temperatures, reduced nighttime cooling, and higher air pollution levels associated with urban heat islands which can affect human health by contributing to general discomfort, respiratory difficulties, heat cramps and exhaustion, non-fatal heat stroke, and heat-related mortality (Grimmond *et al.*, 2011; Lemonsu *et al.*, 2015; Yang *et al.*, 2017; Cao *et al.,* 2018). It is also known that UHI contributes locally and globally to a higher temperature (Jackson *et al.*, 2010; McCarthy *et al.*, 2010; Oleson *et al.*, 2011; Seto *et al.*, 2012;). For instance, the IPCC report (Stocker *et al.*, 2013) estimates that the contribution of UHI to the global warming trend is less than 10% but notes that there could be regional variations. Paranunzio *et al*. (2019) found that the increase of temperature trends observed in Africa and Asia is strongly correlated with the UHI; i.e., the UHI can explain the observed warming in these regions.

Heat islands can also exacerbate the impact of heat waves (Argüeso *et al.*, 2015; Doan *et al.*, 2016; Zhang *et al.,* 2019) which are a prolonged period of abnormally hot weather. Moreover, the occurrence of heat waves has been growing for the past few decades as stated in Chapter 8 of the Contribution of Working Group 2 to the Fifth Assessment Report of the IPCC (Revi *et al.*, 2014).

2.6.2 The impacts of urbanization on the precipitation

Many studies have attempted to assess a possible relationship between rainfall (patterns and characteristics) and urbanization. Results showed a sensitivity of precipitation to urban expansion conditions. However, urbanization's effects on precipitation remain

considerably uncertain with respect to what degree and how urbanization impacts the precipitation behavior. This is because rainfall changes are dynamic and depend on a number of other factors (multi-decanal natural variability, topography, etc.) (Pielke *et al.*, 2011). Urbanization impacts precipitation by changing the atmosphere's thermal and dynamic conditions in the urban atmosphere environment, which can be attributed to UHI interactions, urban roughness effects, underlying surfaces changes, and aerosols emissions. Thus, positive and negative rainfall response to urban modification has been found. For example, Landsberg (1981); Shepherd *et al.* (2002) and Mote *et al.* (2007), using observations datasets, found that there is an enhancement of precipitation amount over and downwind of cities. Furthermore, these findings have also been confirmed by modeling studies such (Lamptey *et al.*, 2005; Zhang *et al.*, 2009; Niyogi *et al.,* 2017) which have demonstrated that urban effects lead to increased precipitation that was 5-25% higher than background values within cities and in the area 50 to 75 km downwind from cities during the summer period. Feng *et al.* (2015), using the WRF coupled with UCM, found that the summer monsoon is slightly strengthened by large-scale urbanization. Similar results were found by Chen and Zhang (2013), who used the global climate model Community Atmosphere version 4.0 (CAM4.0).

Meanwhile, other studies have demonstrated that urbanization can have a negative influence of rainfall patterns and distribution thereby bringing about reduction in precipitation. For instance, Kaufmann *et al.* (2007), using stations datasets, found a rainfall reduction during the dry season in the urbanized Peral River Delta (PRD) of southern China over the period 1988-1996. Also, Zhang *et al.* (2009), using WRF, found that urban expansion led to a decrease in annual precipitation in the Beijing area during the summer season (by more than 40 mm). Also, Shao *et al.* (2013), using RegCM3 with an urban parameterization added to the land surface scheme, found a weak East Asian

monsoon under urban conditions. This was further established by Ma *et al.* (2016) who used the Community Atmosphere version 5.0 (CAM5.0). They suggested that the reduction of rainfall can be explained by thermal heat effect due to urbanization. Arguably, urbanization leads to the UHI which naturally causes the warming of the land surface leading to the intensifying of the land-sea contrast. These changes can have significant impact on the local circulation and meteorological parameters and their association with precipitation. The reduction of monsoon precipitation amount under urban modification can also be explained by the reduction of surface latent heat flux which leads to a decrease in moisture availability and cloud cover and as consequence the decrease of total rainfall especially in the urbanized region (Feng *et al.*, 2015). In sum, the influence of urbanization on precipitation may depend on the climate regime and geographical locations of cities.

2.6.3 The impacts of urbanization on emissions and air pollution

The way urbanization impacts the air quality through pollution has gained a wide scholarly attention (Rosenzweig *et al.,* 2011; Stone *et al.*, 2012; Revi *et al.*, 2014). Areas with high population are characteristically associated with serious pollution issues (Kumar *et al.*, 2017; Gulia *et al.*, 2018). Consequently, the magnitude of air pollution in urban areas is quite alarming and can have impacts on weather systems, crops, water quality and public health (Balogun *et al.*, 2010; Revi *et al.*, 2014). Again, scholars have examined the relationship between aerosols or pollutants and urban climate. The results revealed that many factors are responsible for the increase in emission and air pollution in urban areas. These include: urban power demand, transportation, industrialization, domestic fuel (Seto *et al.*, 2012; Stone *et al.*, 2012; Rodríguez *et al.,* 2016; Gulia *et al.,* 2018).

Undoubtedly, UHI raises demand for electrical energy particularly in summer. Companies that supply electricity typically rely on fossil fuel power plants to meet much of this demand, which in turn leads to an increase in air pollutant and greenhouse gases emissions. These pollutants are harmful to human health and also contribute to complex air quality problems such as the formation of ground-level ozone, fine particulate matter, and acid rain. Increased use of fossil fuel powered plants also increases emissions of greenhouse gases such as carb dioxide, which contribute to global climate change. Studies showed that urbanization is a major cause of CO_2 emission due to the presence of cars, public transport, and industrialization, which in turn leads to a more intense climate change at regional and global scales (Boucher *et al.*, 2013; Bony *et al.*, 2015). For instance, Doumbia *et al*. (2012) ; Knippertz *et al.* (2015) have demonstrated that cities with higher concentration of pollutants in West Africa correspond to urban areas precisely the coastal cities (Lagos, Dakar, Abidjan). Rodríguez *et al.* (2016) found that cities with larger artificial areas and densely populated cities may experience pollutants higher concentration, particularly, NO_2, PM_{10}, and SO_2 concentrations. Naturally, larger populations are associated with increased vehicle usage and longer vehicular movement thus leading to more tailpipes emissions (McCarty and Kaza, 2015; Martin *et al.*, 2017).

It has been proven that air pollution affects the regional climate and water carbon cycles (Giorgi and Meleux, 2007). Anthropogenic atmospheric pollutants can alter the radiative balance between the atmosphere and earth surface by enhancing the scattering and absorption of solar radiation, which leads to a reduction in solar irradiance and a corresponding drop in temperature near the land surface (Pielke *et al.*, 2002; IPCC, 2008). Also, aerosols act as cloud condensation nuclei and ice nuclei in atmospheric

dynamics and thus affect cloud properties as well as precipitation processes *(*Chen *et al.*, 2011; Mahmood *et al.,* 2014; Knippertz *et al.,* 2015).

2.6.4 Other consequences of urbanization

Urbanization can also have impact on wind speed. Wind is an important indicator of the atmospheric circulation. Changes in wind speed are an indication of the circulation change arising from natural anthropogenic activities. Due to the reduction in wind speed observed during the past decades, a lot of studies have tried to probe the rationale for this change. The studies showed that wind speed reduction can be attributed to urbanization. For instance, wind speed in cities can be 20–30% lower than in adjacent areas (Rosenzweig *et al.*, 2011; Wang *et al.,* 2013). Urban terrains are typically rougher than rural landscapes, and built-up urban canopies strongly increase frictional drag, inducing often remarkable modifications of wind speed at the microscale within the urban canopy layer.

Rural and urban wind flows also differ as a result of vertical thermal gradients and convection. Those phenomena (caused by the UHI, discussed above) induce a convergence of low-level winds over cities, so that air flows into them from all directions.

CHAPTER THREE

METHODOLOGY

As already noted in Chapter Two, studying urbanization interaction with climate is a complex exercise. The review of previous studies showed that numerical modeling is an important tool needed to understand the influence of urbanization on climate change at local and regional levels. It was also observed that a little of these studies did not incorporate an urban scheme in climate models. This doctoral thesis aims to investigate the impact of urban land cover changes on climate in West Africa by using RCM. This chapter covers the modeling tools, the data and the methods required to achieve the specific objectives established in Chapter Two.

3.1 Study Area

The study area covers the West African domain (Figure 3.1). The West African domain exhibits complex terrains especially in the southern and eastern regions. Some localized highlands are also present in West Africa; around Cameroun (Cameroun Mountain), Central Nigeria (Jos Plateau) and Guinea (Guinea Highlands) (Figure 3.1).

The vegetation of West Africa under the uniformly high temperatures in the tropics is determined to a large extent by rainfall. Consequently, vegetation zones run parallel to each other from southwest to northeast and are related to rainfall quantity. It could be: (i) tropical rain forest; (ii) tropical deciduous forest, and (iii) tropical xerophytic woodland.

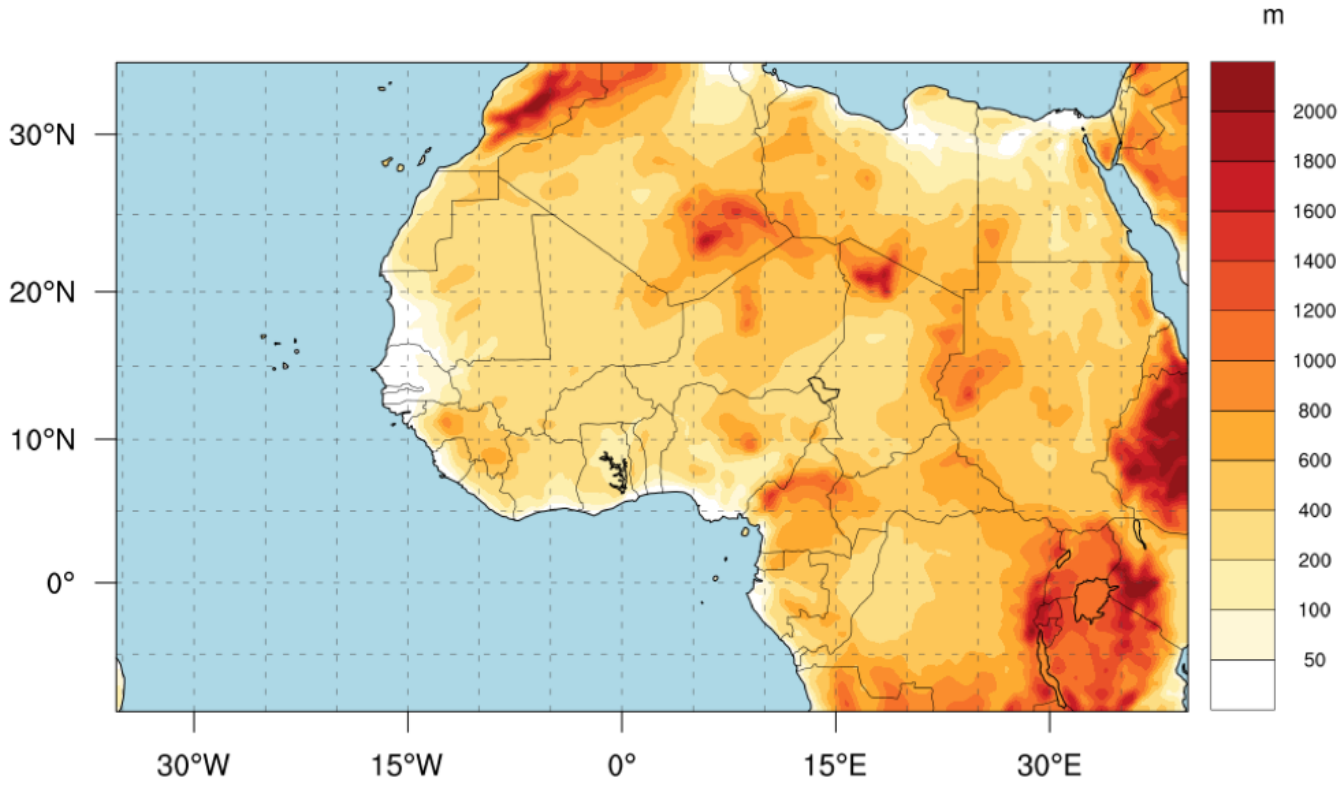

Figure 3.1: Model domain and topography (in meters).

3.2 Data analyses

In this study, many sources of datasets (observations and reanalysis) were used to evaluate the performance of the RegCM4 including the Climatic Research Unit version 4.02 (referred to as CRU TS4. 02) at the University of East Anglia, the University of Delaware (UDEL), the Climate Prediction Center (CPC) of National Oceanic and Atmospheric Administration (NOAA); and reanalysis from ECMWF Reanalysis (ERA5) and the National Centers for Environmental Prediction (NCEP). Multiple observed databases are used to test the model because substantial discrepancies exist among the different observational datasets (Sylla *et al.*, 2013b). It therefore became imperative to use different products to quantify the uncertainties.

3.2.1 Climatic Research Unit (CRU) Dataset

This study utilized monthly datasets, including precipitation and mean temperature from the Climate Research Unit version 4.02 (CRU_TS4.02; just CRU hereafter) to validate RegCM4. CRU dataset produces a global gridded weather dataset that provides monthly estimates on a 0.5 x 0.5 degree latitude/longitude (Harris and Jones, 2017) and is based on the analysis of several homogenized observed parameters from over 4000 weather stations. The 4.02 release of the CRU TS dataset covers the period 1901-2017.

3.2.2 University of Delaware (UDEL) Dataset

We also utilized monthly precipitation and temperature from the University of Delaware dataset version 4.01 (UDEL_v04; just UDEL hereafter). UDEL assimilates historical precipitation observations into 0.5° X 0.5^{o} (Legates and Willmott, 1990). It covers the period 1900-2010.

3.2.3 Climate Prediction Center (CPC) Unified Global Data

The daily global precipitation and temperature of Climate Prediction Center (CPC) dataset was used with a resolution of 0.5º by 0.5º to assess the model performance. CPC products are derived from gauge and gauge-satellite merged analyses of daily precipitation and temperature over both global and regional domains. The data set is derived from a set of quality controlled input gauge and satellite using a robust objective analysis technique (Chen *et al.*, 2008).

3.2.4 National Center for Environmental Prediction (NCEP) reanalysis

The National Center for Environmental Prediction/National Center for Atmospheric Research (NCEP/NCAR) global reanalysis dataset (Kalnay *et al.*, 1996) is an assimilated dataset using a state-of-the-art analysis/forecast system and past data since 1948. The data are provided four times daily at a 6h interval, daily, and monthly values of over 80 climatic variables are available on a 2.5º x 2.5º grid resolution. It has 17 pressures and 28 sigma levels. The NCEP was used to validate the model for the circulation systems.

3.2.5 ERA5

ERA5 is the latest and fifth generation of the global atmospheric reanalysis (Hersbach and Dee, 2016) produced by the European Centre for Medium-Range Weather Forecasts (ECMWF) and it contains a key element of the EU-funded Copernicus Climate Change Service (C3S). ERA5 was carried out to replace the previous atmospheric reanalysis ERA-Interim and covers the period from 1979 onwards. It has important changes relative to the former ERA-Interim including higher spatial and temporal resolutions: from 80 km in the horizontal dimension and 60 levels in the vertical in ERA-Interim to 31 km and 137 levels in ERA5, and from 6-hourly in ERA-Interim to hourly in ERA5

(Hersbach and Dee, 2016; Albergel *et al.*, 2018). ERA5 has the advantage to of being able to use one of the most recent versions of the earth system model and data assimilation methods applied at ECMWF, which make it adaptable to modern parametrizations of earth processes compared to older versions used in ERA-Interim.

3.3 Description of the climate model

3.3.1 Brief introduction to RCM

Urbanization processes affect the climate at local and regional scales. The GCMs resolutions are still too coarse to simulate urban climate. Therefore, high-resolution models are required to assess the impact of this sub-grid process on climate. One technique used to overcome the coarse spatial resolution of coupled GCMs is that of nested modelling. This involves the linking of models of different scales within a global model to provide increasingly detailed analysis of local conditions while using the general analysis of the global output as a driving force for the higher resolution model. RCM operates at much higher resolution (as fine as 50 or 25km) and often, with more detailed topography, land use, local impacts, and physical parameterizations (Giorgi, 2006). The representation is shown in Figure 3.2. It is important to note that the qualities of simulations and predictions of a RCM to reproduce climate depends on the quality of the GCM that drives it (Giorgi, 2006). In addition, the balance between the lateral boundary forcing and internal model dynamics freedom is needed (Giorgi *et al.*, 1993). The development of RCMs helps to obtain more differentiated information about regional climate change and in particular urban climate.

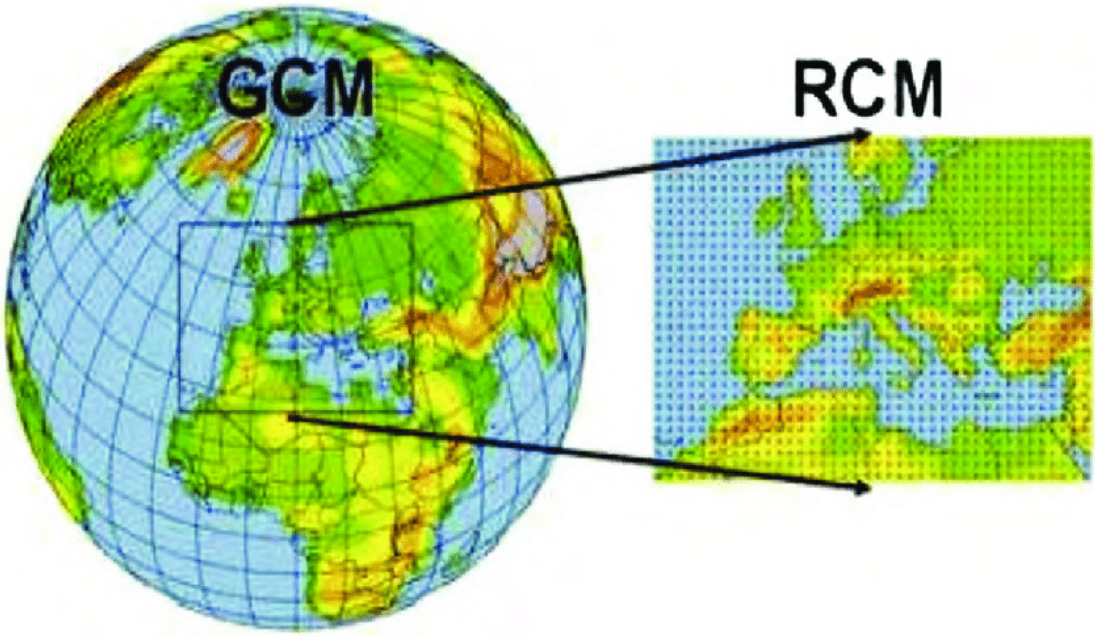

Figure 3.2: Illustration of a nesting approach for RCM that depicts coarse and finer resolutions of GCM and RCM respectively. Source: World Meteorological Organization (WMO:https://www.wmo.int/pages/themes/climate/climate_models.php)

3.3.2 Overview

In this PhD work, the Regional Climate Model version 4 (RegCM4) is used and the specific version used is the recent and upgraded version RegCM4.7.0 (hereafter, referred to as RegCM4). RegCM is originally developed at the National Center for Atmospheric Research (NCAR) (Dickinson *et al.,* 1989; Giorgi and Bates, 1989). It is maintained and distributed by the Earth System Physics (ESP) section of the Abdul Salam International Centre for Theoretical Physics (ICTP). It is the first limited area model developed for long term regional simulation and can be implemented over any region of interest for present and future simulations (Giorgi and Mearns, 1999; Giorgi *et al.,* 2006). It has already been successfully tested over some inter-comparison projects such as CORDEX (Giorgi, 2014).

The RegCM4 model is an improvement on the first version (RegCM1) to the third version (RegCM3) (Pal *et al.,* 2007). The first generation RegCM1 was based on the dynamical component of the Mesoscale Model version 4 (MM4; Anthes *et al.*, 1987) and the radiative transfer Community Climate Model version 1 (CCM1; Kiehl *et al.,* 1987). It is a compressible, finite difference model with hydrostatic balance and vertical σ-sigma coordinates (Dickinson *et al.*, 1989; Giorgi and Bates, 1989). In 1989, series of upgrade was done to the RegCM1 to make the model able to perform long term regional simulations. This led to the development of the second generation (RegCM2; Giorgi *et al.,* 1993), which includes major modifications and addiction of some physical packages such as the Mesoscale Model version 5 (MM5; Grell *et al.*, 1994), the radiation transfer scheme, known as the Community Climate Model version 2 (CCM2; Briegleb, 1992), the surface scheme with the upgraded Biosphere-Atmosphere Transfer Scheme 1 (BATS1) (Dickinson *et al.,* 1993), the non-local planetary boundary layer (PBL) parametrization of Holtslag *et al.* (1990), and a second convective scheme (Grell, 1993).

Next major revisions and modifications led to RegCM3 which reflects major improvement of the physics schemes, surface physics, atmospheric chemistry and aerosols, model input fields and user interface (Pal *et al.,* 2007). In 2012, the fourth generation of the ICTP's regional climate model (RegCM4; Giorgi *et al.,* 2012) was introduced. Many aspects of the model formulation and implementation are identical to the RegCM3, although there are several important changes that have been incorporated into the physical and dynamical packages. This new version: (i) incorporates several recent scientific advances in the understanding and representation of land surface processes, (ii) introduces new convective schemes, and (iii) improves physics schemes.

3.3.3 Description of RegCM4

Like every climate model, RegCM4 model uses physical laws described in terms of mathematical equations to represent the climate as well as the components of the climate system (representing model dynamics). However, some physical processes cannot be resolved by the coarse grid box of the model and must be approximated by what is called parametrizations (representing the model physics).

3.3.3.1 Model dynamics

The model dynamics are the processes that can be characterized by the grid-scale mean quantities. In RegCM4, the dynamical component originated from that of the MM5 (Grell *et al.,* 1994) which is a hydrostatic, compressible, sigma-p vertical coordinate. The model equations are solved on a staggered Arakawa B-grid meaning that the velocity components (u, v) are calculated at the grid center and the masses are evaluated at the grid corners. The model solves a set of equations for mass, momentum and scalar quantities, described as follows:

Horizontal Momentum Equation

$$\frac{\partial p^* u}{\partial t} = -m^2 \left(\frac{\partial p^* u\, u/m}{\partial x} + \frac{\partial p^* v\, u/m}{\partial y} \right) - \frac{\partial p^* u \dot{\sigma}}{\partial \sigma} - m p^* \left[\frac{R T_v}{(p^* + p_t/\sigma} \frac{\partial p^*}{\partial x} + \frac{\partial \phi}{\partial x} \right] + f p^* v + F_H u + F_v u \quad (3.1)$$

$$\frac{\partial p^* v}{\partial t} = -m^2 \left(\frac{\partial p^* v\, u/m}{\partial x} + \frac{\partial p^* v\, v/m}{\partial y} \right) - \frac{\partial p^* v \dot{\sigma}}{\partial \sigma} - m p^* \left[\frac{R T_v}{(p^* + p_t/\sigma} \frac{\partial p^*}{\partial y} + \frac{\partial \phi}{\partial y} \right] - f p^* u + F_H \mathrm{v} + F_v \mathrm{v} \quad (3.2)$$

where u and v are the eastward and northward components of velocity, T_V is virtual temperature, ϕ is the geopotential height, f is the Coriolis parameter, R is the gas constant for dry air, m is the map scale factor for either the Polar Stereographic, Lambert Conformal, or Mercator map projections, $\dot{\sigma} = \frac{d\sigma}{dt}$ and F_H and F_V represent the effects of horizontal and vertical diffusion and $p^* = p_s - p_t$00lp

Continuity and Sigmadot ($\dot{\sigma}$) Equations

$$\frac{\partial p^*}{\partial t} = -m^2 \left(\frac{\partial p^*\, u/m}{\partial x} + \frac{\partial p^*\, v/m}{\partial y} \right) - \frac{\partial p^*\, \dot{\sigma}}{\partial \sigma} \quad (3.3)$$

The vertical integral of Equation 3.3 is used to compute the temporal variation model,

$$\frac{\partial p^*}{\partial t} = -m^2 \int_0^1 \left(\frac{\partial p^*\ u/m}{\partial x} + \frac{\partial p^*\ v/m}{\partial y} \right) d\sigma \quad (3.4)$$

After calculating the surface-pressure tendency $\frac{dp^*}{dt}$, the vertical velocity is computed at each level of the model from the vertical integral of Equation 3.3.

$$\dot{\sigma} = -\frac{1}{p^*} \int_o^\sigma \left[\frac{\partial p^*}{\partial t} + m^2 \left(\frac{\partial p^*\, u/m}{\partial x} + \frac{\partial p^*\, v/m}{\partial y} \right) \right] d\acute{\sigma} \quad (3.5)$$

Where $\acute{\sigma}$ is a dummy variable of integration and $\dot{\sigma}(\sigma = 0) = 0$.

Thermodynamic (or Omega) Equation

The thermodynamic equation is represented by:

$$\frac{\partial p^* T}{\partial t} = -m^2 \left(\frac{\partial p^* u\, T/m}{\partial x} + \frac{\partial p^* v\, T/m}{\partial y} \right) - \frac{\partial p^* T \dot{\sigma}}{\partial \sigma} + \frac{R T_v \omega}{c_{pm}(\sigma + P_t/p_{ast})} + \frac{p^* Q}{C_{pm}} + F_H \mathrm{T} + F_V \mathrm{T} \quad (3.6)$$

Where C_{pm} represents the specific heat for moist air at constant pressure, Q is the diabatic heating, F_HT represents the effect of horizontal diffusion, F_VT is the effect of vertical mixing and dry convective adjustment, and ω is

$$\omega = p^* \dot{\sigma} + \sigma \frac{dp^*}{dt} \quad (3.7)$$

Where $\frac{dp^*}{dt} = \frac{\partial p^*}{\partial t} + m\left(u \frac{\partial p^*}{\partial x} + v \frac{\partial p^*}{\partial y}\right)$

The expression for $C_{pm} = C_p(1 + 0.8q_v)$, where C_p is the specific heat at constant pressure for dry air and q_v is the mixing ratio of water vapor.

Hydrostatic Equation

The hydrostatic equation is used to compute the geopotential heights from the virtual temperature $\mathrm{T_V}$.

$$\frac{\partial \phi}{\partial\, ln(\sigma + p_t/p*)\, \sigma} = -RT_v \left[1 + \frac{q_c + q_r}{1 + q_v}\right] \quad (3.8)$$

Where $T_v = T(1 + 0.608q_v)$, q_v, q_c and q_r represent vapor, cloud water and ice, rain water or snow as well as mixing ratios.

3.3.3.2 Model physics

After the dynamics are completed, the model goes to the model physics which represents phenomena that cannot be properly resolved with physical parameterizations routines. In RegCM4, the model physics correspond to the cloud processes, the absorption and radiating properties of the atmosphere and clouds, and atmospheric interactions with vegetation and other surface features. A brief description of certain schemes that are important in RegCM4 is given below:

3.3.3.3 Radiation transfer scheme

In the RegCM4, the radiation transfer scheme is from the NCAR Community Climate Model 3 (CCC3), which is well described by (Kiehl *et al.*, 1996). This includes calculations for the short-wave and infrared parts of the spectrum, including both atmospheric gases and aerosols. It is parameterized with a δ-Eddington approximation to calculate the solar absorption (Briegleb, 1992) and includes contributions from all main greenhouses gases e.g. H_2O, CO_2, O_3, CH_4, N_2O, and CFCs (Giorgi *et al.*, 2012). Optical properties of clouds determining scattering and absorption of radiation are expressed in terms of cloud water content and an effective droplet radius. When cumulus clouds are formed, the gridpoint fractional cloud cover is such that the total cover for the column extending from the model-computed cloud-base level to the cloud-top level (calculated assuming random overlap) is a function of horizontal gridpoint spacing. The thickness of the cloud layer is assumed to be equal to that of the model layer, and different cloud water content is specified for middle and low clouds.

3.3.3.4 Cumulus Convective Schemes (CCS)

It is perceived that convection is very difficult to model accurately due to its large-scale processes and moist-convective processes (specified grid scale), necessitating the need for parameterization of convection in climate models. The Cumulus Convective

Schemes (CCS) are intended to represent vertical fluxes due to unresolved updrafts and downdrafts and compensating motion outside the clouds. There are several CCS available in RegCM4, which are (i) Grell scheme (Grell *et al.*, 1994), (ii) the Massachusetts Institute of Technology (MIT) Emanuel scheme (Emanuel, 1991; Emanuel and Rothman, 1999), (iii) Tiedtke scheme (Tiedtke, 1989), (iv) Kain and Fritsch scheme (Kain and Fritsch, 1993) and the (v) Modified Kuo scheme (Anthes, 1977). One of the major improvement in the RegCM4 compared to previous versions of RegCM is the possibility to combine the different CCS over land and ocean, a configuration which is referred as to "mixed convection" (Giorgi *et al.,* 2012) instead of using the same CCS over the whole domain.

The Kian-Fritsch scheme is developed based on the assumptions of Fritsch-Chappell scheme (Kain and Fritsch, 1990). It is a mass flux convective scheme model which incorporates the effects of entrainment and detrainment as well as downdrafts associated with evaporation of rain on the convection and large-scale environment. It has both deep and shallow convections and uses a convective available potential energy (CAPE) which reduces the timescale closure. It uses the Lagrangian parcel method, including vertical momentum dynamics, to estimate whether instability exists, or whether any instability will become available for cloud growth and what the properties of any convection encountered by the cloud might be.

The MIT-Emanuel scheme is another convective adjustment scheme proposed by Emanuel (1991), in which the convection is calculated when the level of the neutral buoyancy is greater than the cloud base level. Between these two levels, the air is lifted and the condensed moisture is apportioned between cloud and precipitation. Cloud mixing is considered to be episodic and inhomogeneous, and convective fluxes are

based on a model of sub-cloud-scale updrafts and downdrafts. Precipitation is based on the auto-conversion of cloud water into rain water and accounts for simplified ice processes. Another CCS option is the Grell scheme (Grell, 1993), which assumes that the convective cloud stabilizes the environment. It is based on the Arakawa-Schubert parametrization (AS74, Arakawa and Schubert, 1974) using a mass flux cloud model that considers the cloud as a two steady state circulation having an updraft and downdraft. The mixing between clouds and the adjacent air (entrainment and detrainment) only occurs at the top and bottom of the cloud. The heating and moistening profiles are derived from the latent heat released or absorbed. This is further linked with the updraft-downdraft fluxes and compensating motion. This scheme is triggered when a parcel lifted in the updraft eventually reaches the moist convection level. Two different closures can be adopted: an Arakawa-Schubert type closure in which all buoyant energy is immediately released at the same time and a Fritsch-Chappell type closure in which the available buoyant energy is released with a time scale typically within 30 minutes.

The Modified Kuo scheme is relatively simple and is based on the approach proposed by Kuo (1974), in which convective activity is determined by the convective instability and moisture convergence in the vertical column. Part of this moisture convergence precipitates and the rest is used to moisten the atmosphere. In the vertical, a parabolic profile is used to distribute the latent heat of condensation, so that the maximum heating is located in the upper half of the cloud (Anthes, 1977).

Another improvement in the RegCM4 is the introduction of Tiedtke CCS, which is a mass flux convection scheme using a 1-D bulk model with entrainment and detrainment and the moisture convergence closure (Tiedtke, 1989).

In order to find the "best" convection scheme for this version of RegCM4 for the West African region, a series of preliminary experiments have been conducted using different convection schemes. Results show that the mixed convection configuration (Emanuel over land and Kain-Fritsch over ocean) is the "best" in terms of reproducing the main climatic parameters (rainfall and temperature) in West Africa for this version of RegCM4.

3.3.3.5 Large scale precipitation scheme

In the RegCM4, the resolved-scale cloud microphysics is treated by the Subgrid Explicit Moisture Scheme (SUBEX; Pal *et al*., 2000), which calculates fractional cloud cover as a function of grid point average relative humidity and includes only one prognostic equation for cloud water. Rain is calculated diagnostically and it forms when the in-cloud liquid water exceeds a temperature-dependent threshold (auto conversion). Rain is assumed to fall instantaneously within the model's time step and it grows by accretion of cloud droplets.

3.3.3.6 Land surface parameterization

The Land Surface Models (LSMs) are used to describe the complex interactions (including biophysical, hydrological, and biogeochemical interactions) between land surface and atmosphere at micro- and mesoscales. In addition, it provides relevant information on the land surface and climate data. Numerical parameterization of land surface provides a simple and realistic method of showing the transfer of mass, energy, and momentum between the land surface and atmosphere. Two LSMs are available in RegCM4: the Biosphere-Atmosphere Transfer (BATS; Dickinson *et al.*, 1993) and the Community Land Surface Model version 4.5 (CLM4.5; Oleson *et al.,* 2013).

3.3.3.7 Structure of the Biosphere Atmosphere Transfer Scheme (BATS)

The BATS has been used for many years as a default LSM in early versions of RegCM (versions 1, 2 and 3). This scheme is a surface package designed to describe the role of vegetation and interactive soil moisture in calculating the exchanges of momentum, energy and water vapor associated with surface-atmosphere interactions (Dickinson *et al.,*1993). It includes a vegetation layer, a snow layer, three soil layers, a simple surface runoff parametrization, and 20 vegetation types with 12 soil color and soil texture types. For each vegetation type, there are 27 derived parameters which represent the morphological, physical and physiological properties of vegetation and soil.

The prognostic equations are solved for the soil layer temperatures using a generalization of the force restore method (Dickinson *et al.*, 1993). The temperature of the canopy and canopy foliage is calculated diagnostically via an energy balance formulation including sensible, radiative and latent heat fluxes. The soil hydrology calculations include predictive equations for the water content of the soil layers. The soil water movement formulation is obtained from a high-resolution soil model Dic (1984) and the surface runoff rates are expressed as functions of the precipitation rates and the degree of soil water saturation.

In the much upgraded RegCM4, two new land use types were added to BATS to represent urban and suburban environments. Urban development not only modifies the surface albedo and alters the surface energy balance, but also creates impervious surfaces with large effects on runoff and evapotranspiration.

3.3.3.8 Structure of the Community Land Model version 4.5 (CLM4.5)

The major improvement with respect to the representation the land surface characteristics in RegCM4 is the inclusion of the Community Land Model (CLM). For this study, we have used the version 4.5 of CLM referred to as CLM4.5 (Oleson *et al.,* 2013). The CLM4.5 is a LSM which was developed by the National Center of Atmospheric Research (NCAR) as part of the Community Climate System Model (CCSM). The CLM4.5 gives a more detailed description of land surface processes compared to BATS. It includes different aspects of the land surfaces bio-geophysics, hydrology, biogeochemistry, and ecological dynamics (Figure 3.3). It contains one vegetation layer with a canopy photosynthesis conductance model, 10 unevenly space soil layers, 5 snow layers with an additional representation of trace snow and 22 vegetation types. Table 3.1 summarized vegetation classes and land cover considered in the CLM4.5 scheme.

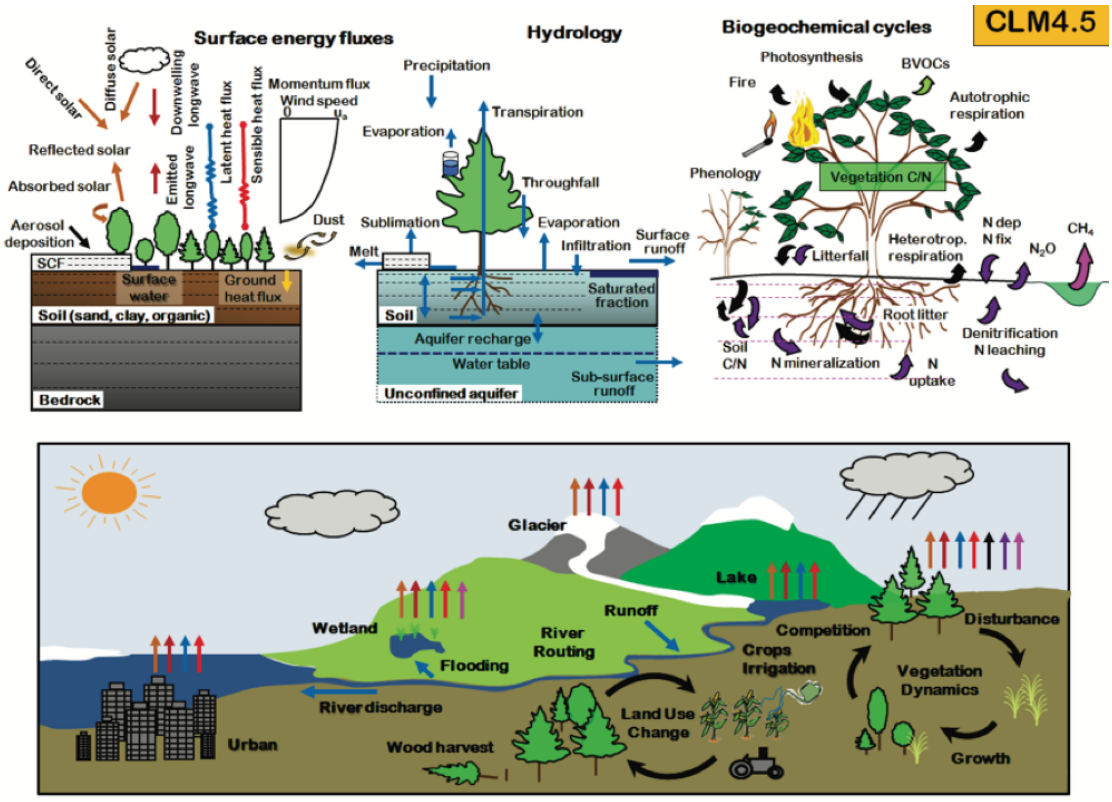

Figure 3.3: Land biogeophysical, biogeochemical, and landscape processes simulated by CLM4.5 [adapted from Oleson *et al.* (2013)].

Table 3.1: Vegetation classes and land cover in CLM4.5

Code	Vegetation classes and land cover
1	Crop/mixed farming
2	Short grass
3	Evergreen needle leaf tree
4	Deciduous needle leaf tree
5	Deciduous broad leaf tree
6	Evergreen broad leaf tree
7	Tall grass
8	Desert
9	Tundra
10	Irrigated Crop
11	Semi desert
12	Ice cap/glacier
13	Bog or marsh
14	Inland water
15	Ocean
16	Evergreen shrub
17	Deciduous shrub
18	Mixed Woodland
19	Forest/Field mosaic
20	Water Land mixture
21	Urban
22	Sub Urban

The CLM4.5 model, as shown in Figure 3.4, presents the land surface characteristics as a nested subgrid hierarchy in which the grid cells are composed of multiple landunits, snow/soil columns, and Plants Functionals Types (PFTs) (Oleson *et al.,* 2010c). Each grid cell can have a different number of landunits, each landunit can have a number of columns, and each column can have multiple PFTs. At the first subgrid level: wetlands, glaciers, vegetation, water and urban, and columns, and at the second subgrid level especially for urban areas: roof, sunlit and shaded walls, pervious and impervious canyon floor. For example, an urban parameterization (CLMU) that is to represent the difference between urban and rural areas has been incorporated into the model since the introduction of CLM4.0 (Oleson *et al.*, 2010). A third subgrid level includes the representation of up to 24 PFTs. A more detailed history and description of the model is provided by Oleson *et al.* (2013).

In this study, the CLM4.5 has been selected because previous studies have shown that CLM4.5 as LSM not only gives a good representation of the West African climate but it also includes an urban canyon model needed to contrast rural and urban energy balance and climate. This is known as the Community Land Model Urban (CLMU. This model has been teste and it has demonstrated its ability to help quantify the urban climate interactions (Oleson *et al.*, 2008a; 2008b; Jackson *et al.,* 2010).

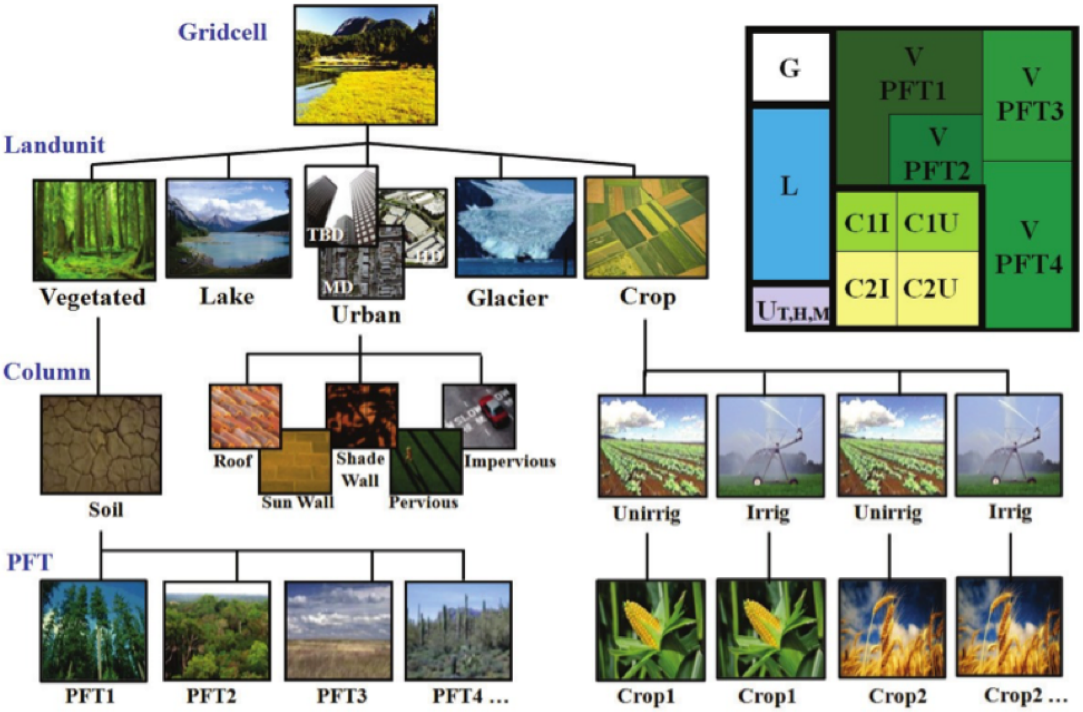

Figure 3.4: Configuration of the CLM4.5 subrid hierarchy [adapted from Oleson *et al.* (2013)]. The urban component is broken into five facets to calculate the exchange of energy between the surfaces and the urban canyon. Note that the Crop land unit is only used when the model is run with the crop model active. Abbreviations: TBD=Tall Building District; HD=High Density; MD=Medium Density, G =Glacier, L=Lake, U=Urban, C=Crop, V=Vegetated, PFT=Plant Functional Type, I= Irrigated, U=Unirrigated.

Description of the Community Land Model Urban

An urban area is probably one of the most complex existing surfaces. A complete reproduction of all the heterogeneity of a "real" city would be too complex and hardly realizable in most cases due to the lack of detailed data. A simplification of the city is therefore needed. During the last few years, several efforts have been made to improve the representation of urban surface characteristics in mesoscales models (Martilli *et al.*, 2002; Grimmond, 2007; Oleson *et al.*, 2008a)

In the CLM4.5, the urban areas are represented by an urban canopy scheme called the Community Land Model Urban (CLMU; Oleson *et al.*, 2008a). The CLMU is represented by up to three urban landunits per gridcell according to density class (Oleson *et al.*, 2013). The CLMU is based on the urban canopy approach of Oke (1987) in which the canyon geometry is described by street width (W) bordered by two facing buildings height (H) as shown in Figure 3.5. The canyon system consists of roofs, walls, and canyon floor. Walls are further divided into shaded and sunlit components. The canyon floor is divided into pervious which includes residential lawns and parks and impervious which includes roads, parking lots and sidewalks fractions. Vegetation is not explicitly modelled for the pervious fraction. Instead evaporation is parameterized by a simplified bulk scheme.

Each of the five urban surfaces is treated as a column within the landunit. Radiation parameterizations account for trapping of solar and longwave radiation inside the canyon. Momentum fluxes are determined for the urban landunit using a roughness length and displacement height appropriate for the urban canyon and stability formulations from CLM (Oleson *et al.*, 2013 for more description). The urban model produces turbulent, momentum and radiative fluxes which are areas averaged with fluxes from non-urban

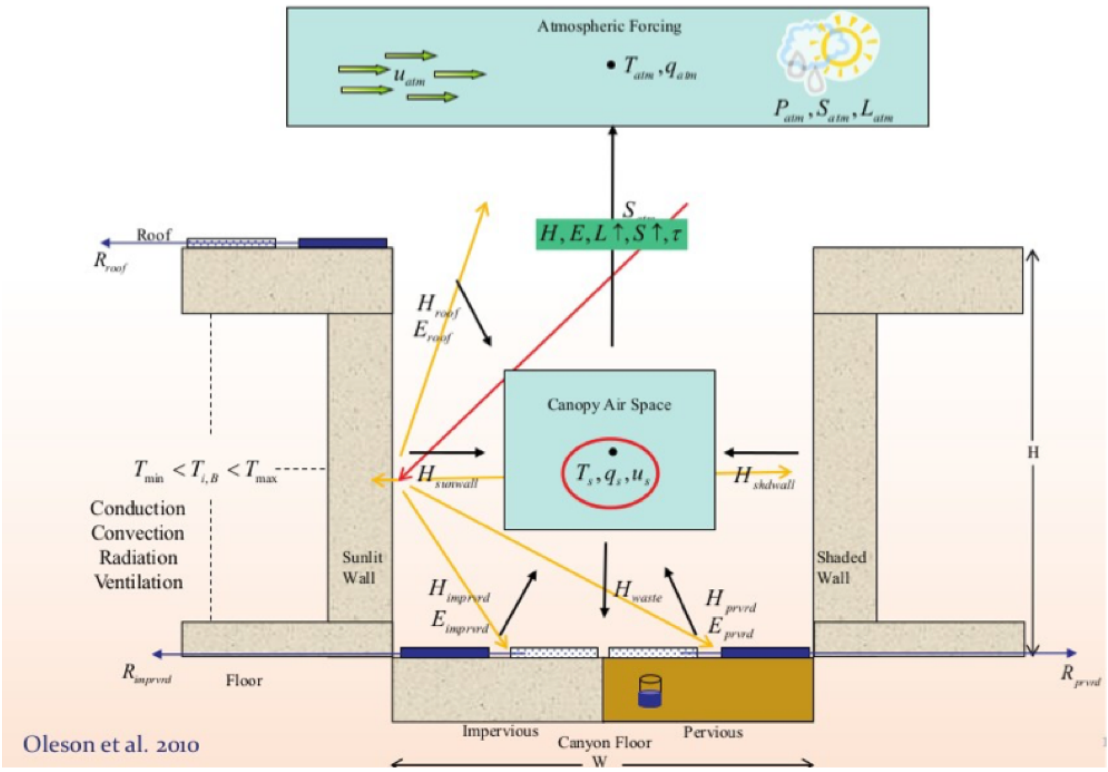

Figure 3.5: Schematic representation of urban and atmospheric model coupling. [adapted from Oleson *et al*. (2013)]. The urban model is forced by the atmospheric model wind (u_{atm}), temperature (T_{atm}), specific humidity (q_{atm}), precipitation (P_{atm}), solar ($S_{atm}\downarrow$) and long-wave ($L_{atm}\downarrow$) radiation at reference height z_{atm}. Fluxes from the urban landunit to the atmosphere: turbulent sensible (H), latent heat (λE), momentum (τ), albedo (I$\uparrow$), emitted longwave (L$\uparrow$), absorbed shortwave ($\vec{S}$), adiation. Air temperature (Tac), specific humidity (q_{ac}) and wind speed (u_c), within the urban canopy layer are diagnosed by the urban model. H is the average building height.

surfaces (e.g. vegetation and lakes) to supply grid cells averaged fluxes to the atmospheric model.

Urban areas are prescribed from a dataset of present day global urban extent and urban properties. Jackson *et al.* (2010) identified 132 regional categories. The globe is divided into 33 regions with similarities in urban characteristics, and each category is subdivided into 4 subcategories representing the different urban classes [tall building district (TBD), and high, medium, and low density (HD, MD, LD)]. This dataset was derived from LandScan 2004, a population density dataset derived from census data, nighttime lights satellite observations, road proximity, and slope (Dobson *et al.*, 2000). The urban morphology includes average building heights (H), urban canyon height-to-width ratios (H:W), and fraction of pervious surface (*e.g.* vegetation), roof area, and impervious surfaces (e.g. roads and sidewalks). Urban morphology also includes fraction of pervious (e.g. vegetation), roof area, and impervious area (e.g. roads and sidewalks). Imagery from Google Earth for each regional category's validation cities provided the primary tool for estimating these fractions. In essence, the spatial extent dataset was used to identify a cluster of pixels within a validation city for the desired urban category (i.e. TBD, HD, MD, LD). For the current implementation, the LD class is not used because it is highly rural and better modelled as a vegetated/soil surface. Although the TBD, HD, and MD classes are represented as individual urban land units, urban model history output is currently a weighted average of the output for individual classes. For each category, (TBD, HD, MD, LD), average building heights (H), urban canyon height to width ratios (H:W), and fractions of pervious surface (e.g., vegetation), roof area and impervious surfaces (e.g., roads and sidewalks), are defined, among other parameters. The urban land unit within the CLM4.5 is represented as a fraction in percentages of

three. A global database of tallest buildings by cities was used for TBDs within each region (Emporis Corporation 2007). Where available, the 25 tallest buildings were averaged for five cities within a region, then the average building heights of these cities were calculated to determine an average regional tall building value. This average was then decreased proportionately to account for the remaining buildings in the TBD resulting in an average TBD building height representative of each regional category. In regions with no TBD (e.g. Greenland), or those with few cities with a TBD (e.g. West Africa), the maximum number of buildings in the buildings database was used in the calculation. For the HD category, Emporis Corporation (2007) data were used where available and were supplemented by imagery of verification cities. By studying imagery of city skylines, building heights could be estimated by comparing TBD heights to HD buildings. To further aid the estimation process, the number of stories of HD buildings was counted in order to approximate heights. For the remaining categories of MD and LD, building heights were determined based primarily on dominant housing types. For instance, a typical two-story frame home in the U.S. is approximately eight meters tall. The intra-urban categories (TBD, HD, MD, and LD) must be adaptable to any location. For example, LD encompasses suburbs in the United States and urban-agriculture in East Africa, and similar differences exist for the other urban classes.

For each of the 33 distinct regions across the globe, thermal (e.g., heat capacity and thermal conductivity), radiative (e.g. albedo and emissivity) and morphological (e.g. height to width ratio, roof fraction, average building height, and previous fraction of the canyon floor) properties are provided for each of the density classes. Building interior minimum and maximum temperatures are prescribed based on climate and socioeconomic considerations.

The urban extent data for TBD, HD, and MD classes are aggregated from the original 1 km resolution. The 1 km resolution dataset is in geographical grid format. For use in the CCSM, data are also aggregated to a half degree grid (i.e. the 0.05 degree resolution data is summed by class to 0.5 degree aggregates), and, based on historical population, estimates and histories of urbanization by region, we have extrapolated urban extent back to 1750.

The CLMU is, thus, designed to be able to predict the degree and characteristic of each city's urban metabolism as well as their cities and own unique heat islands, thermal canopy layers, and climates. CLMU can accommodate only one urban class, and only one set of representative thermal and radiative properties within the TBD, HD, and MD categories can be used. The class selected is based on which is most abundant in a GCM grid cell, and the values are comprised of weighted averages of the three typical wall and roof types within that class. Studies (Oleson *et al*., 2010b; Fischer *et al*., 2012) indicated that the CLM4 with CLMU included provides a useful tool for the studying of climate effects of urbanization. Note that the CLM4.5 can be run with or without an active CLMU.

3.4 Description of the Initial Conditions and Boundary Conditions (ICBC)

In this study, all simulations have been forced with a GCM called the Max-Planck Institute Earth System Model for medium Resolution version (MPI-ESM-MR; Giorgetta *et al.*, 2013). The MPI-ESM-MR, with horizontal resolution ~1.9^{o} x 1.9^{o}, is the latest version of the coupled model of the Max Planck Institute for Meteorology, specifically developed for the CMIP5 exercise which provided the basis for the IPCC AR5. It is a fully coupled atmospheric (Stevens *et al.*, 2013) and ocean (Jungclaus *et*

al., 2013) components and also includes a subsystem models for land, vegetation (Reick *et al.,* 2013; Schneck *et al.,* 2013) and marine biogeochemistry (Ilyina *et al.,* 2013).

The atmospheric component; that is the sixth generation of the atmospheric general circulation model of the European Centre Hamburg Model (ECHAM6) is a hydrostatic and dynamical core which describes the relevant atmospheric processes and variables. The ECHMA6's dynamical part is formulated in spherical harmonics. Thus, atmospheric circulation (vorticity and divergence) temperature, pressure and humidity are solved in a spectral grid. Radiation, clouds, convection and precipitation are solved in a regular Gaussian grid.

This dataset were chosen because previous studies have shown that it is one of the best of the Coupled Model Intercomparison Project Phase 5 (CMIP5) GCMs in terms of giving a good representation of the African (Elguindi *et al.,* 2014) and in particular West African (Gbobaniyi *et al.*, 2014; Sylla *et al.*, 2015) climates with some biases at the regional scale (any bias corrections have not been applied).

3.5 Numerical experiments

The RegCM4 is used to carry out a set of experiments to achieve the aim of this study. In this section, the different experiments design and the change in land surface state are described.

3.5.1 RegCM4 configuration and simulations experiments description

All simulations performed within this study were run on 198x326 gridpoints at a horizontal resolution of 25 km and 23 vertical sigma levels. The model domain covers the West African region (Figure 3.1). A large domain was chosen, on the one hand, to

cover the entire West Africa region, and on the other hand, to capture the main processes that govern the WAM system and also to avoid boundary issues.

All the simulations are forced by the outputs from MPI-ESM-MR (Giorgetta *et al.*, 2013). The RegCM4 configuration and the physics schemes used in this work are provided in Table 3.2.

Table 3.2: RegCM4 configuration and simulation setup.

Contents	**Description**
Model dynamic	Hydrostatic, compressible, σ-p vertical coordinates
Horizontal grid	25 km
Vertical levels	23 sigma levels
Number of points	198x326
Map projection	Mercator
Cumulus scheme	Emanuel over land Kain-Fritsch over ocean
Radiative scheme	NCAR/CCM3
Resolved-scale precipitation	SUBEX
Ocean flux	Zeng *et al.* (1998)
Land surface model	CLM4.5
Urban surface model	CLMU
ICBC	MPI-ESM-MR

3.5.2 Implementation of "idealized" urban land scenarios in the RegCM4-CLM4.5

Conducting researches on urbanization studies will deepen understanding of the physical processes by which urban land cover change affects the regional climate especially in West African climate. In order to clarify the potential effect of urbanization on WASMC, a parametrization for urban surfaces has been incorporated into CLM4.5. In this thesis, we propose two "idealized" urban expansion scenarios to quantify model sensitivity to land cover change and its impacts on West African climate. As mentioned in Chapter Two, most of the megacities in West Africa are located along the coastal band. Hence, these projected "idealized" urban expansion over the coastal region is based on the urban projection from Jackson *et al.* (2010), Seto *et al.* (2012), and the urban class available in CLM4.5. In this work, it is assumed that all the coastal Megacities have the same degree of urbanization.

The urban land surface is parameterized inside the CLM4.5 as follows:

- the first scenario is based on the probabilities of 100% of HD;
- the second one is fixed at 70% for HD, 20% for MD and 10% for TBD.

The first scenario, mostly common in current West African coastal megacities, which are characterized by an important rate of urbanization and the presence of high-rise buildings.

This second scenario (future cities), quite typical of future developed West African, where megacities are projected to have a majority of storey buildings, some smaller, some higher and few very tall ones. Here, vegetated land cover categories is proportionally replaced by urban area along the West African coastal zone (Figure 3.6b).

Some of these cities are Lagos (Nigeria), Abidjan (Côte d'Ivoire), Accra (Ghana) and Dakar (Senegal).

Only grid cells in coastal band are modified for future urbanization, while other grid cells were kept the same current as land cover conditions (Figure 3.6a).

3.5.3 Details of experiments

In West Africa, most urban areas are concentrated along the coastal band. Urban areas have a central role to play in the changing climate. It is, therefore, important to assess the consequences of rapid urbanization on West African climate at the local and regional scales. The objective of this study is to evaluate the potential influence of urbanization on the West African climate. To fulfill this objective, four simulations with the RegCM4-CLM4.5 are performed, in two categories; without urban expansion.

The first experiment represents the present-day climate while the remaining three represent the future climate experiments which differed only in the vegetation cover composition along the West African coastal band.

The first experiment, referred to as is present control simulation (hereafter referred to as CTRL_PRS), corresponds to the present-day climate, and covers the period 1984-2005. In the CTRL_PRS experiment, the default land cover available in CLM 4.5 was used as shown in Figure 3.6a.

The second experiment also called future control simulation (hereafter referred to as CTRL_FTR), is also made without any change in land cover (Figure. 3.6a) under the far future climate, covering the period 2079-2100. It represents the effect of climate change alone with current land cover conditions. This means that in this simulation, the effect of greenhouse gas concentration only as contained in the Representative Concentration Pathway 8.5 (RCP8.5; Moss *et al.*, 2010) scenario was taken into account. In the

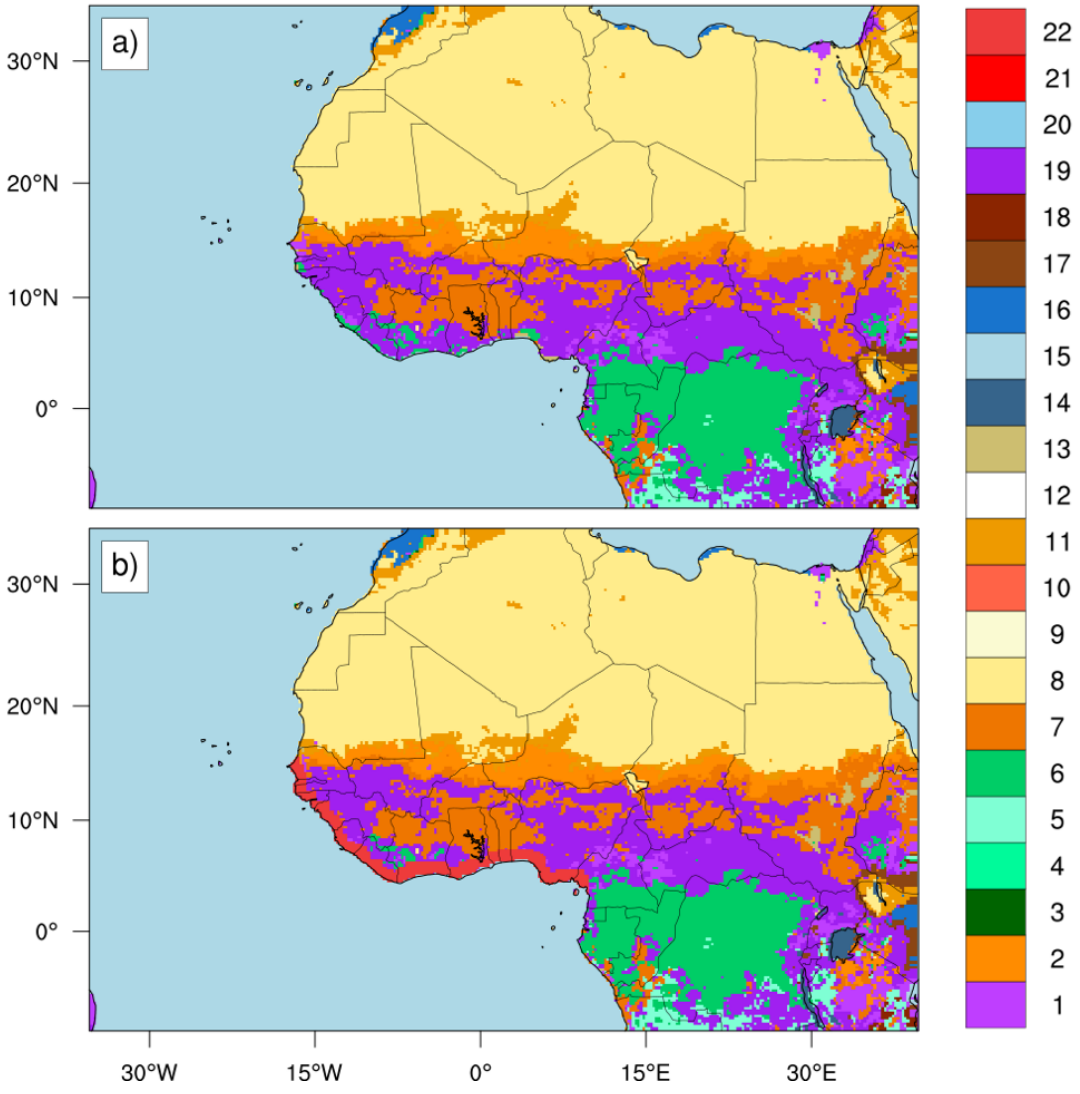

Figure 3.1: Vegetation cover in CLM4.5: a) default vegetation cover, b) modified vegetation land cover: an urban expansion, represented in red color, was added along the coastal band from Dakar (Senegal) to Douala (Cameroon). The meaning of each code is defined in Table 3.1.

CTRL_PRS and CTRL_FTR simulations, the urban fractions of the entire model grid were held to zero during the entire simulation period.

The two remaining experiments represent the sensitivity simulations. The urban conditions (change mentioned above) taken into account in the experiments. They are represented an idealized urbanization experiment in which different states of urbanization in the future climate conditions were added along the coastal band from Dakar (Senegal) to Douala (Cameroon) (Figure. 3.6.b). The first sensitivity experiment; URBAN1, represents the future effect of climate change (under the RCP8.5) plus the "idealized" urban expansion change. It covers the same period like the CTRL_FTR simulation. In this experiment, the first scenario is considered (i.e. 100% of HD).

The second sensitivity experiment, denoted as URBAN2, and represented by 70% of HD, 20% of MD and 10% of TBD, is incorporated into CLM4.5. Both of these sensitivity experiments are performed in order to compare the urban effect under different urban intensification conditions. The summary of the simulations performed is provided in Table 3.3.

Note that all simulations are exposed the same physical conditions and are kept at the same initial conditions and boundary conditions (ICBC) for future simulations. Also, the increase in aerosol concentration due to urban air pollution and its effects on cloud and WAM are not treated. So, potential variables' changes are caused by the combined effect of urban warming and the modification on the land surface properties. The first two years of all simulations are discarded as model spin-up time to establish equilibrium with the initial climate. This means that the remaining 20 years (1986-2005) for present climate and (2081-2100) for future climate are used for the analyses.

Table 3.3: Details of different simulations

Experiment name	Brief description	Urban scheme	Simulation Period (RCPs)
CTRL_PRS	Historical climate simulation	default	1984-2005 (Historical)
CTRL_FTR	Future climate simulation	default	2079-2100 (RCP8.5)
URBAN1	A similar experiment as CTRL_FTR with activation of the urban scheme along the coastal band	100% of HD	2079-2100 (RCP8.5)
URBAN2	A similar experiment as URBAN1 with different urban categories	70 % of HD 20% of MD 10% of TBD	2079-2100 (RCP8.5)

3.6 Analyses methodology

Some mathematical tools are used in this study such as the Empirical Orthogonal Functions (EOFs) and the Principal Components (PC).

In atmospheric science, a mathematical method, known as the Empirical Orthogonal Functions (EOF) analysis and the Principal Components (PC) are often used to study possible spatial patterns of climate variability and how they change with time. EOFs refers to the independent spatial patterns (modes) of variability and are associated with the corresponding principal components (PC) that describe their time varying amplitudes. EOFs can represent mutually orthogonal space patterns where the data variance is concentrated, with the first pattern being responsible for the largest part of the variance, and the second for the largest part of the remaining variance, and so on.

In this work, the EOFs analysis is applied to the whole West African domain averaging JJAS monthly temperature anomalies to extract the coherent spatial and temporal patterns.

CHAPTER FOUR

RESULTS AND DISCUSSION

This chapter presents and discusses all the results from this study. It provides an improvement on the previously known effects of urbanization effects on West African climate. It starts by evaluating model performance. Thus, the effects arising from the coastal urban expansion on the mean and variability of climate are delivered. Finally, we will evaluate the urbanization influence of monsoon features. All the results presented here are based on model and observation results for JJAS and they correspond the monsoon months.

4.1 Assessment of the model performance of the CTRL_PRS experiment

The focus of this section is to evaluate RegCM4 performance. For that, the output results from the CTRL_PRS are compared with observations and reanalyses to evaluate the model performance representing the WASMC.

4.1.1 Mean summer monsoon climatology of temperature and precipitation

A comparison of the temperature and precipitation by observations (CPC, CRU, UDEL) and RegCM4 runs from 1986 to 2005 was carried out.

Figure 4.1 presents the JJAS mean temperature climatology from CPC, CRU, UDEL, and RegCM4 outputs, respectively. From the figure, it is obvious that all different datasets show a zonal pattern of temperature with long-term mean lower temperatures (between 24ºC and 26 ºC) observed in the Guinea Coast, and a higher 38ºC temperature in the Sahara region. Lower temperatures are also found in the orographic regions such as Cameroun Mountains, Jos Plateau, and Guinean Highlands. Almost all the observed

temperature has similar pattern and RegCM4 simulation agrees well with the observed. However, RegCM4 overestimates temperature in the central part of the Sahara which corresponds to the SHL region, some parts of Liberia and Sierra Leone, and around the Cameroun region, and it underestimates temperature in the central part of Nigeria. These observable temperature biases were noted in several RCMs simulations as demonstrated by Giorgi *et al.* (2012) and Sylla *et al.* (2012; 2013b). They revealed that these biases can originate from a number of factors such as cloudiness, surface albedo, temperature advection, surface water, and energy fluxes. Generally, RegCM4 reproduces the seasonal surface temperature patterns quite well.

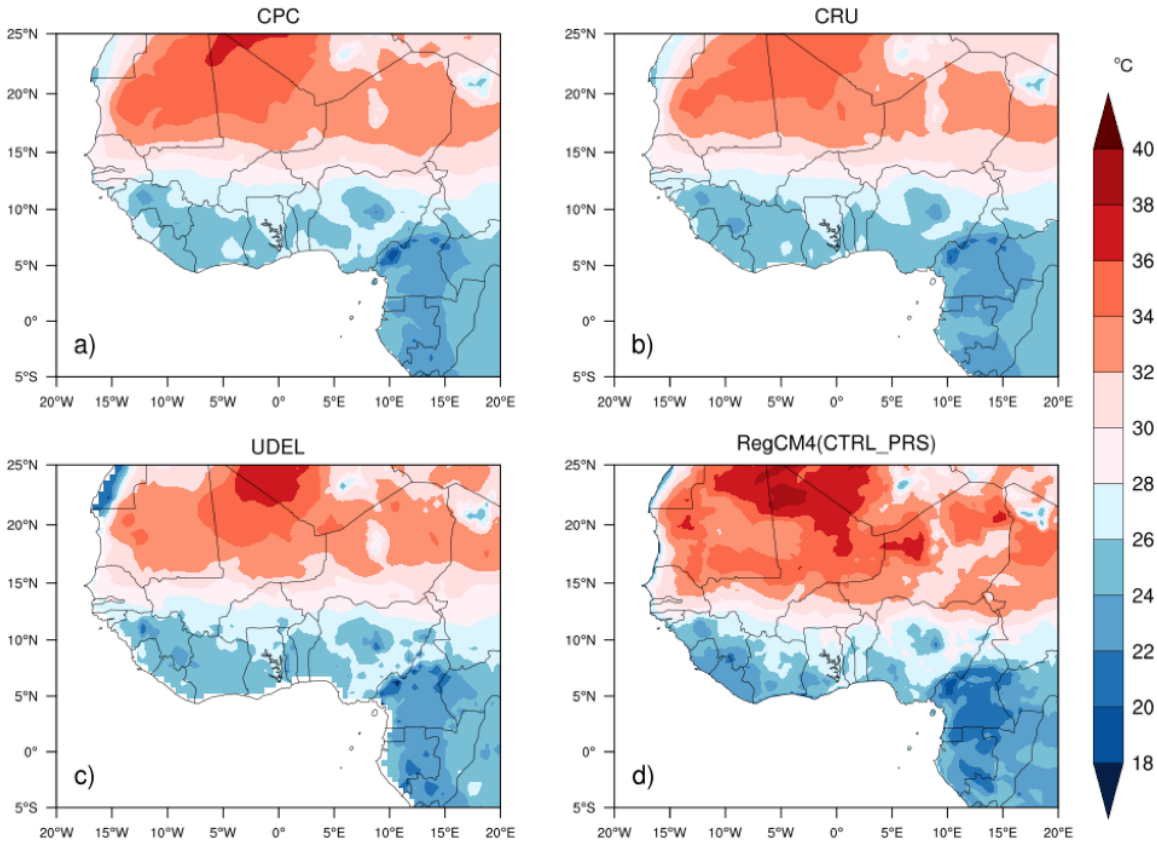

Figure 4.1: Seasonal JJAS mean temperature (°C) during1986-2005 from: (a) CPC, (b) CRU, (c) UDEL, (d) RegCM4.

The spatial distribution of mean JJAS precipitation climatology (1986-2005) from CPC, CRU, UDEL, and RegCM4 outputs, respectively, are shown in Figure 4.2a-d. It is observed that rainfall mostly occurred in the latitudinal belt between 5ºN and 18ºN during the summer monsoon with the Guinea Coast having the highest rainfall. In addition, precipitation maxima are also located in mountainous regions of Cameroun Mountains, Jos Plateau, and Guinean Highlands, which also experience the coldest temperatures indicating large evaporating cooling over these areas (Sylla *et al.*, 2013a). It is observed that the rainfall monsoon decreases northward and southward of the zonal ITD band. However, a number of differences can be observed both between observational datasets on the one hand and observational datasets and RegCM4 results on the other hand. For instance, both CRU and UDEL show intense rainfall amounts in orographic regions which are not well presented in CPC dataset. Some differences have also been noted between CRU and UDEL. The issue of discrepancies across different observed climatologies has been discussed by Sylla *et al.* (2012; 2013b). They concluded that these uncertainties are due to limitations in density and quality of available stations, extraction algorithms, interpolation techniques, and techniques for data blending. This analysis is a confirmation of the fact that significant uncertainties are present in observed precipitation climatologies and RegCM4 precipitation output is within the range of these uncertainties.

Even though RegCM4 is close to UDEL, but it underestimates the rainfall amount in orography regions. In addition, the simulated rainfall peaks agree with CRU and UDEL with an underestimation in the Sahel region. Despite the differences, it should be noted that RegCM4 resolves, quite well, the orographic rainfall maxima compared to CRU and UDEL, but it underestimates the amount. Similar underestimations in rainfall monsoon amount have been found in regional model simulations over West Africa

(Diallo *et al.*, 2012; Sylla e*t al.,* 2012). The underestimations of rainfall may be related to the choice of convection used (Afiesimama *et al.*, 2006) or the model's failure to resolve topography accurately (Akinsanola and Ogunjobi, 2017).

Overall, RegCM4 captures well the spatial distribution of rainfall, particularly the ITD position, and precipitation maxima over orographic regions.

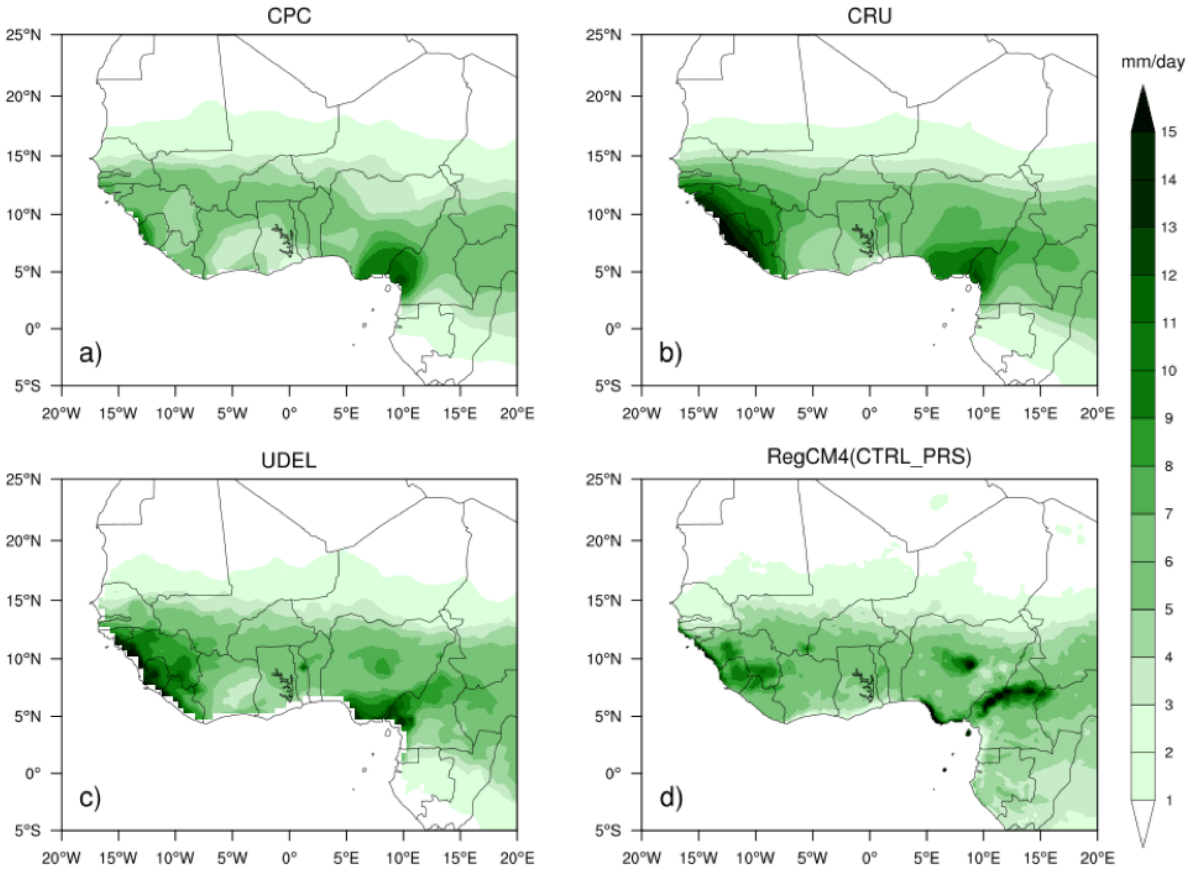

Figure 4.2: Seasonal JJAS mean precipitation (mm/day) during 1986-2005 from: (a) CPC, (b) CRU, (c) UDEL, (d) RegCM4.

The temporal mean variability of temperature and precipitation is also analyzed. It is expressed by the time-latitude cross sections averaged between 15°W and 15°E for the period 1986-2005. Figure 4.3 shows the latitude-time cross-section of the mean surface temperature from CPC, CRU, UDEL, and RegCM4 runs, respectively. The West African climate is characterized by latitudinal variation in mean annual temperature, which increases from the Guinea Coast to the Saharan region (Figure 4.3). As a result, a large temperature gradient exists that favours the SHL, which appears as the area with very low pressure and higher temperature. Lower temperatures in highland regions (Jos Plateau, Fouta Djallon, and Cameroon Mountains) and higher temperature over the northern Sahel and central Sahara are observable.

In general, the time-latitude cross-section of temperature is used for tracking the position and shift of the SHL, which is demonstrated as an important feature of the WASMC (Lavaysse *et al.*, 2009).

It was observed that RegCM4 (in Figure 4.3d) reproduces the temporal evolution of the mean temperature quite well. For instance, the model is capable of reproducing the north-south temperature gradient, the intensification and northward migration of the SHL from the northern Sahel (April–May) to the Sahara (July–August). Gbobaniyi *et al.* (2014); Sylla *et al.* (2013a) associated this migration with a progressive increase in the lower-level temperature gradient between the Gulf of Guinea and the Sahara, strengthening and shifting northwards the features triggering and maintaining the WAM which ultimately favour intense convection over the Sahel. However, compared to observations, we find that RegCM4 overestimates the intensity of the SHL and enhances a more northeastward extension of the SHL position.

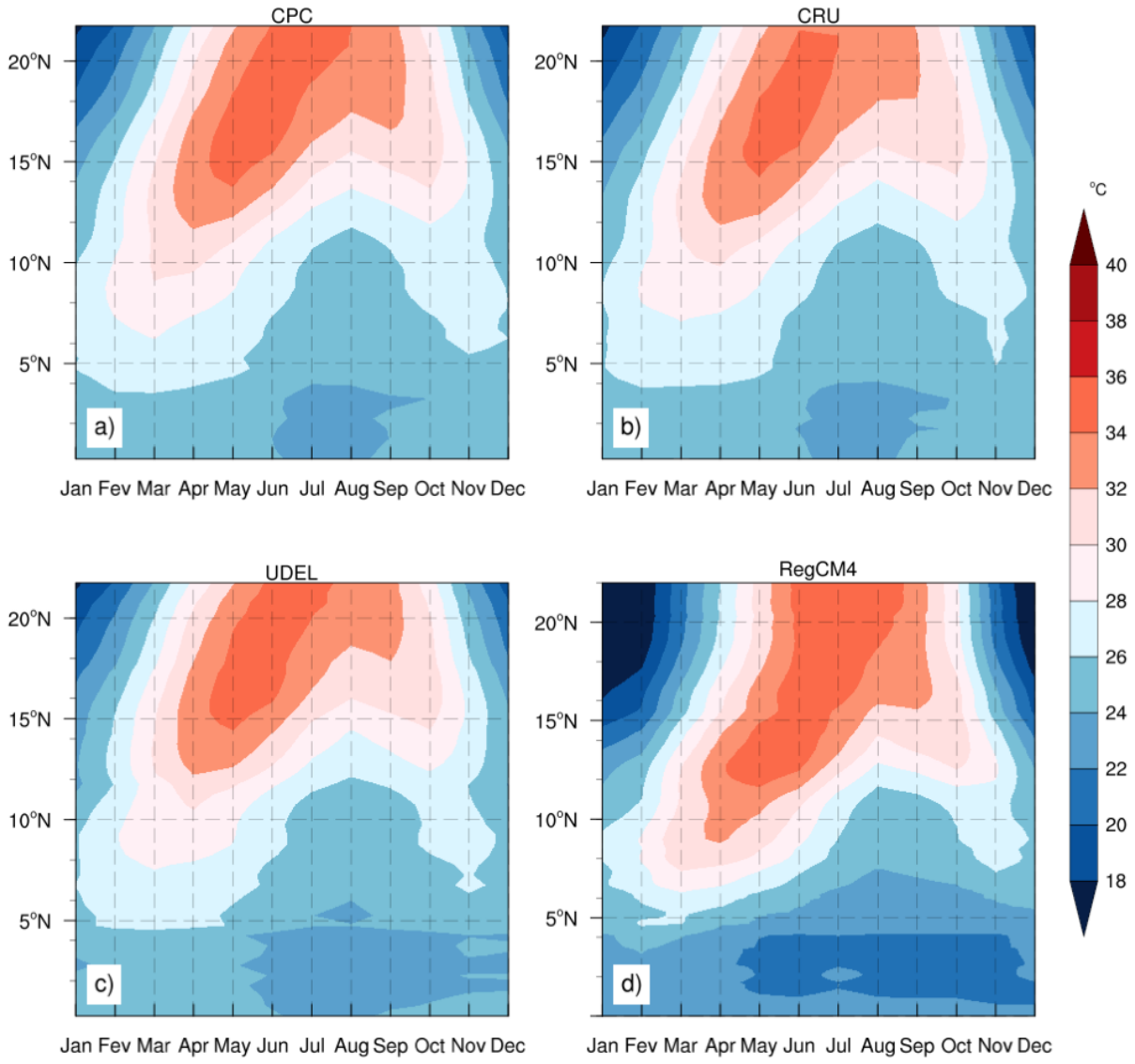

Figure 4.3: Latitude-time cross section of temperature (°C) during1986-2005 from: (a) CPC, (b) CRU, (c) UDEL, (d) RegCM4.

Figure 4.4 shows the latitude-time cross-section diagram for precipitation. Compared to the annual evolution of temperature, the temporal evolution of precipitation is more complex. Three distinct phases of rainfall maxima associated with the south-north-south displacement of the ITD can be identified. The first phase corresponds to the onset phase and represents the northward movement of the rainbelt from the coast to about 7^{o}N between March and June. This onset phase is characterized by rain band intensification along the Guinea Coast. The second phase represents the monsoon jump which is characterized by a sudden northward shift in the rainbelt into the Sahel region within the months of June to August. It is consistent with the northernmost position of the ITCZ (Sultan and Janicot, 2003). The rainbelt at this period is located between 8^{o}-13^{o}N in observational datasets but in RegCM4, it is located between 9º-11ºN. This is the period of high rainfall amounts over the Sahel and the sudden termination of heavy precipitation along the Guinea Coast. The last phase of the WAM season corresponds to the retreat (cessation) of rain belt towards the equator from the month of September. During this period, rainfall amount decreases and gradually retreats southwards to its southernmost position at the coast, and it is consistent with the southernmost position of the ITD.

In all, RegCM4 clearly identifies the main characteristics of WAM (onset phase, monsoon jump, monsoon peak and retreat of monsoon). However, some differences can be found among observed datasets and model with regard to the magnitude and spatial extent of these features. For instance, RegCM4 underestimates the intensity of pre- and post-monsoon rainfall compared to CRU or UDEL and the monsoon jump is advanced. The noticeable advance of the monsoon jump can be linked to the northeastward position of the core of maximum temperature found there.

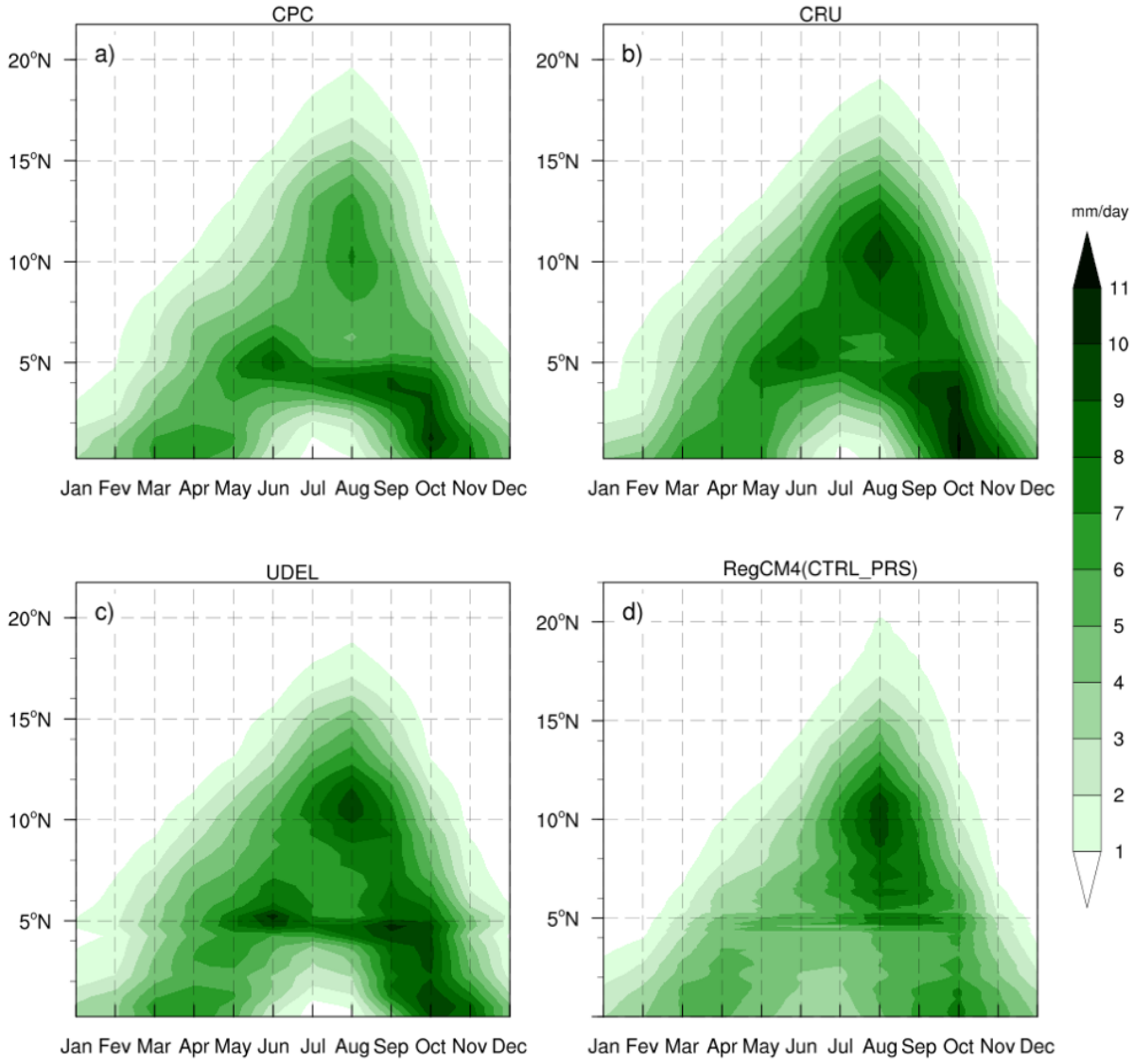

Figure 4.4: Latitude-time cross section of precipitation rate (mm/day) during1986-2005 from: (a) CPC, (b) CRU, (c) UDEL, (d) RegCM4.

4.1.2 Mean summer monsoon climatology of atmospheric circulation

This section presents the performance of RegCM4 in simulating the atmospheric circulation.

The vertical cross section of zonal wind averaged between 15ºW and 15ºE is displayed in Figure 4.5a-c both for reanalysis (ERA5 and NCEP) dataset and model runs during the JJAS summer months. The key monsoon features present in both the reanalysis are reasonably reproduced in the model namely: (1) The low-level monsoonal flow between approximately 2ºN and 20ºN (Figure 4.5a-c). (2) A low-level easterly flow (harmattan) confined between 20ºN and 30°N. (3) The AEJ, about 600-700 mb, is also well captured by the model with the core located around 12ºN-15ºN in ERA5, 10ºN -14ºN in NCEP, 10-15ºN in RegCM4. The regional model captures the AEJ location but its strength is weaker by about 4m/s with respect to ERA5 and NCEP. (4) An upper-level easterly flow (TEJ) located between 200-150 hPa and centered around 9ºN-10ºN in reanalysis, is also well represented by the model. However, ERA5 agrees very closely to RegCM4 concerning the TEJ location and intensity. In addition, a remarkable difference in the TEJ core between ERA5 and NCEP is observable. The low NCEP resolution could be the possible cause for this difference.

Due to the importance of the AEJ, which is one of the most complex and intriguing dynamical features in tropical meteorology (Nicholson, 2013), a research has been done at 700 hPa for a further description of the AEJ structure. It is displayed in Figure 4.5d-f.

RegCM4 is able to reproduce the location as well as the intensity of the AEJ although with few discrepancies (Figure 4.5d-f). For instance, it underestimates the jet speed more than 4 ms^{-1}. The model reproduces the northward shift of the core of the AEJ in both ERA5 and NCEP reasonably. However, RegCM4 has the closest to the ERA5,

which is more recent and has a higher resolution compared to NCEP. We also found an equatorward position of the jet position in RegCM4, which can cause the underestimation of rainfall in the Sahel region as demonstrated by Jenkins *et al.* (2005) and Raj *et al.* (2019).

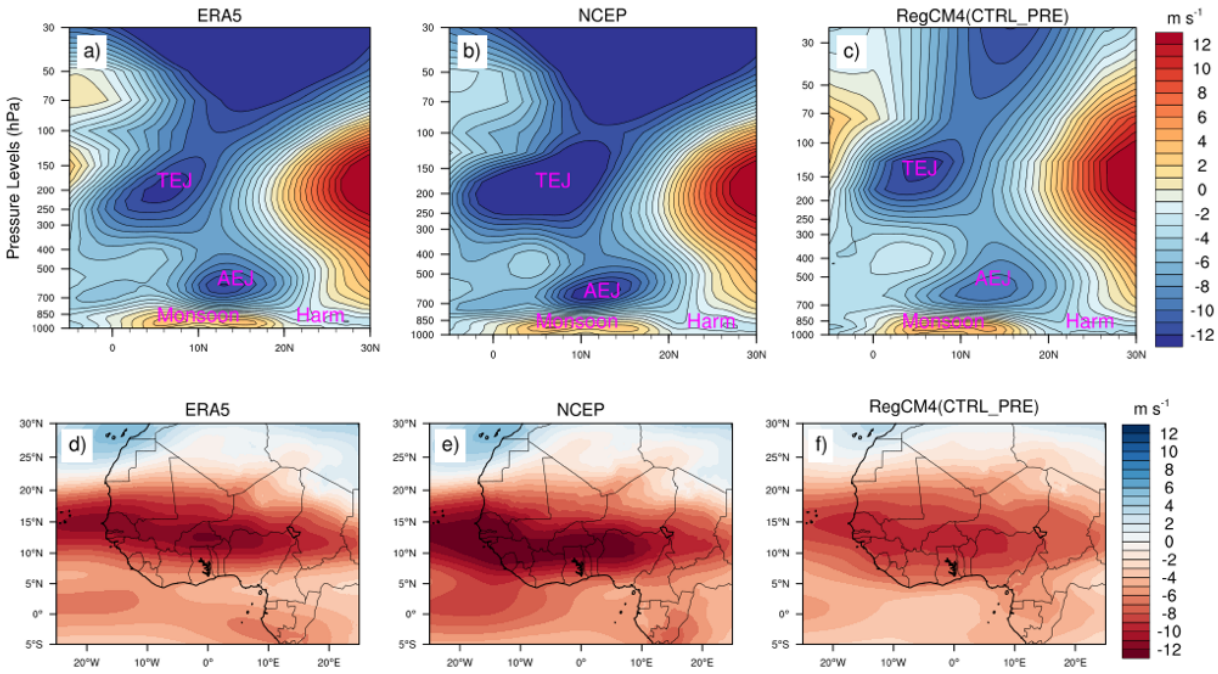

Figure 4.5: Latitude-pressure of zonal wind and seasonal AEJ position and strength in the period 1986-2005. The top panel (a-c) represents the latitude-pressure of zonal wind from: (a) ERA5, (b) NCEP, (c) RegCM4, while the bottom (d-f) represents the AEJ position from: (d) ERA5, (e) NCEP, (f) RegCM4.

Other key elements that can influence the WASM through the AEJ are the surface meridional temperature gradient (see Figure 4.6a-c) and the potential temperature (Figure 4.6d-f). These factors are used to determine the structure of the atmospheric boundary layer.

The meridional temperature gradient is a key factor in the latitudinal position of the AEJ, with positive gradients corresponding to the AEJ (Hall and Peyrillé, 2006; Raj *et al.*, 2019). It is obserable that a positive temperature gradient band with the core centered 15^{o}N develops near the surface and extends up to 700 hPa, and at that altitude, a reversal in the sign occurs, implying westerly shear with height, or weakening easterlies, as shown in Figure 4.6a-c. The AEJ, thus, develops at this transition point along with the monsoon flow in summer at about 12-15^{o}N (Hall and Peyrillé, 2006).

RegCM4 (Figure 4.6c) captures the structure of the temperature gradient and the pattern, especially the positive gradient band which corresponds to AEJ. The core of the maxima is located in 15ºN in ERA5, 13ºN in NCEP, and 14ºN in RegCM4. Similar pattern is observable between observations but a reversal in the sign is strong in NCEP, which confirms the possibility of a stronger AEJ in NCEP. However, few differences must be noted. For instance, a more extended reversal of temperature gradient exists in RegCM4.

Another factor that can influence the strength of the meridional circulation is the potential temperature whose the profile is displayed in Figure 4.6(d, e, f). It is observed that the potential temperature increases with height and a maximum near the surface at 20-25ºN (Sylla *et al.*, 2011). Note that the level of the AEJ (700-650 hPa) occurs in correspondence with the isentrope 315 K. The isentropes exhibit a large deflection towards the ground from 10°N, suggesting that baroclinicity increases north of that

latitude. This is consistent with the findings of Sylla *et al.* (2011). The model gives a good representation of the potential temperature profile.

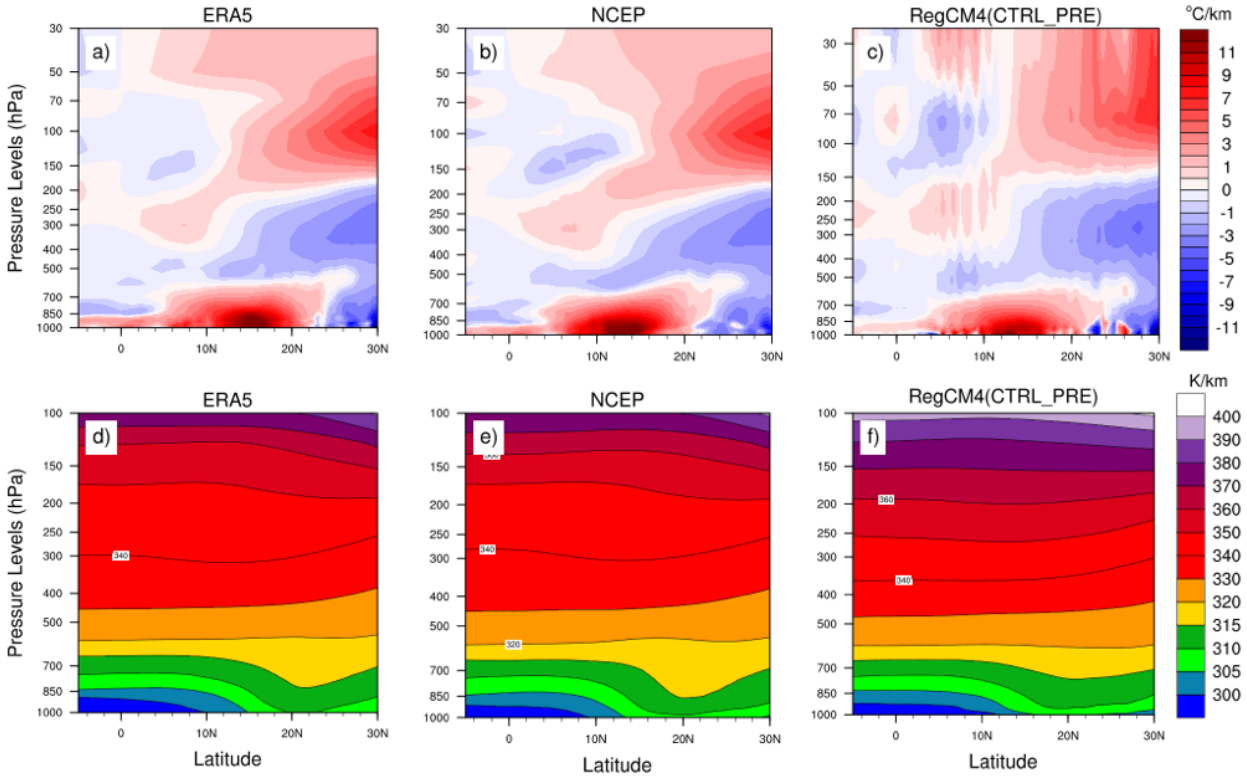

Figure 4.6: Seasonal JJAS of meridional temperature and potential temperature in the period 1986-2005. The top panel (a-c) represents meridional temperature from: (a) ERA5, (b) NCEP, (c) RegCM4, and the bottom (d-f) represents the potential temperature from: (d) ERA5, (e) NCEP, (f) RegCM4.

4.2 Influence of urbanization on the mean and variability of climatic variables

One focus of this study is to assess the potential influence of urbanization on the mean and variability of West African climate, especially temperature and precipitation.

4.2.1 Influence of urbanization on mean and variability temperature changes

In this section, we investigate the plausibility of the modelled effect of urban expansion on the mean temperature and precipitation, which are the major determinant parameters for West African climates. As mentioned in Chapter Two, urbanization can affect regional temperature through the mean temperature (Grimmond and Oke, 1999; McCarthy *et al.,* 2010; Argüeso *et al.*, 2014). Also, it is well known that temperature is one of the climatic variables that define West African climate.

In Figure 4.7(a-c), the projected changes of mean temperature for the period 2081-2100 relative to 1986-2005 are presented. The possible change in the future for the 21st century is computed by subtracting the present-day climate from the future's.

With respect to temperature, the projected changes show a gradient in warming, extending from south to north. By the end of the 21st century, all the model simulations (Figure 4.7a-c) project significant warming in the entire West African domain with the greatest temperatures located between 10^{o}N and 25^{o}N corresponding to the Sahel band, the Sahara desert especially the north-east Sahara. Higher temperature will also be experienced along the coastal band, which corresponds to the "perturbed" region (Figure 4.7 b, c). In particular, the climate signal is up to more than 5^{o}C in Sahara region and some parts of Sahel band, and up to 2 and 3^{o}C in the Guinean Coast**.** The highest warming in Sahara leads to a strong temperature gradient. These results are consistent with the ranges of changes projected by Niang *et al.* (2014); Sylla *et al.* (2016a); Diallo *et al*. (2012); Dosio and Panitz (2016) and the IPCC report. These studies demonstrated that strong warming is expected by the end of this century in many parts of West Africa. In

addition, higher temperatures are also found in the "perturbed" region, which marks the impact of the urbanized area (Figure 4.7 b, c). These changes from both urbanized simulations are almost identical and the magnitude of the changes could be up to 7ºC. These results are consistent with findings from Grimmond *et al.* (2011), McCarthy *et al.* (2010), Oleson *et al.* (2012), and Paranunzio *et al.* (2019). These researchers revealed that urbanization accelerates warming at regional scale through the UHI.

To evaluate the contribution of urban expansion, we calculated the difference between the urban simulations (URBAN1 and URBAN2), which included both climate change and urban expansion, and the future control simulation (CTRL_FTR), which described the climate change alone. The differences between URBAN1 (URBAN2) and CTRL_FUT reflect the sum effects arising from urbanization alone on the one hand and the coupling of climate change and urban development on the other hand. The differences in mean temperature between future simulations are presented in Figure 4.7d-f. As expected, a significant difference between the control future experiment (CTRL_FTR) and the urbanizations experiments (URBAN1 and URBAN2) is noticed. The impact of the extension of the cities is clearly identifiable: warming of more than 3ºC is observed and it is essentially located in the "urbanized" region indicating an impact at the local scale. The changes in urban mean temperature can be explained by changes in surface thermal properties such as heat capacity and thermal conductivity. Obviously, transforming the natural land surface to urbanized area results in more energy being stored as ground heat flux during the daytime whereas the appearance of more positive ground heat flux appears during the night indicates more energy being released (warming the atmosphere) and leads to warmer air temperatures (Oke, 1987; Lemonsu *et al.*, 2015; Yang *et al.*, 2016). This simulated response of temperature to urban expansion aligns well with the studies of Argüeso *et al.* (2014; 2015) and Georgescu *et*

al. (2014). Georgescu *et al.* (2014), for example, using WRF coupled with an urban canopy model, estimated contribution to future mean warming from urban structures to be within the range of 1-2ºC by the end of the century. Chen and Frauenfeld (2016) also assessed the impacts of future urban expansion for China as a whole, via utility of a high-probability urban growth scenario derived from global projections of urban expansion with WRF (under RCP 4.5) and found warming up to 3°C on the regional scale. Also, Cao *et al.* (2018), using WRF under future urban expansion scenarios, found near-surface warming up to 2ºC, 3ºC, and 5ºC for 100%, high-, and low-probability urban growth scenarios.

It is observed that the difference between URBAN1 and URBAN2 shows a maximum value of 0.6ºC for the URBAN2 simulation. The presence of tall buildings in URBAN2 could be responsible for this difference. It shows a sensitivity of the UHI results to the urban land cover class. This result establishes a relationship between the size of an urban area and the intensity of the UHI. For instance, Atkinson (2003) performed a series of simulations in which the horizontal dimension of the city was increased from 6 km to 10 km, in steps of 2 km. The study indicated that the maximum UHI intensity for the largest urban area was only 0.2 K greater than that of the smallest urban area.

In a nutshell, urban structures affect local temperatures (perturbed region only). The changes in land cover that are observable in urban experiments confirm the sensitivity of local temperatures to the land surface changes (Zheng and Eltahir, 1997; Abiodun *et al.*, 2008; Paeth *et al.*, 2009; Sylla *et al.*, 2016a).

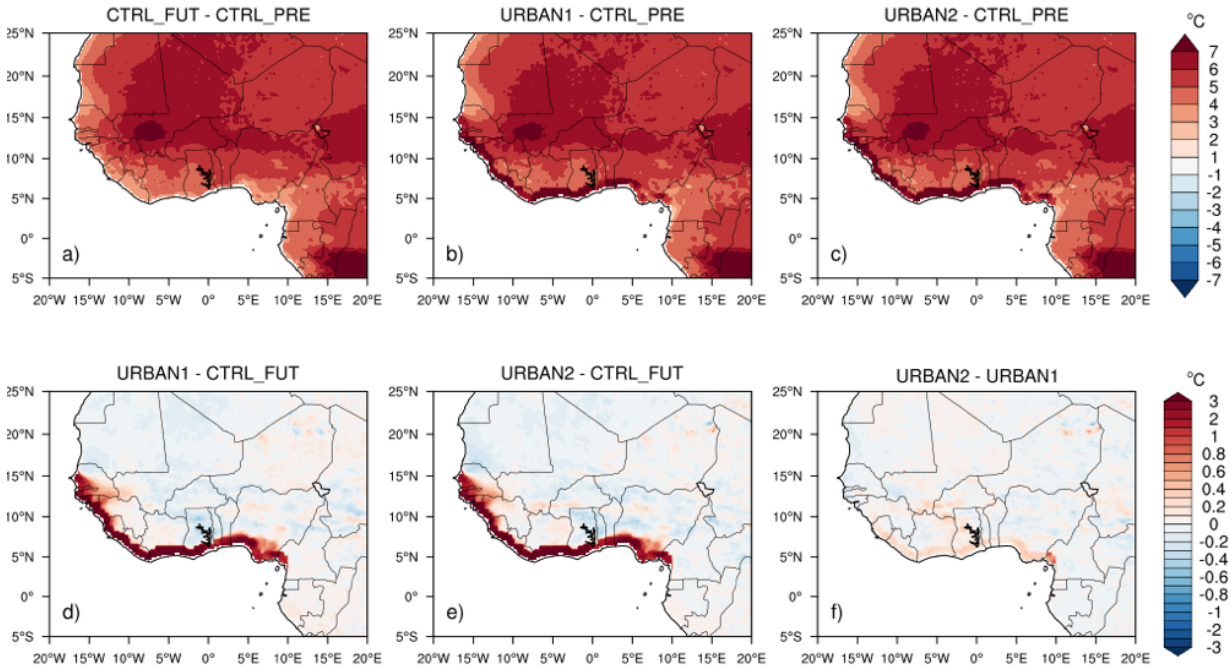

Figure 4.7: Projected changes of JJAS temperature between the future (2081-2100) and the reference period (1986-2005) and future simulations differences. The top panel (a-c) represents the projected changes and bottom panel (d-f) represents the future simulations differences.

In the previous sub-section, the study focused on the analyses of the influence of urbanization on the temperature mean. Here, we investigate the influence of urbanization on the temperature variability. In Figure 4.8 and Figure 4.9, the variability in temperature is displayed. This variability is evaluated through the EOFs and PC analyses.

The first five leading EOFs of temperature from the CTRL_PRS explain about 90 % of the total variance, i.e. most of the spatial variability in JJAS surface temperature can be explained by the first three modes of variability. The first mode EOF1 of CTRL_PRS (Figure 4.8a) explains 64.7% of the total interannual variability of the region. It shows positive values covering almost the whole West Africa with the strongest weights over the Sahel region. It may be placed in the broader context of the regionally observed warming trend over these last decades in the West Africa, especially in the Sahel region. It corresponds to the Sahelian mode.

The second pattern EOF2 (Figure 4.8b) explains 16.0% of the total variance. In this mode, we observe a bimodal distribution with positive and weak anomalies in the central West Africa region and negative values in the parts of Sahara. It corresponds to the Guinean and Saharan modes, respectively. The third mode which explains 5.3%, shows that positive values occur over the Western Sahara and some parts of the Sahel band and negative anomalies exist along the coast of the Gulf of the Guinea and the eastern Sahara. The other patterns, which represent the fourth and fifth modes respectively, explain respectively 3% and 1.9% of the total variance of seasonal JJAS temperature, with varying spatial patterns indicating that these patterns have become less independent of physical mechanisms.

The PCs associated with the different modes are displayed in Figure 4.9 (top row). The Sahelian regime (PC1) of the control present simulation is characterized by a low interannual variability. This suggests the persistence of the warming over the Sahel region during the last decades. Conversely, the other PCs show a strong interannual variability especially for the Guinean Coast and the Saharan modes (PC2, PC3, in Figure 4.9).

For all the future simulations (second, third, and fourth rows), it is noticed the same pattern with the CTRL_PRS experiment but with opposite signs and increasing percentage variance. This is most noticeable especially with the first EOFs. Hence, the changing of temperature variability under global warming. This correlates with the projected warming in West Africa at the end of this century. Lower values are found along the Sahel region which confirms the results that high warming is expected in this area. In the Guinean Coast mode (PC2, second row), we find a low interannual variability and this result is in line with the above findings of the expected warming over Guinea Coast which is not much compared to the Sahel or Sahara regions. For the Saharan mode, a strong interannual variability with positive values is observed in the CTRL_FTR experiment. This confirms the result that high temperatures are expected in Sahara region at the end of the 21st century.

Considering the changes in vegetation land cover along the coastal region (third and fourth rows), it is observed an inconsequential change from the first EOF pattern and the PC (PC1 of URBAN1 and URBAN2). However, a change is observed in the second PC2 corresponding to the Guinea Coast mode confirming the sensitivity of temperature variability to the land surface conditions. This is in line with Charney (1975) and Zheng

and Eltahir (1997) who demonstrated the change of variability under change of land surface conditions.

In summary, urbanization leads to a change of the annual variability of temperature in the area where the changes are made.

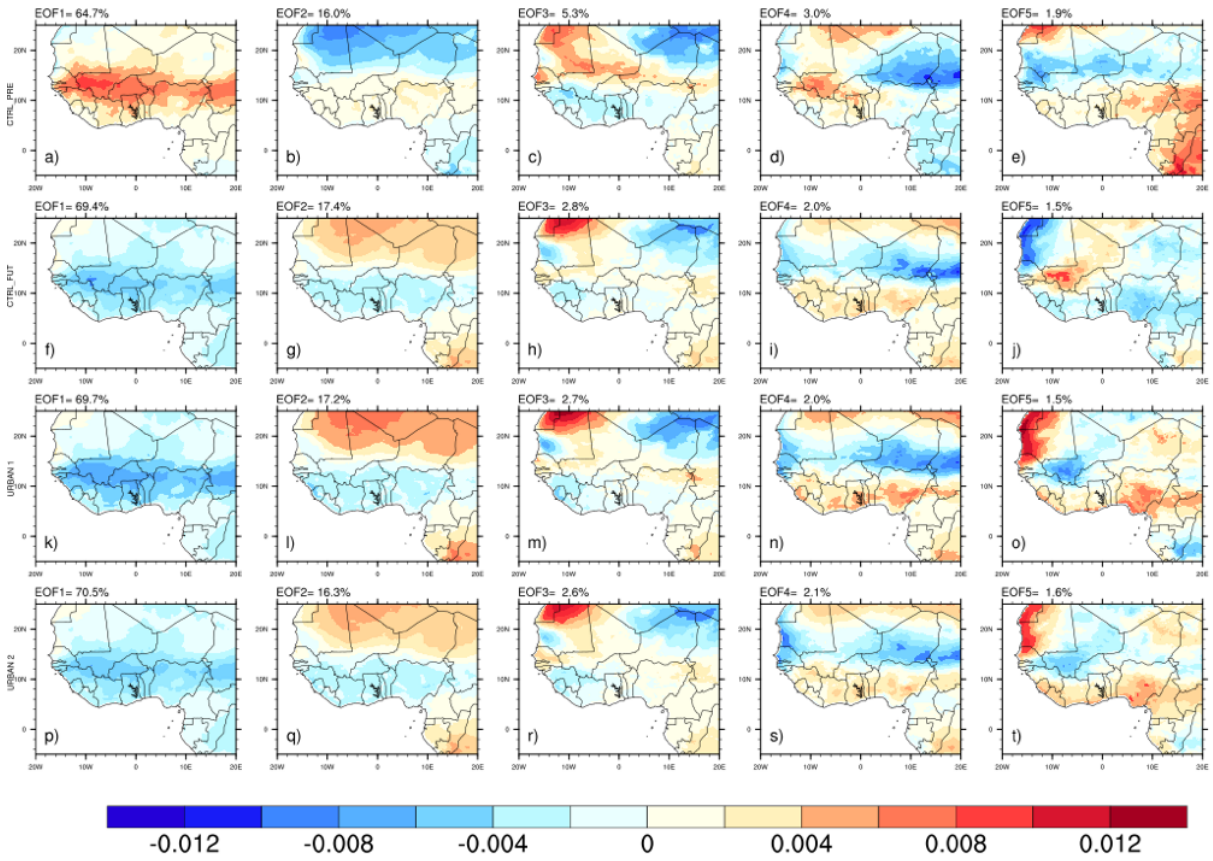

Figure 4.8: The first five EOFs of the monthly mean temperature for CTRL_PRS (first row), CTRL_FTR (second row), URBAN1(third row) and URBAN2 (fourth row).

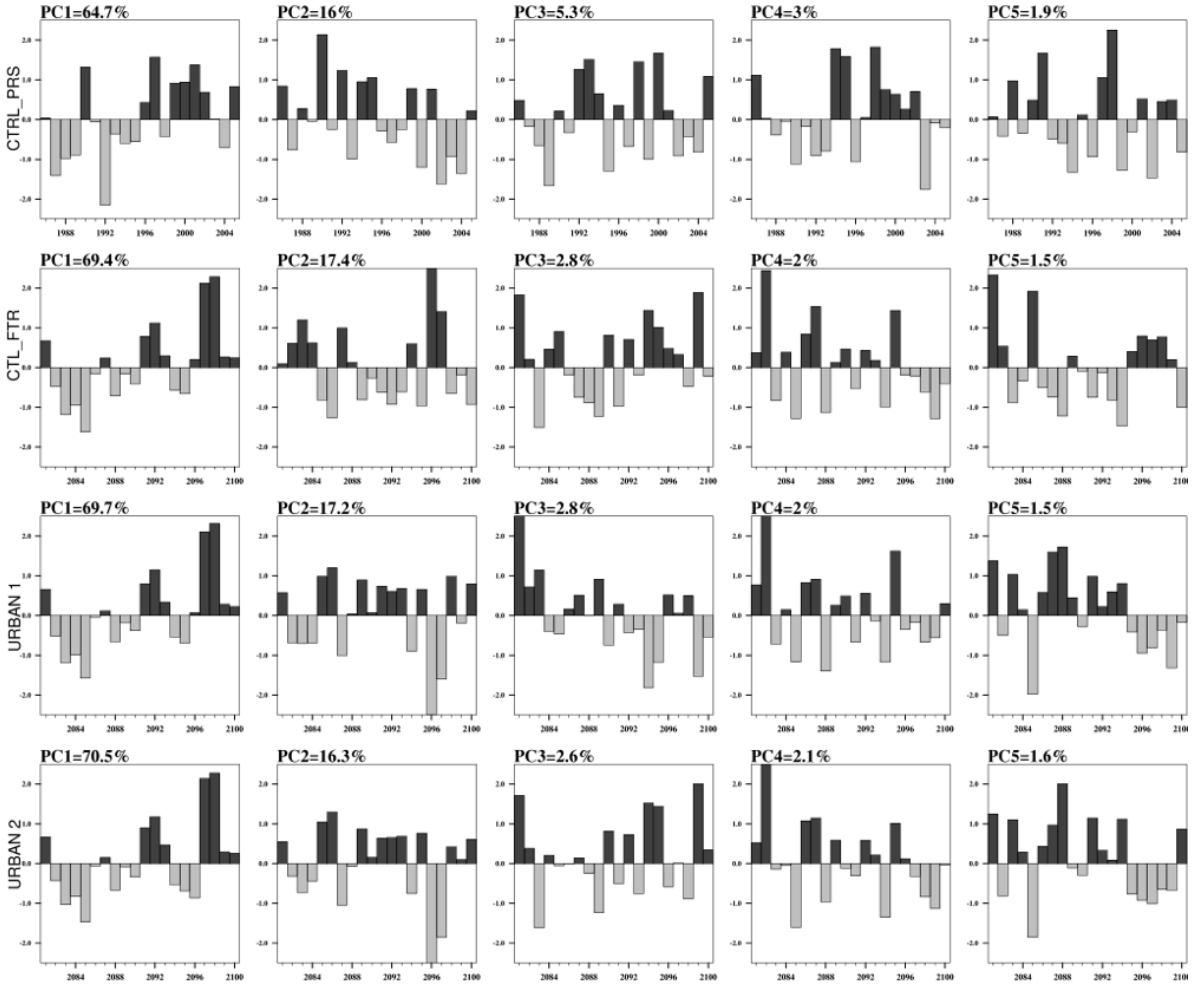

Figure 4.9: The corresponding PCs of the first five modes of temperature EOFs for CTRL_PRS (first row), CTRL_FTR (second row), URBAN1 (third row), and URBAN2 (fourth row).

4.2.2 Influence of urbanization on mean precipitation changes

The projected mean precipitation changes for the period 2081-2100 relative to 1986-2005 are presented in Figure 4.10(a-c). For all the different simulations, a reduction of rainfall, exceeding 30%, is projected at the end of the 21st century in almost the entire West African domain (Figure 4.10a-c) expect some parts of the eastern Sahel which appear to be wet, most especially in the sensitivity simulations. This decrease in precipitation during the JJAS season is mostly associated with the large warming found there, probably as a result of lower evaporative cooling and cloudiness (Diallo *et al.*, 2016; Sylla *et al*., 2016b). A great decrease in precipitation (~50%) can be seen in Nigeria and some parts of Mali. Also, the projected drier conditions were more pronounced in the CTRL_FTR simulation compared to the urban simulations. However, there are opposing views in the literature regarding the projected changes in precipitation.

In general, it should be noted that many of the GCMs or RCMs disagree with the future precipitation change patterns in West Africa. Some studies are projected an increase in precipitation in Guinean Coast and eastern Sahel during the JJAS monsoon season and a reduction in precipitation in the western Sahel (Niang *et al*., 2014; Sylla *et al*., 2015, 2016c; Dosio and Panitz, 2016; Diallo *et al*., 2016) while others would experience a decrease of precipitation in the entire West Africa at the end of the 21st century (Elguindi *et al.*, 2014). The lack of agreement on the sign of changes in precipitation is discussed in previous works such as Giorgi (2014); Niang *et al.* (2014); Sylla *et al.* (2015). They concluded that the projected regional rainfall changes are more uncertain than regional temperature changes due to the complexity of the climate models adopted to resolve convective scales.

When considering the contribution of urbanization alone (the climate change signal has been removed) (Figure 4.10d, e), it is noted that urbanization has a positive effect on the mean precipitation. An increase in rainfall, (more of 15%), in both urban simulations is observed especially in the "perturbed" region (Figure 4.9d, e). This result agrees with findings of Lamptey *et al.* (2005), Zhang *et al*. (2009). Chen and Zhang (2013) and Niyogi *et al*. (2017), who demonstrated that urbanization leads to increase in precipitation. According to them, urbanization includes enhanced convergence, boundary layer destabilization, increased aerosols, or alterations of existing storms (Lamptey *et al.*, 2005). Another important finding is that the effects are not only locally felt but an increase in precipitation is also observable in the non-urban areas such as Mali, and Niger. This result is in line with Lamptey e*t al.* (2005) who demonstrated that urban expansion leads to an enhancement of precipitation within cities and in the area 50 to 75 km downwind from cities during the summer period. Both local and regional processes drive this pattern of precipitation and it is called remote effects. Numerous studies have suggested that remote biophysical effects of LULCC could affect regional precipitation through a shift in major features of the climate system that modulates rainfall amount (Zheng and Eltahir, 1997; Quesada *et al.,* 2017). In summary, urbanization leads to an enhancement of rainfall at the local and regional scales.

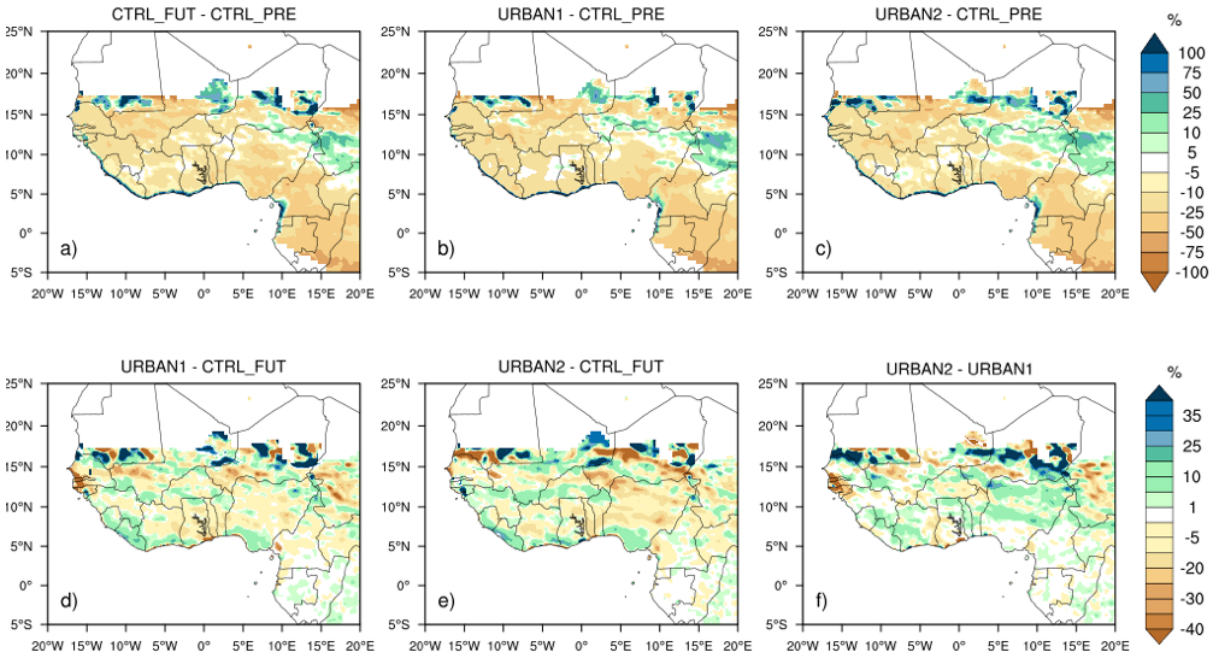

Figure 4.10: Projected changes of JJAS rainfall (in %) between the future (2081-2100) and the reference period (1986-2005) and future simulations differences. The top panel (a-c) represents the projected changes and the bottom panel (d-f) represents the future simulations differences.

Like the temperature, the EOFs and PC of precipitation variability under these different experiments is examined and it is displayed in Figure 4.11 and Figure 4.12. The spatial dominant patterns of precipitation during the summer months (first EOF) for the control present simulation (CTRL_PRS) explains 35.1% of the total variance with negative or weak values over the whole West Africa region. It is characterized by a uniform pattern through all the regions. The second EOF associated with 10.9% of the total variance shows a tripole-like pattern of loadings with negative values in Guinea Coast and Sahara and positive values over the Sahel (which corresponds to the Sahelian mode). In contrast, the third EOF (Figure 4.11c) associated with 3.8% of the total variance**,** shows opposite patterns between West Africa and the Sahara regions.

The corresponding PC (Figure 4.12) show a strong interannual precipitation variability in all modes especially for the PC2 and PC3 (first row) and corresponds to the decrease in mean precipitation.

Under climate change (Figure 4.11, second row) and both climate change and urban expansion (Figure 4.11, third and fourth row) scenarios, it is noted a change in the pattern of variability for all the first EOFs. The observed variability in the end of the 21st century appears to be consistent with global warming forcing. These basic processes are likely responsible for the greenhouse gases (greenhouse gases plus urban expansion) induced climate change case, thus contributing to the similar change patterns. The results suggest long-term greenhouse gases forcing, and that any additional processes from land cover change would play a dominant role in precipitation variability by the end of the 21st century.

The results from the corresponding PCs from the future simulations (CTRL_FTR, URBAN1 and URBAN2) show a strong inter-annual variability of the precipitation confirming the difficulties involved in assessing the rainfall pattern in West Africa.

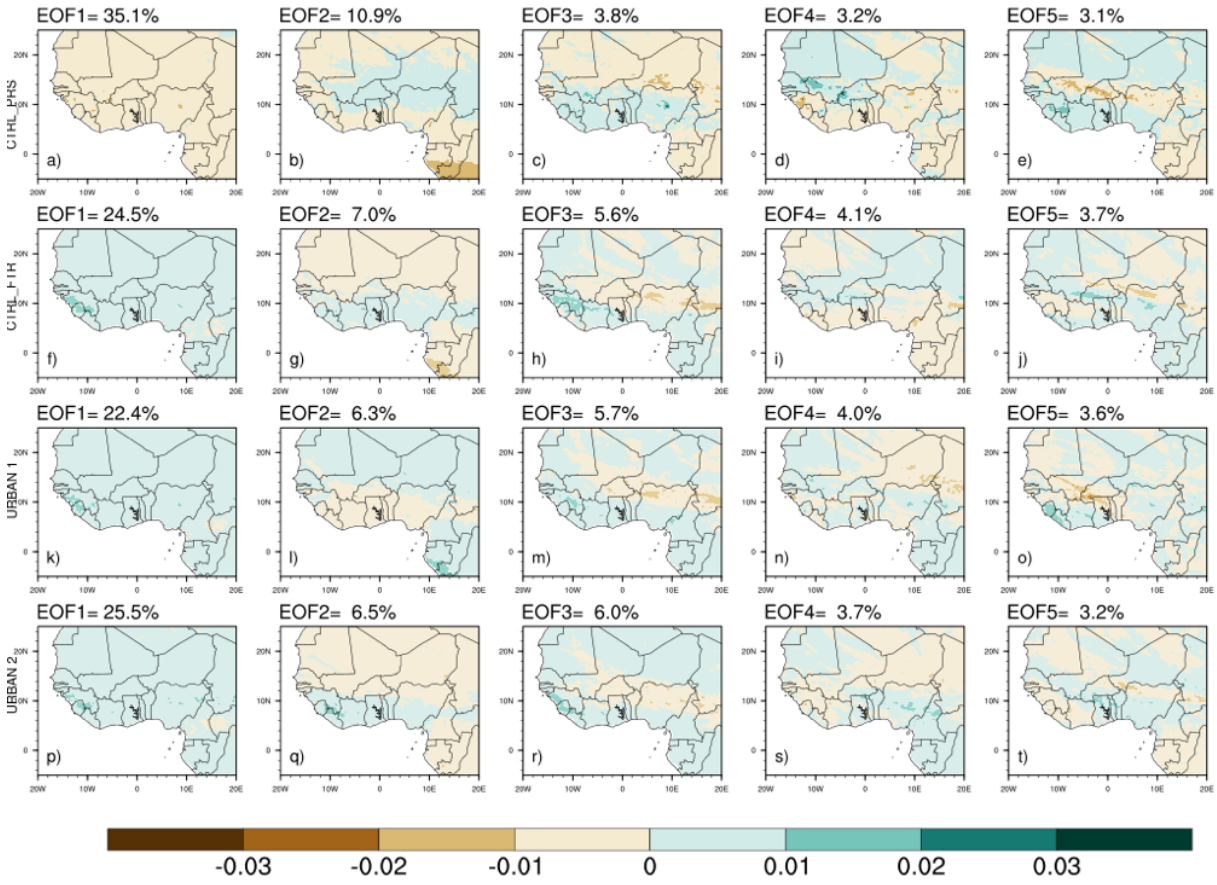

Figure 4.11: The first five EOFs of the monthly mean precipitation for CTRL_PRS (first row), CTRL_FTR (second row), URBAN1 (third row), and URBAN2 (fourth row).

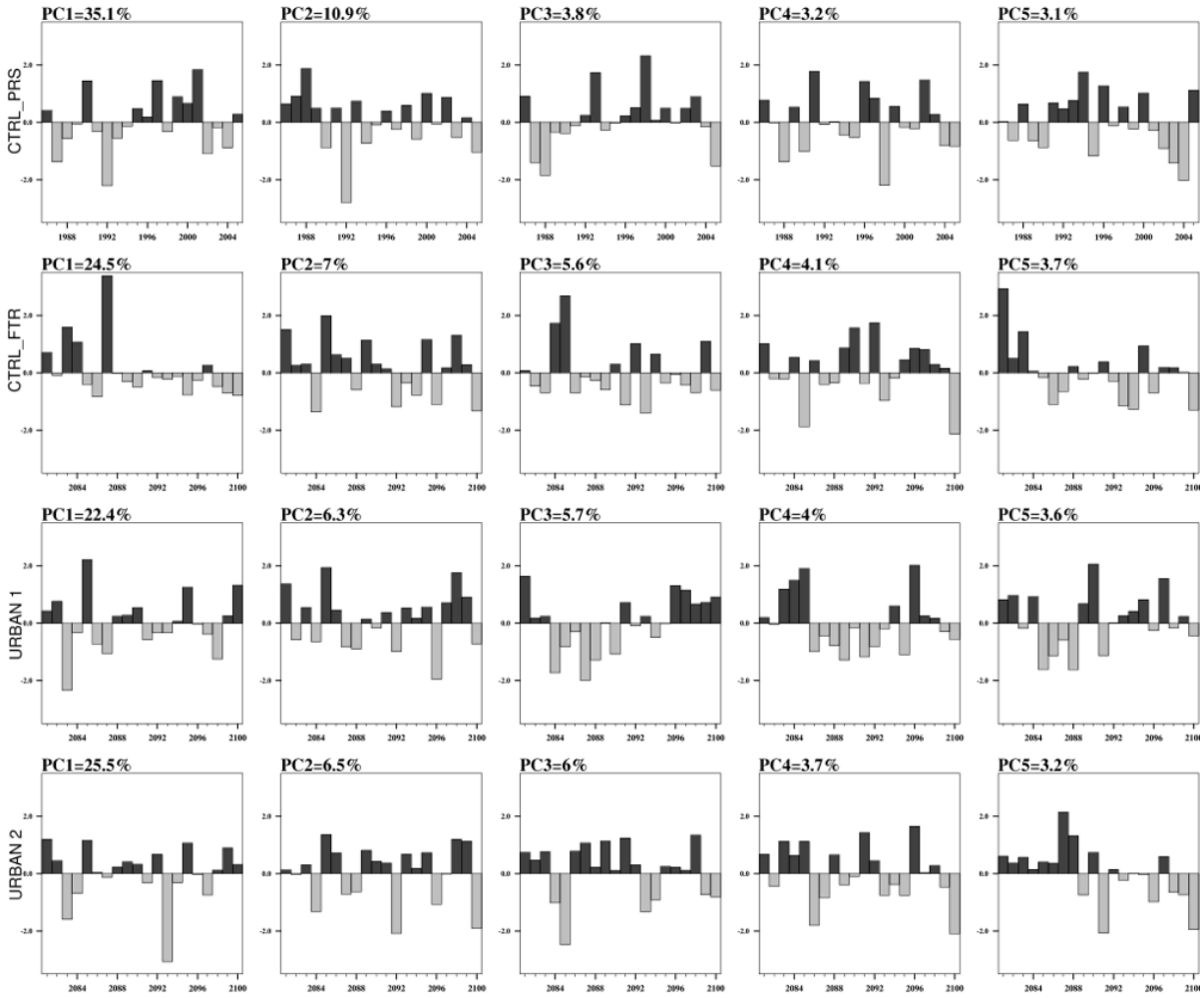

Figure 4.12: The corresponding PCs of the first five modes of precipitation EOFs for CTRL_PRS (first row), CTRL_FTR (second row), URBAN1(third row) and URBAN2 (fourth row).

4.3 Impact on the atmospheric circulation

Scholars have proven that in West Africa, the monsoon system plays a key role in increasing/decreasing the seasonal precipitation. The monsoon circulation system is mainly determined by various components such as the wind, the temperature gradient, the potential temperature, the vertical velocity, etc.

In this section, we will discuss the changes in various components of summer monsoon systems, and also the potential urbanization impacts on the atmospheric circulation.

4.3.1 Changes in African Easterly Jet

The projected mean changes and future simulations differences in AEJ position and strength are displayed in Figures 4.13. All the experiments (Figure 4.13a-c) show a southward displacement of the AEJ core, in response to enhanced radiative forcing in the RCP8.5 pathway (Figure 4.13 a) and both RCP8.5 pathway and urban expansion (Figure 4.13 b, c). It is, thus, clear that all the different experiments produce a lower AEJ during the late 21st century across West Africa, particularly over the Guinea Coast. However, the latitudinal change in maximum jet remains relatively stationary. This south displacement of the AEJ can explain the projected low precipitation in JJAS over West Africa, particularly, in the Sahel region by the end of the 21st century. Parallel work has supported this result. For example, Nicholson and Grist (2003) and Jenkins *et al.* (2005) have demonstrated that a southward position in the latitude of the AEJ corresponds to a decrease in rainfall in West Africa, especially in the Sahel region.

When considering only the contribution of urbanization to the AEJ, we find a southward displacement and positive value, suggesting a stronger AEJ. This strong value of the AEJ leads to low humidity, causing a divergence which impacts the convection, thereby creating drying conditions in West Africa. These results contradict with the findings of

Jenkins et al. (2005) and Nicholson (2008), who revelated that a strong and southward displacement of the AEJ cause drier conditions over the region.

In conclusion, urbanization leads to a stronger AEJ but does not affects the position of the jet. However, compared to the rainfall pattern shown above, it is noticed that AEJ is not the only feature controlling the WAM rainfall during the summer months.

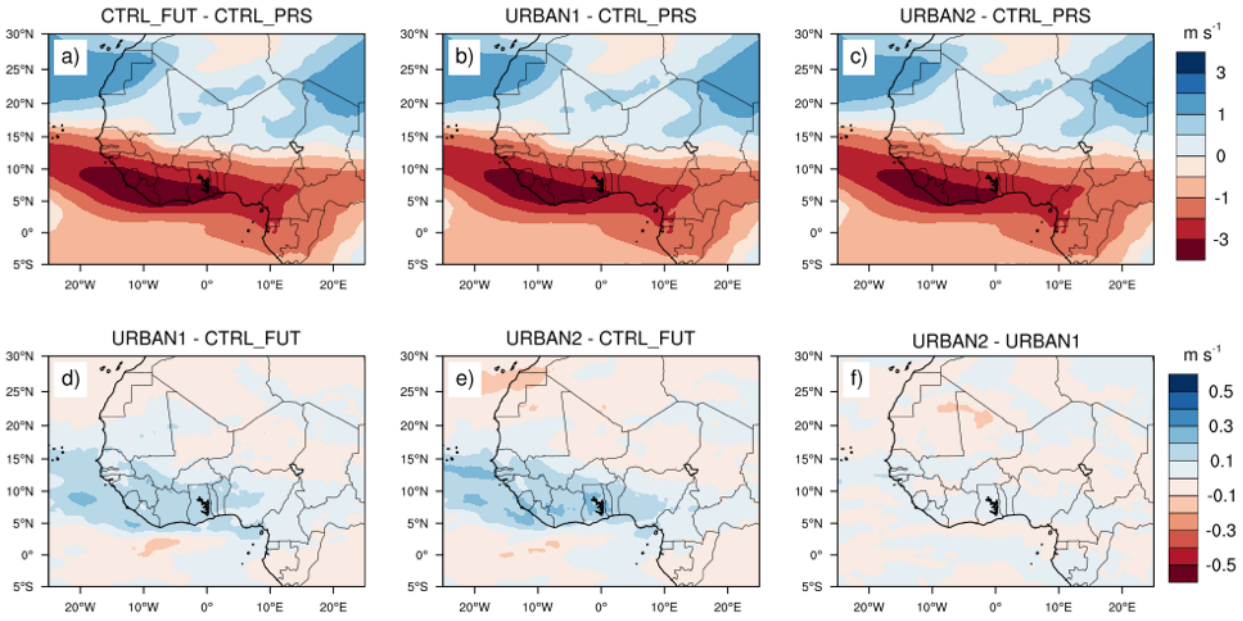

Figure 4.13: Projected changes of JJAS zonal wind (m/s) at 700 hPa between the future (2081-2100) and the reference period (1986-2005) and future simulations differences. The top panel (a-c) represents the projected changes and the bottom panel (d-f) represents the future simulations differences.

4.3.2 Change in meridional temperature

To further reveal the physical mechanism which accounts for the response of atmospheric circulation to urban land use in the West African coast, the meridional temperature gradient change is examined. The strength of the AEJ depends strongly on the position and the intensity of meridional surface temperature gradient.

Under the RCP8.5 pathway (Figure 4.14 a) and both RCP8.5 pathway and urbanization effects (Figure 4.14 b, c), it is observed that all the simulations projected a positive meridional temperature gradient from the lower level (surface) to 650 hPa with the maximum located around 10^{o}N and a negative gradient over the Sahara extending from the surface to the upper tropospheric level. Changes in the meridional temperature gradients in the upper troposphere will alter the structure of zonal wind through the thermal wind relationship and modify the propagation of planetary waves (Cook, 1999; Thorncroft and Blackburn, 1999).

The meridional temperature gradient anomalies diagnosed in response to future urbanization change along the West African coastal region are very small (Figure 4.14 d, e, f). This means that urbanization has not so great influence on the meridional temperature gradient.

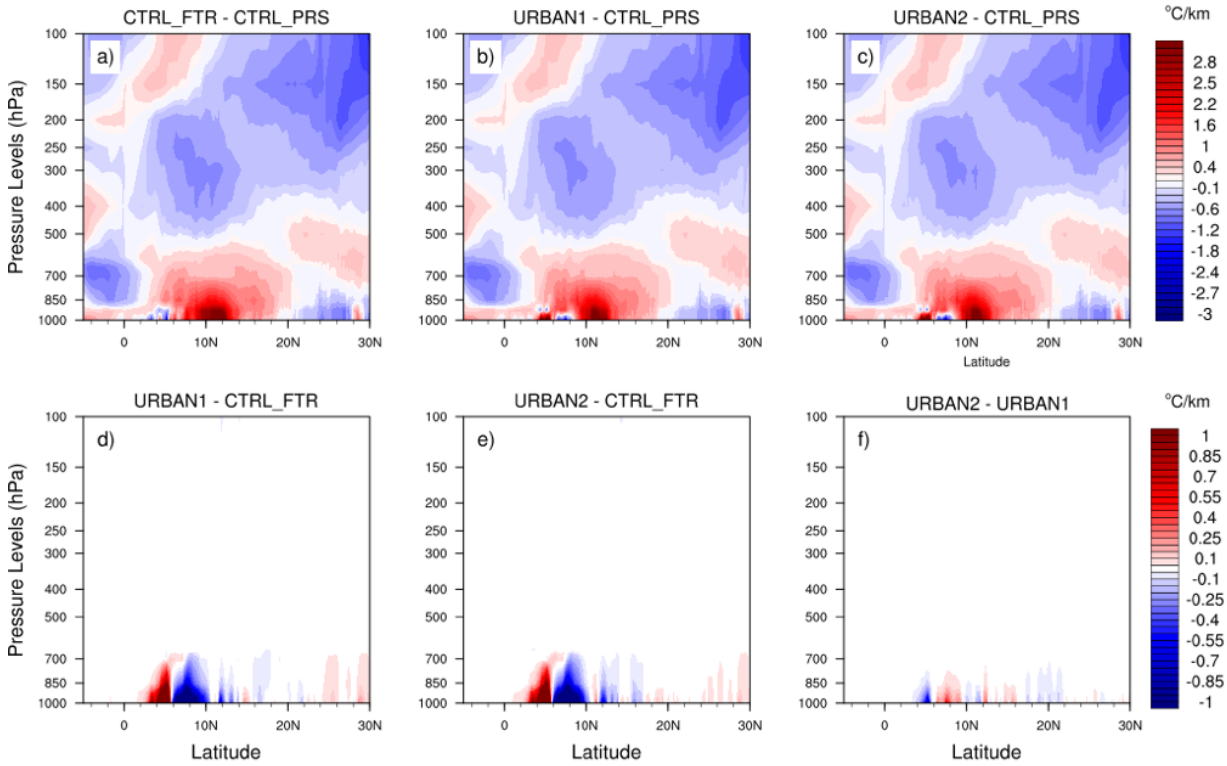

Figure 4.14: Projected changes of meridional temperature between the future (2081-2100) and the reference period (1986-2005) and future simulations differences. The top panel (a-c) represents the projected changes and the bottom panel (d-f) represents the future simulations differences.

4.3.3 Changes in potential temperature

In Figure 4.15(a, b, c), the summer potential temperature gradient change averaged between10ºE and 20ºW is displayed. The surface temperature gradient plays a significant role in the lower and middle troposphere in generating the intensity of the AEJ at 650 mb. All the simulations project a similar increase of potential temperature with height. The mean potential temperature increases by 7K/km to 13K/km in the mi-levels of the troposphere (~500-100hPa). Such shift in meridional temperature gradient is likely going to affect the zonal atmospheric circulation pattern through the thermal wind relationship (Cook, 1999; Cornforth et *al*., 2009). It could also have substantial impact on the position and the strength of AEJ.

When assessing urbanization contribution alone, a minor impact of changes in potential temperature is observed.

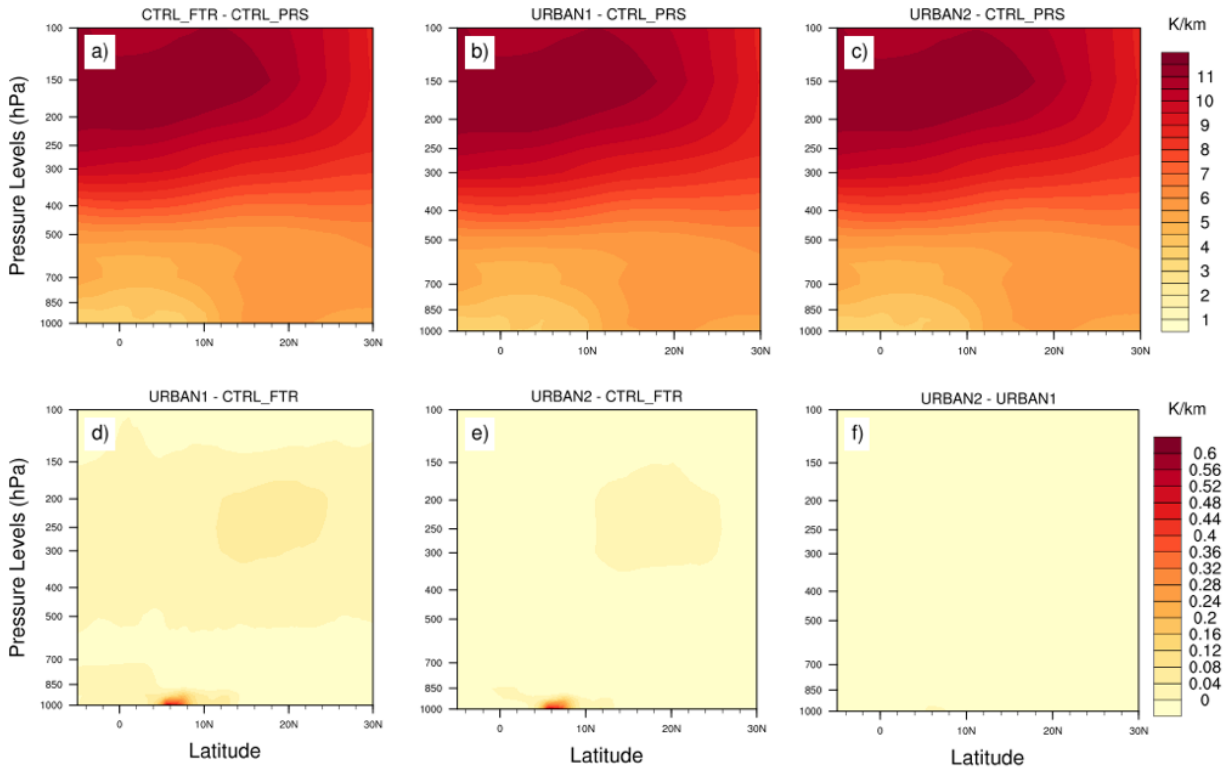

Figure 4.15: Projected changes of Potential temperature between the future (2081-2100) and the reference period (1986-2005) and future simulations differences. The top panel (a-c) represents the projected changes and the bottom panel (d-f) represents the future simulations differences.

4.3.4 Changes in African Easterly Waves

The next phase is to estimate the projected change in the AEWs. To calculate the AEWs, we used the meridional component of the wind at 700 mb (Diedhiou *et al* 1999). To isolate variations in flow associated with the passing of AEWs, we filter the daily time series of meridional wind during JJAS a 3- to 5- (2- to 10-) day band pass filter. We then calculate the variance of the filtered time series at each grid point for each season to attain a proxy of mean seasonal AEWs activity. This approach is advantageous for detecting AEWs within long-term climate time series because it is computationally efficient, and yields a clear, coherent spatial pattern of mean AEW activity over Africa. All simulations agree that AEWs activities (3-5 filtered day) are projected to decrease when the maximum change is located between 15 and 25°N i.e. along the Sahel-Sahara border and the Nigeria part (Figure 4.16a, b, c) at the end of the 21st century. This region with decreased AEWs activities is located north of the projected future location of the AEJ core (Figure 4.16a, b, c).

Similar pattern is also found for the JJAS mean variance of the 2-10 day filtered meridional wind at 700 mb (Figure 4.17a, b, c).

However, when assessing the urbanization contribution, an increase of AEWs activity is noted in both cases. Strong AEWs activity may weaken the jet temporally through barotropic conversions, as noted by the simple modeling results. Also, as long as the strong surface temperature gradient exists, the jet will restore its strength through a thermally direct ageostrophic meridional circulation.

In consistence with the studies of Skinner and Diffenbaugh (2013), these results imply that most of the precipitation over West Africa is generated by the AEWs (Omotosho, 1985).

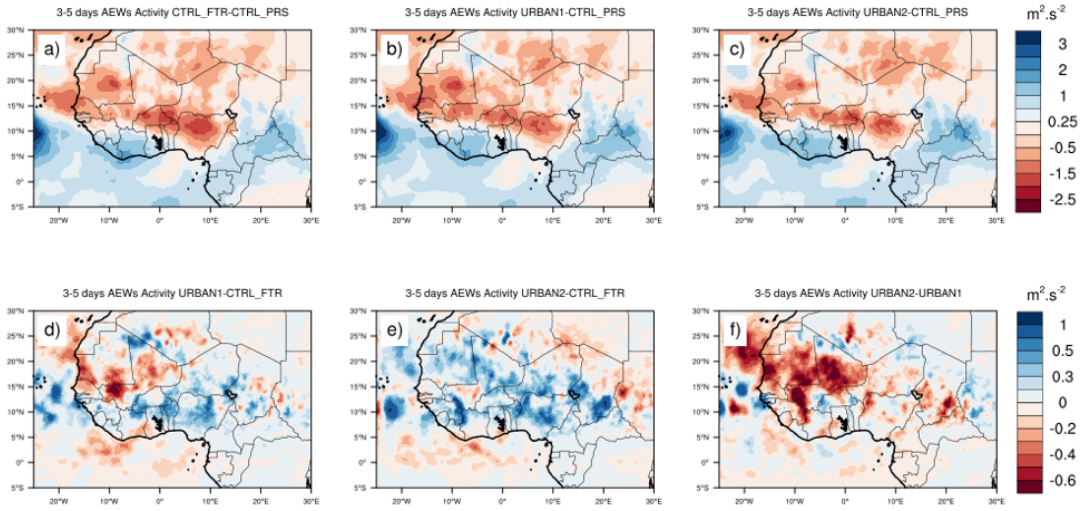

Figure 4.16: JJAS average difference between the futures(2081-2100) and the reference period (1986-2005) of the 3- to 5-d filtered meridional wind at 700 mb.

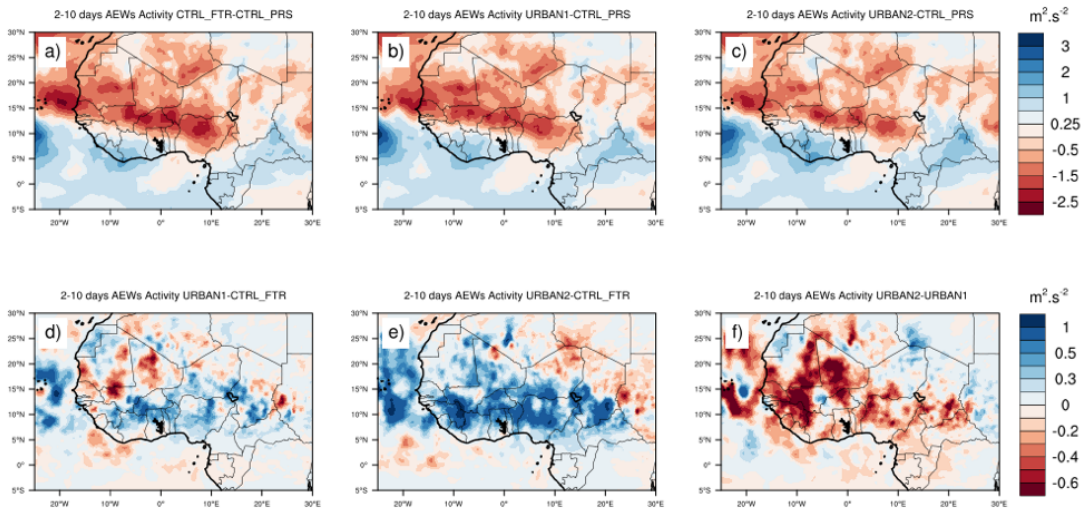

Figure 4.17: JJAS average difference between the future (2081-2100) and the reference period (1986-2005) of the 2- to 10-d filtered meridional wind at 700 mb.

CHAPTER FIVE

CONCLUSION AND RECOMMENDATIONS

5.1 Conclusion

This thesis examined the effects of coastal urbanization on the West African summer climate using the Regional Climate Model Version 4 (RegCM4) coupled with the Community Land Surface Model version 4.5 (CLM4.5). This study has provided one of the first descriptive influence of land use changes from urbanization in the West Africa region. A series of experiments were done, on the modern-day climate (1984-2005) and the far future climate (2079-2100) under RCP8.5, with and without activating an urban expansion scheme. The sensitivities simulations account for the potential urban expansion influence on the West African climate by adding different states of "idealized" future urbanization scenarios along the coastal band from Dakar (Senegal) to Douala (Cameroon). These "idealized" scenarios were constructed based on the assumptions of the future expansion from Jackson *et al.* (2010), Seto *et al.* (2012), and also to the urban classes present in CLM4.5.

First, we have demonstrated the capability of RegCM4 simulations to reproduce the main characteristics of West African climate during the JJAS summer months. A comparison of the RegCM4 temperature and rainfall with different observations datasets such as CPC, CRU, UDEL was also done. The atmospheric circulations are evaluated using reanalyses from ERA5 and NCEP.

Results establish the ability of RegCM4 to simulate the long-term spatial distribution of the temperature and precipitation over West Africa as well as the temporal evolution. For example, the model gives realistic patterns regarding the zonal temperature over West Africa with cool temperature in the Gulf of Guinea and high temperatures in the

Sahel and the Sahara regions. Concerning precipitation, the model captures well the southward-northward rainfall distribution over West Africa and the maximum rainfall amount over highland regions (Guinean Highlands, Jos Plateau, and Cameroun Mountains), and the essential phases (onset, monsoon jump, retreat). However, some biases were noted. For instance, RegCM4 underestimates maxima rainfall over the highland regions compared to observation datasets. Also, this study confirms the difference within observation datasets itself.

The model ability to simulate atmospheric circulation was also assessed. The vertical structure of the zonal wind from the control present experiment aligned with ERA5 and NCEP. RegCM4 was able to simulate the essential features over West Africa (monsoon flux, harmattan, AEJ, TEJ). Other atmospheric processes such as the potential temperature and meridional temperature was also analyzed. RegCM4 was capable to simulate all the processes.

Furthermore, the influence of climate change and land cover change (from urbanization) on the mean and variability temperature and precipitation were analyzed. Results revealed that all the different simulations project significant warming in temperature over the entire West Africa at the end of the 21st century. Higher temperature was experienced in the Sahel-Sahara region and along the West African coastal region over the "perturbed" region in the sensitivity simulations. When removing the climate change signal, we found that urbanization has a strong influence on temperature at the local scale. This warming from urbanization called the 'Urban Heat Island' can reach 3ºC. The results of this study imply that urban effects can reach the same magnitude as global warming effects.

Another important finding of this study is that the sensitivity of temperature to urban areas depends on the form of the urbanization.

With respect to precipitation, all the different simulations projected precipitation decrease at the end of the 21st century over the whole West African domain except for part of the Sahel which was projected to be wet. However, the expected drier conditions in the 21st century are more pronounced in CTRL_FTR experiment, which represents the effects of climate change alone, compared to sensitivity simulations, which represent both climate change and urbanization.

When calculating the urbanization contribution alone, it is noted that variation in urban land use in the West African coastal region could impact precipitation positively. Such impact is not limited to coastal regions with changing urban land use; the impact can reach the central and northern part of Nigeria, Mali, western part of Togo and Benin. Contrary to temperatures, both regional and local processes (remote effects) control the rainfall over the West African region.

Moreover, the variability of temperature and precipitation under these different conditions was also examined. Results showed the changes in natural vegetation land cover can perturb the variability of the temperature and rainfall pattern. Under climate change conditions alone, a strong inter-annual variability especially for precipitation over the whole West African region is observed. This confirmed the local and regional influence of urbanization on precipitation. As for the temperature, we noticed a change of variability especially along the urbanized areas.

This work also examined the response of the atmospheric circulation drivers to the urban land-use change. The results revealed that the changes in natural vegetation land cover

influence the dynamic circulation of variables like AEJ and AEWs or other atmospheric variables. Under urban conditions, we observed a strong and southward position of the AEJ which can cause less precipitation in the region while more convective activities (AEWs) are detected along the same direction. This means that urbanization leads more convection over the urbanized area and its surrounding areas.

5.2 Recommendations

Although some limitations exist in our simulation, the present results for the extensive coastal urban agglomerations still have the important value and will provide some basic findings, which may serve as a reference for future studies using relevant methods.

For better understanding of the effects of the urbanization on the West African climate, the variation in land cover should be extended to other regions such as the Sahel and/or the Guinea Coast. This is because previous studies which have demonstrated the response of West African climate to land surfaces change merely depended on the location and position where the changes were made.

This study used a single climate model driven by a single global climate model. For future studies, the utilization of more RCMs, forced with different GCMs and under different RCPs or an ensemble simulation encompassing several regional climate models could help to reduce uncertainties and make the results more robust.

Future studies could also include the incorporation of more precise historical land cover data within the model. Whilst this allows an interesting comparison between different forms of urbanization, these results could be better related to historic conditions with better land cover information.

Finally, future studies could take into account the impact of both urban land-use change and anthropogenic aerosols. Perhaps, the activation of aerosols schemes could permit a clear investigation into the effects of the urban area on regional climate.

REFERENCES

Abiodun, B. J., Pal, J. S., Afiesimama, E. A., Gutowski, W. J. and Adedoyin, A. (2008). Simulation of West African monsoon using RegCM3 Part II: Impacts of deforestation and desertification. *Theoretical and Applied Climatology*, 93(3-4), 245-261. https://doi.org/10.1007/s00704-007-0333-1

Abiodun, Babatunde J., Adeyewa, Z. D., Oguntunde, P. G., Salami, A. T. and Ajayi, V. O. (2012). Modeling the impacts of reforestation on future climate in West Africa. *Theoretical and Applied Climatology*, 110(1-2), 77-96. https://doi.org/10.1007/s00704-012-0614-1

Abiodun, Babatunde J., Adegoke, J., Abatan, A. A., Ibe, C. A., Egbebiyi, T. S., Engelbrecht, F. and Pinto, I. (2017). Potential impacts of climate change on extreme precipitation over four African coastal cities. *Climatic Change*, 143(3-4), 399-413. https://doi.org/10.1007/s10584-017-2001-5

Afiesimama, E. A., Pal, J. S., Abiodun, B. J., Gutowski, W. J. and Adedoyin, A. (2006). Simulation of West African monsoon using the RegCM3. Part I: Model validation and interannual variability. *Theoretical and Applied Climatology*, 86(1-4), 23-37. https://doi.org/10.1007/s00704-005-0202-8

African Development Bank, OECD and United Nations Development Programme. (2016). *African Economic Outlook 2016: Sustainable Cities and Structural Transformation*. https://doi.org/10.1787/aeo-2016-en

Ajay, P., Pathak, B., Solmon, F., Bhuyan, P. K. and Giorgi, F. (2019). Obtaining best parameterization scheme of RegCM 4.4 for aerosols and chemistry simulations over the CORDEX South Asia. *Climate Dynamics*. https://doi.org/10.1007/s00382-018-4587-3

Akinsanola, A. A., Ogunjobi, K. O., Gbode, I. E. and Ajayi, V. O. (2015). Assessing the Capabilities of Three Regional Climate Models over CORDEX Africa in Simulating West African Summer Monsoon Precipitation. *Advances in Meteorology*, 2015, 1-13. https://doi.org/10.1155/2015/935431

Akinsanola, A. A. and Ogunjobi, K. O. (2017). Evaluation of present-day rainfall simulations over West Africa in CORDEX regional climate models. *Environmental Earth Sciences*, 76(10). https://doi.org/10.1007/s12665-017-6691-9

Alaka, G. J. and Maloney, E. D. (2017). Internal Intraseasonal Variability of the West African Monsoon in WRF. *Journal of Climate*, 30(15), 5815-5833. https://doi.org/10.1175/JCLI-D-16-0750.1

Albergel, C., Dutra, E., Munier, S., Calvet, J.-C., Munoz-Sabater, J., de Rosnay, P. and Balsamo, G. (2018). ERA-5 and ERA-Interim driven ISBA land surface model simulations: Which one performs better? *Hydrology and Earth System Sciences*, 22(6), 3515-3532. https://doi.org/10.5194/hess-22-3515-2018

Alcala, A. C. and Russ, G. R. (2006). No-take Marine Reserves and Reef Fisheries Management in the Philippines: A New People Power Revolution. *AMBIO: A Journal of the Human Environment*, 35(5), 245-254. https://doi.org/10.1579/05-A-054R1.1

Anthes, R. A. (1977). A Cumulus Parameterization Scheme Utilizing a One-Dimensional Cloud Model. *Monthly Weather Review*, 105(3), 270-286. https://doi.org/10.1175/1520-0493(1977)105<0270:ACPSUA>2.0.CO;2

Arakawa, A. and Schubert, W. H. (1974). Interaction of a Cumulus Cloud Ensemble with the Large-Scale Environment, Part I. *Journal of the Atmospheric Sciences*, 31(3), 674-701. https://doi.org/10.1175/1520-0469(1974)031<0674:IOACCE>2.0.CO;2

Argüeso, D., Evans, J. P., Fita, L. and Bormann, K. J. (2014). Temperature response to future urbanization and climate change. *Climate Dynamics*, 42(7-8), 2183-2199. https://doi.org/10.1007/s00382-013-1789-6

Argüeso, D., Evans, J. P., Pitman, A. J. and Di Luca, A. (2015). Effects of City Expansion on Heat Stress under Climate Change Conditions. *PLOS ONE,* 10(2), e0117066. https://doi.org/10.1371/journal.pone.0117066

Atkinson, B. W. (2003). Numerical Modelling of Urban Heat-Island Intensity. *Boundary-Layer Meteorology*, 109(3), 285-310. https://doi.org/10.1023/A:1025820326672

Bai, X., Shi, P. and Liu, Y. (2014). Society: Realizing China's urban dream. *Nature*, 509(7499), 158-160. https://doi.org/10.1038/509158a

Balogun, A. A., Balogun, I. A. and Adeyewa, Z. D. (2010). Comparisons of urban and rural heat stress conditions in a hot–humid tropical city. *Global Health Action*, 3(1), 5614. https://doi.org/10.3402/gha.v3i0.5614

Bamba, A., Diallo, I., Touré, N. E., Kouadio, K., Konaré, A., Dramé, M. S., Diedhiou, A., Silué, S., Doumbia, M., and Tall, M. (2018). Effect of the African greenbelt position on West African summer climate: A regional climate modeling study. *Theoretical and Applied Climatology*. https://doi.org/10.1007/s00704-018-2589-z

Bayo Omotosho, J. (1985). The separate contributions of line squalls, thunderstorms and the monsoon to the total rainfall in nigeria. *Journal of Climatology*, 5(5), 543-552. https://doi.org/10.1002/joc.3370050507

Beauchemin, C. and Bocquier, P. (2004). Migration and Urbanisation in Francophone West Africa: An Overview of the Recent Empirical Evidence. *Urban Studies*, 41(11), 2245-2272. https://doi.org/10.1080/0042098042000268447

Bony, S., Stevens, B., Frierson, D. M. W., Jakob, C., Kageyama, M., Pincus, R., Shepherd, T. G., Sherwood, S. C., Siebesma, A. P., Sobel, A. H., Watanabe, M., and Webb, M. J. (2015). Clouds, circulation and climate sensitivity. *Nature Geoscience*, 8(4), 261-268. https://doi.org/10.1038/ngeo2398

Boone, A. A., Xue, Y., De Sales, F., Comer, R. E., Hagos, S., Mahanama, S., Schiro, K., Song, G., Wang, G., Li, S. and Mechoso, C. R. (2016). The regional impact of Land-Use Land-cover Change (LULCC) over West Africa from an ensemble of global climate models under the auspices of the WAMME2 project. *Climate Dynamics*, 47(11), 3547-3573. https://doi.org/10.1007/s00382-016-3252-y

Boucher O., Randall D., Artaxo P., Bretherton C., Feingold G., Forster P., Kerminen, V. M., Liao, H., Lohmann, U., Rasch, P., Sherwood, S., Bjorn, S. B. and Zhang X.Y. (2013). Clouds and Aerosols. In: Climate Change 2013: The Physical Science Basis. Contribution of Working Group I to the Fifth Assessment Report of the Intergovernmental Panel on Climate Change [Stocker, T.F., D. Qin, G.-K. Plattner, M. Tignor, S.K. Allen, J. Boschung, A. Nauels, Y. Xia, V. Bex and P.M. Midgley (eds.)]. Cambridge University Press, Cambridge, United Kingdom and New York, NY, USA. https://pure.mpg.de/rest/items/item_2007900/component/file_2007948/content

Briegleb, B. P. (1992). Delta-Eddington approximation for solar radiation in the NCAR community climate model. *Journal of Geophysical Research*, 97(D7), 7603. https://doi.org/10.1029/92JD00291

Browne, N. A. K. and Sylla, M. B. (2012). Regional Climate Model Sensitivity to Domain Size for the Simulation of the West African Summer Monsoon Rainfall. *International Journal of Geophysics*, 2012, 1-17. https://doi.org/10.1155/2012/625831

Burdett M. (2018). Urban growth projections https://geographycasestudysite.wordpress.com/urban-growth-to-2050/

Burpee, R. W. (1972). The Origin and Structure of Easterly Waves in the Lower Troposphere of North Africa. *Journal of the Atmospheric Sciences*, 29(1), 77-90. https://doi.org/10.1175/1520-0469(1972)029<0077:TOASOE>2.0.CO;2

Cao, Q., Yu, D., Georgescu, M. and Wu, J. (2016). Impacts of urbanization on summer climate in China: An assessment with coupled land-atmospheric modeling: Impacts of urbanization on climate. *Journal of Geophysical Research: Atmospheres*, 121(18), 10,505-10,521. https://doi.org/10.1002/2016JD025210

Cao, Q., Yu, D., Georgescu, M., Wu, J. and Wang, W. (2018). Impacts of future urban expansion on summer climate and heat-related human health in eastern China. *Environment International*, 112, 134-146. https://doi.org/10.1016/j.envint.2017.12.027

Cárdenas Rodríguez, M., Dupont-Courtade, L. and Oueslati, W. (2016). Air pollution and urban structure linkages: Evidence from European cities. *Renewable and Sustainable Energy Reviews*, 53, 1-9. https://doi.org/10.1016/j.rser.2015.07.190

Charney, J. G. and Stern, M. E. (1962). On the Stability of Internal Baroclinic Jets in a Rotating Atmosphere. *Journal of the Atmospheric Sciences*, 19(2), 159-172. https://doi.org/10.1175/1520-0469(1962)019<0159:OTSOIB>2.0.CO;2

Charney, J. G. (1975). Dynamics of deserts and drought in the Sahel. *Quarterly Journal of the Royal Meteorological Society*, 101(428), 193-202. https://doi.org/10.1002/qj.49710142802

Chen, H. and Zhang, Y. (2013). Sensitivity experiments of impacts of large-scale urbanization in East China on East Asian winter monsoon. *Chinese Science Bulletin*, 58(7), 809–815. https://doi.org/10.1007/s11434-012-5579-z

Chen, J., Chen, J., Liao, A., Cao, X., Chen, L., Chen, X., He, C., Han, G., Peng, S., Lu, M., Zhang, W., Tong, X. and Mills, J. (2015). Global land cover mapping at 30m resolution: A POK-based operational approach. *ISPRS Journal of Photogrammetry and Remote Sensing*, 103, 7-27. https://doi.org/10.1016/j.isprsjprs.2014.09.002

Chen, L. and Frauenfeld, O. W. (2016). Impacts of urbanization on future climate in China. *Climate Dynamics*, 47(1-2), 345-357. https://doi.org/10.1007/s00382-015-2840-6

Chen, M., Shi, W., Xie, P., Silva, V. B. S., Kousky, V. E., Wayne Higgins, R. and Janowiak, J. E. (2008). Assessing objective techniques for gauge-based analyses of global daily precipitation. *Journal of Geophysical Research*, 113(D4). https://doi.org/10.1029/2007JD009132

Chen, Q., Yin, Y., Jin, L., Xiao, H. and Zhu, S. (2011). The effect of aerosol layers on convective cloud microphysics and precipitation. *Atmospheric Research*, 101(1-2), 327-340. https://doi.org/10.1016/j.atmosres.2011.03.007

Cook, K. H. (1999). Generation of the African Easterly Jet and Its Role in Determining West African Precipitation. *Journal of Climate*, 12(5), 1165-1184. https://doi.org/10.1175/1520-0442(1999)012<1165:GOTAEJ>2.0.CO;2

Cornforth, R. J., Hoskins, B. J. and Thorncroft, C. D. (2009). The impact of moist processes on the African easterly jet-African easterly wave system. *Quarterly Journal of the Royal Meteorological Society*, 135(641), 894-913. https://doi.org/10.1002/qj.414

Daniel, M., Lemonsu, A., Déqué, M., Somot, S., Alias, A. and Masson, V. (2019). Benefits of explicit urban parameterization in regional climate modeling to study climate and city interactions. *Climate Dynamics*, 52(5-6), 2745-2764. https://doi.org/10.1007/s00382-018-4289-x

Diallo, I., Sylla, M. B., Giorgi, F., Gaye, A. T. and Camara, M. (2012). Multimodel GCM-RCM Ensemble-Based Projections of Temperature and Precipitation over West Africa for the Early 21st Century. *International Journal of Geophysics*, 201*2*, 1-19. https://doi.org/10.1155/2012/972896

Diallo, I., Giorgi, F., Deme, A., Tall, M., Mariotti, L. and Gaye, A. T. (2016). Projected changes of summer monsoon extremes and hydroclimatic regimes over West Africa for the twenty-first century. *Climate Dynamics*, 47(12), 3931-3954. https://doi.org/10.1007/s00382-016-3052-4

Diasso, U. and Abiodun, B. J. (2017). Drought modes in West Africa and how well CORDEX RCMs simulate them. *Theoretical and Applied Climatology*, 128(1–2), 223-240. https://doi.org/10.1007/s00704-015-1705-6

Diba, I., Camara, M., Sarr, A. and Diedhiou, A. (2018). Potential Impacts of Land Cover Change on the Interannual Variability of Rainfall and Surface Temperature over West Africa. *Atmosphere*, 9(10), 376. https://doi.org/10.3390/atmos9100376

Dickinson, R. E., Errico, R. M., Giorgi, F. and Bates, G. T. (1989). A regional climate model for the western United States. *Climatic Change*, 15(3). https://doi.org/10.1007/BF00240465

Dickinson, R. E., Henderson-Sellers, A. and Kennedy, P. (1993). Biosphere-atmosphere Transfer Scheme (BATS) Version 1e as Coupled to the NCAR Community Climate Model. https://doi.org/10.5065/D67W6959

Diedhiou, A., Janicot, S., Viltard, A., de Felice, P. and Laurent, H. (1999). Easterly wave regimes and associated convection over West Africa and tropical Atlantic: Results from the NCEP/NCAR and ECMWF reanalyses. *Climate Dynamics*, 15(11), 795-822. https://doi.org/10.1007/s003820050316

Doan, Q. V., Kusaka, H. and Ho, Q. B. (2016). Impact of future urbanization on temperature and thermal comfort index in a developing tropical city: Ho Chi Minh City. *Urban Climate*, 17, 20-31. https://doi.org/10.1016/j.uclim.2016.04.003

Dobigny, G., Gauthier, P., Houéménou, G., Choplin, A., Dossou, H.-J., Badou, S., Etougbétche, J., Koffi, S., Durski, K., Bertherat, E. and Picardeau, M. (2018). Leptospirosis and Extensive Urbanization in West Africa: A Neglected and Underestimated Threat? *Urban Science*, 2(2), 29. https://doi.org/10.3390/urbansci2020029

Dobson, J. E., Edward A. B., Phllllp R. C., Rlchard C. D. and Brian A. W. (2000). LandScan: A Global Population Database for Estimating Populations at Risk. *Photogram. Eng. Rem. Sens*, 66, 849-857.

Dorning, M. A., Koch, J., Shoemaker, D. A. and Meentemeyer, R. K. (2015). Simulating urbanization scenarios reveals tradeoffs between conservation planning strategies. *Landscape and Urban Planning*, 136, 28-39. https://doi.org/10.1016/j.landurbplan.2014.11.011

Dosio, A. and Panitz, H. J. (2016). Climate change projections for CORDEX-Africa with COSMO-CLM regional climate model and differences with the driving global climate models. *Climate Dynamics*, 46(5-6), 1599-1625. https://doi.org/10.1007/s00382-015-2664-4

Douglas, I., Alam, K., Maghenda, M., Mcdonnell, Y., Mclean, L. and Campbell, J. (2008). Unjust waters: Climate change, flooding and the urban poor in Africa. *Environment and Urbanization*, 20(1), 187-205. https://doi.org/10.1177/0956247808089156

Doumbia, E. H. T., Liousse, C., Galy-Lacaux, C., Ndiaye, S. A., Diop, B., Ouafo, M., Assamoi, E. M., Gardrat, E., Castera, P., Rosset, R., Akpo., A. and Sigha, L. (2012). Real time black carbon measurements in West and Central Africa urban sites. *Atmospheric Environment*, 54, 529-537. https://doi.org/10.1016/j.atmosenv.2012.02.005

Elguindi, N., Giorgi, F. and Turuncoglu, U. (2014). Assessment of CMIP5 global model simulations over the subset of CORDEX domains used in the Phase I CREMA. *Climatic Change*, 125(1), 7-21. https://doi.org/10.1007/s10584-013-0935-9

Eltahir, E. A. B. and Gong, C. (1996). Dynamics of Wet and Dry Years in West Africa. *Journal of Climate*, 9(5), 1030-1042. https://doi.org/10.1175/1520-0442(1996)009<1030:DOWADY>2.0.CO;2

Emanuel, K. A. (1991). A Scheme for Representing Cumulus Convection in Large-Scale Models. *Journal of the Atmospheric Sciences*, 48(21), 2313-2329. https://doi.org/10.1175/1520-0469(1991)048<2313:ASFRCC>2.0.CO;2

Emanuel, K. A. and Živković-Rothman, M. (1999). Development and Evaluation of a Convection Scheme for Use in Climate Models. *Journal of the Atmospheric Sciences*, 56(11), 1766-1782. https://doi.org/10.1175/1520-0469(1999)056<1766:DAEOAC>2.0.CO;2

Feng, J. M., Wang, Y. L. and Ma, Z. G. (2015). Long-term simulation of large-scale urbanization effect on the East Asian monsoon. *Climatic Change*, 129(3–4), 511-523. https://doi.org/10.1007/s10584-013-0885-2

Field, C. B. (2014). *Climate Change 2014 – Impacts, Adaptation and Vulnerability: Regional Aspects*. Cambridge University Press.

Fink, A. and Reiner, A. (2003). Spatiotemporal variability of the relation between African Easterly Waves and West African Squall Lines in 1998 and 1999. *Journal of Geophysical Research*, 108(D11). https://doi.org/10.1029/2002JD002816

Fischer, E. M., Oleson, K. W. and Lawrence, D. M. (2012). Contrasting urban and rural heat stress responses to climate change: Heat stress response to climate change. *Geophysical Research Letters*, 39(3). https://doi.org/10.1029/2011GL050576

Fischer, E. M. and Schär, C. (2010). Consistent geographical patterns of changes in high-impact European heatwaves. *Nature Geoscience*, 3(6), 398-403. https://doi.org/10.1038/ngeo866

Fontaine, B., Trzaska, S. and Janicot, S. (1998). Evolution of the relationship between near global and Atlantic SST modes and the rainy season in West Africa: Statistical analyses and sensitivity experiments. *Climate Dynamics*, 14(5), 353-368. https://doi.org/10.1007/s003820050228

Fontaine, B., Philippon, N. and Camberlin, P. (1999). An improvement of June-September rainfall forecasting in the Sahel based upon region April-May moist static energy content (1968-1997). *Geophysical Research Letters*, 26(14), 2041-2044. https://doi.org/10.1029/1999GL900495

Fontaine, B., Garcia-Serrano, J., Roucou, P., Rodriguez-Fonseca, B., Losada, T., Chauvin, F., Gervois, S., Sijikumar, S., Ruti, P. and Janicot, S. (2010). Impacts of warm and cold situations in the Mediterranean basins on the West African monsoon: Observed connection patterns (1979–2006) and climate simulations. *Climate Dynamics*, 35(1), 95-114. https://doi.org/10.1007/s00382-009-0599-3

Fortune, M. (1980). Properties of African Squall Lines Inferred from Time-Lapse Satellite Imagery. *Monthly Weather Review*, 108(2), 153-168. https://doi.org/10.1175/1520-0493(1980)108<0153:POASLI>2.0.CO;2

Gaye, A., Viltard, A. and de Félice, P. (2005). Squall lines and rainfall over Western Africa during summer 1986 and 87. *Meteorology and Atmospheric Physics*, 90(3–4), 215–224. https://doi.org/10.1007/s00703-005-0116-0

Gbobaniyi, E., Sarr, A., Sylla, M. B., Diallo, I., Lennard, C., Dosio, A., Dhiediou, A., Kamga, A., Kluste, N. A. B., Hewitson, B., Nikulin, G. and Lamptey, B. (2014). Climatology, annual cycle and interannual variability of precipitation and temperature in CORDEX simulations over West Africa: CORDEX simulations over West Africa. *International Journal of Climatology*, 34(7), 2241-2257. https://doi.org/10.1002/joc.3834

Georgescu, M., Morefield, P. E., Bierwagen, B. G. and Weaver, C. P. (2014). Urban adaptation can roll back warming of emerging megapolitan regions. *Proceedings of the National Academy of Sciences*, 111(8), 2909-2914. https://doi.org/10.1073/pnas.1322280111

Giorgetta, M. A., Jungclaus, J., Reick, C. H., Legutke, S., Bader, J., Böttinger, M., Brovkin, V., Crueger, T., Esch, M., Fieg, K., Glushak, K., Gayler, V., Haak, H., Hollweg,. H. D., Ilyina, T., Kinne, S., Notz, D., Six, K. D., Wegner, J. and Stevens, B. (2013). Climate and carbon cycle changes from 1850 to 2100 in MPI-ESM simulations for the Coupled Model Intercomparison Project phase 5: Climate Changes in MPI-ESM. *Journal of Advances in Modeling Earth Systems*, 5(3), 572-597. https://doi.org/10.1002/jame.20038

Giorgi, F. and Bates, G. T. (1989). The Climatological Skill of a Regional Model over Complex Terrain. *Monthly Weather Review*, 117(11), 2325-2347. https://doi.org/10.1175/1520-0493(1989)117<2325:TCSOAR>2.0.CO;2

Giorgi, F. and Mearns, L. O. (1991). Approaches to the simulation of regional climate change: A review. *Reviews of Geophysics*, 29(2), 191. https://doi.org/10.1029/90RG02636

Giorgi, F., Marinucci, M. R. and Bates, G. T. (1993). Development of a Second-Generation Regional Climate Model (RegCM2). Part I: Boundary-Layer and Radiative Transfer Processes. *Monthly Weather Review*, 121(10), 2794-2813. https://doi.org/10.1175/1520-0493(1993)121<2794:DOASGR>2.0.CO;2

Giorgi, F. and Mearns, L. O. (1999). Introduction to special section: Regional Climate Modeling Revisited. *Journal of Geophysical Research: Atmospheres*, 104(D6), 6335-6352. https://doi.org/10.1029/98JD02072

Giorgi, F. (2006a). Regional climate modeling: Status and perspectives. *Journal de Physique IV (Proceedings)*, 139(1), 101-118. https://doi.org/10.1051/jp4:2006139008

Giorgi, F., Pal, J. S., Bi, X., Sloan, L., Elguindi, N. and Solmon, F. (2006b). Introduction to the TAC special issue: The RegCNET network. *Theoretical and Applied Climatology*, 86(1–4), 1–4. https://doi.org/10.1007/s00704-005-0199-z

Giorgi, F. and Meleux, F. (2007). Modelling the regional effects of climate change on air quality. *Comptes Rendus Geoscience*, 339(11-12), 721-733. https://doi.org/10.1016/j.crte.2007.08.006

Giorgi, F, Coppola, E., Solmon, F., Mariotti, L., Sylla, M., Bi, X., Elguindi, N., Diro, G.T., Nair, V., Guiliani, G., Turuncoglu, U., Cozzini, S., Güttler, I., O'Brien, T. A., Tawfik, A. B., Stordal, F., Sloan, L. C. and Brankovic, C. (2012). RegCM4: Model description and preliminary tests over multiple CORDEX domains. *Climate Research*, 52, 7-29. https://doi.org/10.3354/cr01018

Giorgi, F. (2014). Introduction to the special issue: The phase I CORDEX RegCM4 hyper-matrix (CREMA) experiment. *Climatic Change*, 125(1), 1-5. https://doi.org/10.1007/s10584-014-1166-4

Grell, G. A. (1993). Prognostic Evaluation of Assumptions Used by Cumulus Parameterizations. *Monthly Weather Review*, 121(3), 764-787. https://doi.org/10.1175/1520-0493(1993)121<0764:PEOAUB>2.0.CO;2

Grell, G. A., Dudhia, J. and Stauffer, D. R. (1994). *A Description of the Fifth-Generation Penn State/NCAR Mesoscale Model (MM5)*. 128.

Grimmond, C. S. B. and Oke, T. R. (1999). Heat Storage in Urban Areas: Local-Scale Observations and Evaluation of a Simple Model. *Journal of Applied Meteorology*, 38(7), 922-940. https://doi.org/10.1175/1520-0450(1999)038<0922:HSIUAL>2.0.CO;2

Grimmond, C. S. B. (2007). Urbanization and global environmental change: Local effects of urban warming. *The Geographical Journal*, 173(1), 83-88. https://doi.org/10.1111/j.1475-4959.2007.232_3.x

Grimmond, C. S. B., Blackett, M., Best, M. J., Baik, J.-J., Belcher, S. E., Beringer, J., Bohnenstengel, S. I.,Calmet, I., Chen, F., Coutts, A., Kawai, T., Kawamoto, Y., Lee, S. H., Martilli, V., Miao, S., Oleson, K., Voogt, J. A., Young, D. T. and Zhang, N. (2011). Initial results from Phase 2 of the international urban energy balance model comparison. *International Journal of Climatology*, 31(2), 244-272. https://doi.org/10.1002/joc.2227

Grist, J. P., Nicholson, S. E. and Barcilon, A. I. (2002). Easterly Waves over Africa. Part II: Observed and Modeled Contrasts between Wet and Dry Years. *Monthly Weather Review*, 130(2), 212-225. https://doi.org/10.1175/1520-0493(2002)130<0212:EWOAPI>2.0.CO;2

Gulia, S., Nagendra, S. M. S., Barnes, J. and Khare, M. (2018). Urban local air quality management framework for non-attainment areas in Indian cities. *Science of The Total Environment*, 619-620, 1308-1318. https://doi.org/10.1016/j.scitotenv.2017.11.123

Hagos, S. M. and Cook, K. H. (2007). Dynamics of the West African Monsoon Jump. *Journal of Climate*, 20(21), 5264-5284. https://doi.org/10.1175/2007JCLI1533.1

Hagos, S. M., Leung, L. R., Xue, Y., Boone, A., de Sales, F., Neupane, N., Huang, M. and Yoon, J. H. (2014). Assessment of uncertainties in the response of the African monsoon precipitation to land use change simulated by a regional model. *Climate Dynamics*, 43(9-10), 2765-2775. https://doi.org/10.1007/s00382-014-2092-x

Hall, N. M. J. and Peyrillé, P. (2006). Dynamics of the West African monsoon. *Journal de Physique IV (Proceedings)*, 139(1), 81-99. https://doi.org/10.1051/jp4:2006139007

Hamdi, R., Van de Vyver, H., De Troch, R. and Termonia, P. (2014). Assessment of three dynamical urban climate downscaling methods: Brussels's future urban heat island under an A1B emission scenario: Brussels's future urban heat island. *International Journal of Climatology*, 34(4), 978-999. https://doi.org/10.1002/joc.3734

Harris, I.C and Jones, P.D. (2017). CRU TS4.01*:* Climatic Research Unit (CRU) Time-Series (TS) version 4.01 of high-resolution gridded data of month-by-month variation in climate *(Jan. 1901- Dec. 2016)*. https://doi.org/10.5285/58a8802721c94c66ae45c3baa4d814d0

Hassan, Z., Shabbir, R., Ahmad, S. S., Malik, A. H., Aziz, N., Butt, A. and Erum, S. (2016). Dynamics of land use and land cover change (LULCC) using geospatial techniques: A case study of Islamabad Pakistan. *SpringerPlus*, 5(1). https://doi.org/10.1186/s40064-016-2414-z

Hersbach, H., and D. Dee. (2016). ERA5 reanalysis is in production. ECMWF Newsletter, No. 147, ECMWF, Reading, United Kingdom, 5-6. https://www.ecmwf.int/sites/default/files/elibrary/2016/16299-newsletter-no147-spring-2016.pdf

Holtslag, A. A. M., De Bruijn, E. I. F. and Pan, H. L. (1990). A High Resolution Air Mass Transformation Model for Short-Range Weather Forecasting. *Monthly Weather Review*, 118(8), 1561-1575. https://doi.org/10.1175/1520-0493(1990)118<1561:AHRAMT>2.0.CO;2

Hourdin, F., Musat, I., Guichard, F., Ruti, P. M., Favot, F., Filiberti, M. A., Pham, M., Grandpeix , J. Y., Polcher, J., Marquet, P., Boone, A., Lafore, J. P., Redelsperger, J. L., Dell, A., Doval, T. L., Traore, A. K. and Gallée, H. (2010). AMMA-Model Intercomparison Project. *Bulletin of the American Meteorological Society*, 91(1), 95-104. https://doi.org/10.1175/2009BAMS2791.1

Huszar, P., Karlický, J., Ďoubalová, J., Šindelářová, K., Nováková, T., Belda, M., Halenka, T., Žák, M. and Pišoft, P. (2019). The urban canopy meteorological forcing and its impact on ozone and PM2.5: Role of the vertical turbulent transport. *Atmospheric Chemistry and Physics Discussions*, 1-58. https://doi.org/10.5194/acp-2019-486

IFRC. (2010). World Disasters Report 2010: Focus on Urban Risk. International Federation of Red Cross and Red Crescent Societies (IFRC), Geneva, Switzer. https://www.ifrc.org/Global/Publications/disasters/WDR/WDR2010-full.pdf

Ilyina, T., Six, K. D., Segschneider, J., Maier-Reimer, E., Li, H. and Núñez-Riboni, I. (2013). Global ocean biogeochemistry model HAMOCC: Model architecture and performance as component of the MPI-Earth system model in different CMIP5 experimental realizations: The Model Hamocc within Mpi-Esm in Cmip5. *Journal of Advances in Modeling Earth Systems*, 5(2), 287-315. https://doi.org/10.1029/2012MS000178

IPCC (Ed.). (2008). *Towards new scenarios for analysis of emissions, climate change, impacts and response strategies: IPCC expert meeting report, 19-21 September 2007, Noordwijkerhout, the Netherlands.* Geneva: IPCC.

Jackson, T. L., Feddema, J. J., Oleson, K. W., Bonan, G. B. and Bauer, J. T. (2010). Parameterization of Urban Characteristics for Global Climate Modeling. *Annals of the Association of American Geographers*, 100(4), 848-865. https://doi.org/10.1080/00045608.2010.497328

Janicot, S. (1992). Spatiotemporal Variability of West African Rainfall. Part II: Associated Surface and Airmass Characteristics. *Journal of Climate*, 5(5), 499-511. https://doi.org/10.1175/1520-0442(1992)005<0499:SVOWAR>2.0.CO;2

Jenkins, G. S., Gaye, A. T. and Sylla, M. B. (2005). Late 20th century attribution of drying trends in the Sahel from the Regional Climate Model (RegCM3): Drying trends in the Sahel from RegCM3. *Geophysical Research Letters*, 32(22). https://doi.org/10.1029/2005GL024225

Jungclaus, J. H., Fischer, N., Haak, H., Lohmann, K., Marotzke, J., Matei, D., Mikolajewicz, U., Notz, D. and von Storch, J. S. (2013). Characteristics of the ocean simulations in the Max Planck Institute Ocean Model (MPIOM) the ocean component of the MPI-Earth system model: Mpiom CMIP5 Ocean Simulations. *Journal of Advances in Modeling Earth Systems*, 5(2), 422-446. https://doi.org/10.1002/jame.20023

Kain, J. S. and Fritsch, J. M. (1990). A One-Dimensional Entraining/Detraining Plume Model and Its Application in Convective Parameterization. *Journal of the Atmospheric Sciences*, 47(23), 2784-2802. https://doi.org/10.1175/1520-0469(1990)047<2784:AODEPM>2.0.CO;2

Kain, J. S. and Fritsch, J. M. (1993). Convective Parameterization for Mesoscale Models: The Kain-Fritsch Scheme. In K. A. Emanuel & D. J. Raymond (Eds.), The Representation of Cumulus Convection in Numerical Models. 165-170. https://doi.org/10.1007/978-1-935704-13-3_16

Kalnay, E., Kanamitsu, M., Kistler, R., Collins, W., Deaven, D., Gandin, L., Iredell, M., Saha, S., White, G., Woollen, J., Zhu, Y., Leetmaa, A., Reynolds, R., Mo, K. C., Wang, J., Jenne, R. and Joseph, D. (1996). The NCEP/NCAR 40-Year Reanalysis Project. *Bulletin of the American Meteorological Society*, 77(3), 437-471. https://doi.org/10.1175/1520-0477(1996)077<0437:TNYRP>2.0.CO;2

Kalnay, E. and Cai, M. (2003). Impact of urbanization and land-use change on climate. *Nature*, 423(6939), 528-531. https://doi.org/10.1038/nature01675

Kaufmann, R. K., Seto, K. C., Schneider, A., Liu, Z., Zhou, L. and Wang, W. (2007). Climate Response to Rapid Urban Growth: Evidence of a Human-Induced Precipitation Deficit. *Journal of Climate*, 20(10), 2299-2306. https://doi.org/10.1175/JCLI4109.1

Kiehl, J., Hack, J., Bonan, G., Boville, B., Briegleb, B., Williamson, D. and Rasch, P. (1996). Description of the NCAR Community Climate Model (CCM3). https://doi.org/10.5065/D6FF3Q99

Kiehl, T., Wolski, J. G., Briegleb, P. and Ramanthan, V. (1987). Documentation of Radiation and Cloud Routines in the NCAR Community Climate Model (CCM1). https://doi.org/10.5065/D6JS9NDG

Kiladis, G. N., Thorncroft, C. D. and Hall, N. M. J. (2006). Three-Dimensional Structure and Dynamics of African Easterly Waves. Part I: Observations. *Journal of the Atmospheric Sciences*, 63(9), 2212-2230. https://doi.org/10.1175/JAS3741.1

Kithiia, J. (2011). Climate change risk responses in East African cities: Need, barriers and opportunities. *Current Opinion in Environmental Sustainability*, 3(3), 176-180. https://doi.org/10.1016/j.cosust.2010.12.002

Knippertz, P., Coe, H., Chiu, J. C., Evans, M. J., Fink, A. H., Kalthoff, N., Liousse, C., Mari, C., Allan, R. B., Brooks, B., Danou, S., Flamant, C., Jegede, O. O., Lohou, F. and Marsham, J. H. (2015a). The DACCIWA Project: Dynamics–Aerosol–Chemistry–Cloud Interactions in West Africa. *Bulletin of the American Meteorological Society*, *96*(9), 1451-1460. https://doi.org/10.1175/BAMS-D-14-00108.1

Knippertz, P., Evans, M. J., Field, P. R., Fink, A. H., Liousse, C. and Marsham, J. H. (2015b). The possible role of local air pollution in climate change in West Africa. *Nature Climate Change*, 5(9), 815-822. https://doi.org/10.1038/nclimate2727

Kueppers, L. M., Snyder, M. A. and Sloan, L. C. (2007). Irrigation cooling effect: Regional climate forcing by land-use change. *Geophysical Research Letters*, 34(3). https://doi.org/10.1029/2006GL028679

Kumar, P., Gulia, S., Harrison, R. M. and Khare, M. (2017). The influence of odd–even car trial on fine and coarse particles in Delhi. *Environmental Pollution*, 225, 20–30. https://doi.org/10.1016/j.envpol.2017.03.017

Kuo, H. L. (1974). Further Studies of the Parameterization of the Influence of Cumulus Convection on Large-Scale Flow. *Journal of the Atmospheric Sciences*, 31(5), 1232-1240. https://doi.org/10.1175/1520-0469(1974)031<1232:FSOTPO>2.0.CO;2

Lafore, J. P., Flamant, C., Giraud, V., Guichard, F., Knippertz, P., Mahfouf, J. F., Mascart, P., Williams, P. and Williams, E. R. (2010). Introduction to the AMMA Special Issue on 'Advances in understanding atmospheric processes over West Africa through the AMMA field campaign.' *Quarterly Journal of the Royal Meteorological Society*, 136(S1), 2-7. https://doi.org/10.1002/qj.583

Lamptey, B., Barron, E. and Pollard, D. (2005). Impacts of agriculture and urbanization on the climate of the Northeastern United States. *Global and Planetary Change*, 49(3-4), 203-221. https://doi.org/10.1016/j.gloplacha.2005.10.001

Landsberg, H. E. (1981). *The Urban Climate*. Academic Press.

Landsea, C. W. and Gray, W. M. (1992). The Strong Association between Western Sahelian Monsoon Rainfall and Intense Atlantic Hurricanes. *Journal of Climate*, 5(5), 435-453. https://doi.org/10.1175/1520-0442(1992)005<0435:TSABWS>2.0.CO;2

Laurent, H., D'Amato, N. and Lebel, T. (1998). How important is the contribution of the mesoscale convective complexes to the Sahelian rainfall? *Physics and Chemistry of the Earth*, 23(5-6), 629-633. https://doi.org/10.1016/S0079-1946(98)00099-8

Laux, P., Nguyen, P. N. B., Cullmann, J. and Kunstmann, H. (2017). Impacts of Land-Use/Land-Cover Change and Climate Change on the Regional Climate in the Central Vietnam. In A. Nauditt & L. Ribbe (Eds.), *Land Use and Climate Change Interactions in Central Vietnam*. 143-151. https://doi.org/10.1007/978-981-10-2624-9_9

Lavaysse, C., Flamant, C. and Janicot, S. (2009). Regional-scale convection patterns during strong and weak phases of the Saharan heat low. *Atmospheric Science Letters*, 11(4), 255-264. https://doi.org/10.1002/asl.284

Lebel, T. and Ali, A. (2009). Recent trends in the Central and Western Sahel rainfall regime (1990–2007). *Journal of Hydrology*, 375(1-2), 52-64. https://doi.org/10.1016/j.jhydrol.2008.11.030

Legates, D. R. and Willmott, C. J. (1990). Mean seasonal and spatial variability in gauge-corrected, global precipitation. *International Journal of Climatology*, 10(2), 111-127. https://doi.org/10.1002/joc.3370100202

Lemonsu, A., Viguié, V., Daniel, M. and Masson, V. (2015). Vulnerability to heat waves: Impact of urban expansion scenarios on urban heat island and heat stress in Paris (France). *Urban Climate*, 14, 586-605. https://doi.org/10.1016/j.uclim.2015.10.007

Li, Weibiao, Chen, S., Chen, G., Sha, W., Luo, C., Feng, Y., Wen, Z. and Wang, B. (2011). Urbanization signatures in strong versus weak precipitation over the Pearl River Delta metropolitan regions of China. *Environmental Research Letters*, 6(3), 034020. https://doi.org/10.1088/1748-9326/6/3/034020

Li, Weiyue, He, X., Scaioni, M., Yao, D., Mi, C., Zhao, J.,Chen, Y., Gao, J. and Li, X. (2019). Annual precipitation and daily extreme precipitation distribution: Possible trends from 1960 to 2010 in urban areas of China. *Geomatics, Natural*

Hazards and Risk, 10(1), 1694-1711. https://doi.org/10.1080/19475705.2019.1609604

Liang, C., Li, D., Yuan, Z., Liao, Y., Nie, X., Huang, B., Wu, X. and Xie, Z. (2019). Assessing urban flood and drought risks under climate change, China. *Hydrological Processes*, 33(9), 1349-1361. https://doi.org/10.1002/hyp.13405

Liaqut, A., Younes, I., Sadaf, R. and Zafar, H. (2019). Impact of Urbanization Growth on Land Surface Temperature using remote sensing and GIS: A Case Study of Gujranwala City, Punjab, Pakistan. *International Journal of Economic and Environmental Geology*, 44-49.

Ma, H., Jiang, Z., Song, J., Dai, A., Yang, X. and Huo, F. (2016). Effects of urban land-use change in East China on the East Asian summer monsoon based on the CAM5.1 model. *Climate Dynamics*, 46(9-10), 2977-2989. https://doi.org/10.1007/s00382-015-2745-4

Mahmood, R., Pielke, R. A., Hubbard, K. G., Niyogi, D., Dirmeyer, P. A., McAlpine, C., Carleton, A. M., Hale, R., Gameda, S., Beltrán-Przekurat, A., Legates, D. R., Du, J., Nair, U. S. and Fall, S. (2014). Land cover changes and their biogeophysical effects on climate: Land cover changes and their biogeophysical effects on climate. *International Journal of Climatology*, 34(4), 929-953. https://doi.org/10.1002/joc.3736

Martilli, A., Clappier, A. and Rotach, M. W. (2002). An Urban Surface Exchange Parameterisation for Mesoscale Models. *Boundary-Layer Meteorology*, 104(2), 261-304. https://doi.org/10.1023/A:1016099921195

Martin, A. C., Cornwell, G. C., Atwood, S. A., Moore, K. A., Rothfuss, N. E., Taylor, H., DeMott, P. J., Kreidenweis, S. M., Petters M. D. and Prather, K. A. (2017). Transport of pollution to a remote coastal site during gap flow from California's

interior: Impacts on aerosol composition, clouds, and radiative balance. *Atmospheric Chemistry and Physics*, 17(2), 1491-1509. https://doi.org/10.5194/acp-17-1491-2017

Martin, G. M., Peyrillé, P., Roehrig, R., Rio, C., Caian, M., Bellon, G., Cordon, F., Lafore, J. P., Poan, D. E. and Idelkadi, A. (2017). Understanding the West African Monsoon from the analysis of diabatic heating distributions as simulated by climate models: WAM diabatic heating distributions. *Journal of Advances in Modeling Earth Systems*, 9(1), 239-270. https://doi.org/10.1002/2016MS000697

Maynard, K., Royer, J. F. and Chauvin, F. (2002). Impact of greenhouse warming on the West African summer monsoon. *Climate Dynamics*, 19(5-6), 499-514. https://doi.org/10.1007/s00382-002-0242-z

McCarthy, M. P., Best, M. J. and Betts, R. A. (2010). Climate change in cities due to global warming and urban effects: climate change in cities. *Geophysical Research Letters*, 37(9). https://doi.org/10.1029/2010GL042845

McCarty, J. and Kaza, N. (2015). Urban form and air quality in the United States. *Landscape and Urban Planning*, 139, 168-179. https://doi.org/10.1016/j.landurbplan.2015.03.008

Miao, S., Chen, F., LeMone, M. A., Tewari, M., Li, Q. and Wang, Y. (2009). An Observational and Modeling Study of Characteristics of Urban Heat Island and Boundary Layer Structures in Beijing. *Journal of Applied Meteorology and Climatology*, 48(3), 484-501. https://doi.org/10.1175/2008JAMC1909.1

Miao, S., Chen, F., Li, Q. and Fan, S. (2011). Impacts of Urban Processes and Urbanization on Summer Precipitation: A Case Study of Heavy Rainfall in Beijing on 1 August 2006. *Journal of Applied Meteorology and Climatology*, 50(4), 806-825. https://doi.org/10.1175/2010JAMC2513.1

Miao, Y., Liu, S., Zheng, Y., Wang, S. and Chen, B. (2015). Numerical Study of the Effects of Topography and Urbanization on the Local Atmospheric Circulations over the Beijing-Tianjin-Hebei, China. *Advances in Meteorology*, *2015*, 1-16. https://doi.org/10.1155/2015/397070

Moss, R. H., Edmonds, J. A., Hibbard, K. A., Manning, M. R., Rose, S. K., van Vuuren, D. P., Carter, T. R., Emori., S., Kainuma., M., Kram, T., Meehl, G. A., Mitchell, J. F. B., Nakicenovic, N., Riahi, K., Smith, S. J., Stouffer, R. J.,Thomson, A. M., Weyant, J. P. and Wilbanks, T. J. (2010). The next generation of scenarios for climate change research and assessment. *Nature*, 463(7282), 747-756. https://doi.org/10.1038/nature08823

Mote, T. L., Lacke, M. C. and Shepherd, J. M. (2007). Radar signatures of the urban effect on precipitation distribution: A case study for Atlanta, Georgia. *Geophysical Research Letters*, 34(20). https://doi.org/10.1029/2007GL031903

Niang, I., Ruppel, O. C., Abdrabo, M. A., Essel, A., Lennard, C., Padgham, J. and Urquhart, P. (2014). *Africa. In: Climate Change 2014: Impacts, Adaptation, and Vulnerability. Part B: Regional Aspects. Contribution of Working Group II to the Fifth Assessment Report of the Intergovernmental Panel on Climate Change.Cambridge, UK: Cambridge University Press*. 67.

Nicholson, S. (2001). Climatic and environmental change in Africa during the last two centuries. *Climate Research*, 17, 123-144. https://doi.org/10.3354/cr017123

Nicholson, S. E. and Grist, J. P. (2001). A conceptual model for understanding rainfall variability in the West African Sahel on interannual and interdecadal timescales. *International Journal of Climatology*, 21(14), 1733-1757. https://doi.org/10.1002/joc.648

Nicholson, S. E. and Grist, J. P. (2003). The Seasonal Evolution of the Atmospheric Circulation over West Africa and Equatorial Africa. *Journal of Climate*, 16(7), 1013-1030. https://doi.org/10.1175/1520-0442(2003)016<1013:TSEOTA>2.0.CO;2

Nicholson, S. E. (2008). The intensity, location and structure of the tropical rainbelt over west Africa as factors in interannual variability. *International Journal of Climatology*, 28(13), 1775-1785. https://doi.org/10.1002/joc.1507

Nicholson, S. E. (2013). The West African Sahel: A Review of Recent Studies on the Rainfall Regime and Its Interannual Variability. *ISRN Meteorology*, 2013, 1-32. https://doi.org/10.1155/2013/453521

Nikulin, G., Jones, C., Giorgi, F., Asrar, G., Büchner, M., Cerezo-Mota, R., Christensen, O. B., Déqué, M., Fernandez, J., Hänsler, A., van Meijgaard, E., Samuelsson, P., Sylla, M. B. and Sushama, L. (2012). Precipitation Climatology in an Ensemble of CORDEX-Africa Regional Climate Simulations. *Journal of Climate*, 25(18), 6057-6078. https://doi.org/10.1175/JCLI-D-11-00375.1

Nithila Devi, N., Sridharan, B. and Kuiry, S. N. (2019). Impact of urban sprawl on future flooding in Chennai city, India. *Journal of Hydrology*, 574, 486-496. https://doi.org/10.1016/j.jhydrol.2019.04.041

Niyogi, D., Lei, M., Kishtawal, C., Schmid, P. and Shepherd, M. (2017). Urbanization Impacts on the Summer Heavy Rainfall Climatology over the Eastern United States. *Earth Interactions*, 21(5), 1-17. https://doi.org/10.1175/EI-D-15-0045.1

Oke, T. R. (1981). Canyon geometry and the nocturnal urban heat island: Comparison of scale model and field observations. *Journal of Climatology*, 1(3), 237-254. https://doi.org/10.1002/joc.3370010304

Oke, T. R. (1987). *Boundary Layer Climates (2nd edition). Routledge, London.* https://www.academia.edu/16752781/T._R._Oke_-_Boundary_Layer_Climates_1988_.PDF

Oleson, K. W., Bonan, G. B., Feddema, J., Vertenstein, M. and Grimmond, C. S. B. (2008a). An Urban Parameterization for a Global Climate Model. Part I: Formulation and Evaluation for Two Cities. *Journal of Applied Meteorology and Climatology*, 47(4), 1038-1060. https://doi.org/10.1175/2007JAMC1597.1

Oleson, K. W., Niu, G.-Y., Yang, Z. L., Lawrence, D. M., Thornton, P. E., Lawrence, P. J., Stöckli R., Dickinson, R. E., Bonan, G. B., Levis, S., Dai, A. and Qian, T. (2008b). Improvements to the Community Land Model and their impact on the hydrological cycle: Community Land Model Hydrology. *Journal of Geophysical Research: Biogeosciences*, 113(G1). https://doi.org/10.1029/2007JG000563

Oleson, K. W., Bonan, G. B. and Feddema, J. (2010a). Effects of white roofs on urban temperature in a global climate model: Effects of white roofs on temperature. *Geophysical Research Letters*, 37(3). https://doi.org/10.1029/2009GL042194

Oleson, W., Bonan, B., Feddema, J., Vertenstein, M. and Kluzek, E. (2010b). *Technical Description of an Urban Parameterization for the Community Land Model (CLMU)*. https://doi.org/10.5065/D6K35RM9

Oleson, K. W., Bonan, G. B., Feddema, J. and Jackson, T. (2011). An examination of urban heat island characteristics in a global climate model. *International Journal of Climatology*, 31(12), 1848-1865. https://doi.org/10.1002/joc.2201

Oleson, K. (2012). Contrasts between Urban and Rural Climate in CCSM4 CMIP5 Climate Change Scenarios. *Journal of Climate*, 25(5), 1390-1412. https://doi.org/10.1175/JCLI-D-11-00098.1

Oleson, K., Lawrence, D., Bonan, G., Drewniak, B., Huang, M., Koven, C., Levis, S., Li, F., Riley, W., Subin, Z., Swenson, S., Thornton, P., Bozbiyik, P., Fisher, R., Head, C., Leung, L., Sun, Y., Tang, J. and Yang, Z. L. (2013). *Technical description of version 4.5 of the Community Land Model (CLM)*. https://doi.org/10.5065/D6RR1W7M

Oleson, K. W., Monaghan, A., Wilhelmi, O., Barlage, M., Brunsell, N., Feddema, J., Hu, L. and Steinhoff, D. F. (2015). Interactions between urbanization, heat stress, and climate change. *Climatic Change*, 129(3-4), 525-541. https://doi.org/10.1007/s10584-013-0936-8

Paeth, H., Born, K., Girmes, R., Podzun, R. and Jacob, D. (2009). Regional Climate Change in Tropical and Northern Africa due to Greenhouse Forcing and Land Use Changes. *Journal of Climate*, 22(1), 114-132. https://doi.org/10.1175/2008JCLI2390.1

Pal, J. S., Small, E. E. and Eltahir, E. A. B. (2000). Simulation of regional-scale water and energy budgets: Representation of subgrid cloud and precipitation processes within RegCM. *Journal of Geophysical Research: Atmospheres*, 105(D24), 29579-29594. https://doi.org/10.1029/2000JD900415

Pal, J. S., Giorgi, F., Bi, X., Elguindi, N., Solmon, F., Gao, X., Rauscher, S. A., Francisco, R., Zakey, A., Bell, J. L., Konare, A., Martinez, D., Sloan, L. C. and Steiner, A. L. (2007). Regional Climate Modeling for the Developing World: The ICTP RegCM3 and RegCNET. *Bulletin of the American Meteorological Society*, 88(9), 1395-1410. https://doi.org/10.1175/BAMS-88-9-1395

Paranunzio, R., Ceola, S., Laio, F. and Montanari, A. (2019). Evaluating the Effects of Urbanization Evolution on Air Temperature Trends Using Nightlight Satellite Data. *Atmosphere*, 10(3), 117. https://doi.org/10.3390/atmos10030117

Parker, D. J., Thorncroft, C. D., Burton, R. R. and Diongue-Niang, A. (2005). Analysis of the African Easterly Jet, using aircraft observations from the JET2000 experiment. *Quarterly Journal of the Royal Meteorological Society*, 131(608), 1461-1482. https://doi.org/10.1256/qj.03.189

Pielke, R. A., Pitman, A., Niyogi, D., Mahmood, R., McAlpine, C., Hossain, F., Goldewijk, K. K., Nair, U., Betts, R., Fall, S., Reichstein, M., Kabat., P. and de Noblet, N. (2011). Land use/land cover changes and climate: Modeling analysis and observational evidence: Land use/land cover changes and climate: modeling analysis and observational evidence. *Wiley Interdisciplinary Reviews: Climate Change*, 2(6), 828-850. https://doi.org/10.1002/wcc.144

Pielke, R. A., Marland, G., Betts, R. A., Chase, T. N., Eastman, J. L., Niles, J. O., Niyogi, D. S. and Running, S. W. (2002). The influence of land-use change and landscape dynamics on the climate system: Relevance to climate-change policy beyond the radiative effect of greenhouse gases. *Philosophical Transactions of the Royal Society of London. Series A: Mathematical, Physical and Engineering Sciences*, 360(1797), 1705-1719. https://doi.org/10.1098/rsta.2002.1027

Quesada, B., Devaraju, N., de Noblet-Ducoudré, N. and Arneth, A. (2017). Reduction of monsoon rainfall in response to past and future land use and land cover changes: Reduced Monsoon Rainfall Due To LULCC. *Geophysical Research Letters*, 44(2), 1041-1050. https://doi.org/10.1002/2016GL070663

Raj, J., Bangalath, H. K. and Stenchikov, G. (2019). West African Monsoon: Current state and future projections in a high-resolution AGCM. *Climate Dynamics*, 52(11), 6441-6461. https://doi.org/10.1007/s00382-018-4522-7

Redelsperger, J.-L., Thorncroft, C. D., Diedhiou, A., Lebel, T., Parker, D. J. and Polcher, J. (2006). African Monsoon Multidisciplinary Analysis: An International Research Project and Field Campaign. *Bulletin of the American Meteorological Society*, 87(12), 1739-1746. https://doi.org/10.1175/BAMS-87-12-1739

Reed, R. J., Norquist, D. C. and Recker, E. E. (1977). The Structure and Properties of African Wave Disturbances as Observed During Phase III of GATE. *Monthly Weather Review*, 105(3), 317-333. https://doi.org/10.1175/1520-0493(1977)105<0317:TSAPOA>2.0.CO;2

Reick, C. H., Raddatz, T., Brovkin, V. and Gayler, V. (2013). Representation of natural and anthropogenic land cover change in MPI-ESM: Land Cover in MPI-ESM. *Journal of Advances in Modeling Earth Systems*, 5(3), 459-482. https://doi.org/10.1002/jame.20022

Revi, D. E. S. A., Fernando Aragón-Durand, J. C. M., Robert B. R., Kiunsi, M. P. and William Solecki. (2014). Urban areas. In: Climate Change 2014: Impacts, Adaptation, and Vulnerability. Part A: Global and Sectoral Aspects. Contribution of Working Group II to the Fifth Assessment Report of the Intergovernmental Panel on Climate Change. In *Cambridge University Press, Cambridge, United Kingdom and New York, NY, USA*. 535-612.

Richard A. Anthes, Eirh-Yu Hsie and Ying-Hwa Kuo. (1987). *Description of the l Penn State/NCAR Mesoscale Model Version 4 (MM4)*.

Rizwan, A. M., Dennis, L. Y. C. and Liu, C. (2008). A review on the generation, determination and mitigation of Urban Heat Island. *Journal of Environmental Sciences*, 20(1), 120-128. https://doi.org/10.1016/S1001-0742(08)60019-4

Rodríguez-Fonseca, B., Janicot, S., Mohino, E., Losada, T., Bader, J., Caminade, C., Chauvin, F., Fontaine, B., Garcìa-Serrano, J., Gervois, S., Joly, M., Polo, I., Ruti, P., Roucou, P. and Voldoire, A. (2011). Interannual and decadal SST-forced responses of the West African monsoon. *Atmospheric Science Letters*, 12(1), 67-74. https://doi.org/10.1002/asl.308

Rosenzweig, C., William D. Solecki, Stephen A. Hammer and Shagun Mehrotra (Eds.). (2011). *Climate change and cities: First assessment report of the Urban Climate Change Research Network*. Cambridge : New York: Cambridge University Press.

Schlueter, A., Fink, A. H., Knippertz, P. and Vogel, P. (2019). A Systematic Comparison of Tropical Waves over Northern Africa. Part I: Influence on Rainfall. *Journal of Climate*, *32*(5), 1501-1523. https://doi.org/10.1175/JCLI-D-18-0173.1

Schneck, R., Reick, C. H. and Raddatz, T. (2013). Land contribution to natural CO_2 variability on time scales of centuries: Land Contribution to CO_2 Variability. *Journal of Advances in Modeling Earth Systems*, 5(2), 354-365. https://doi.org/10.1002/jame.20029

Seto, Karen C., Fragkias, M., Güneralp, B. and Reilly, M. K. (2011). A Meta-Analysis of Global Urban Land Expansion. *PLoS ONE*, 6(8), e23777. https://doi.org/10.1371/journal.pone.0023777

Seto, K. C., Guneralp, B. and Hutyra, L. R. (2012). Global forecasts of urban expansion to 2030 and direct impacts on biodiversity and carbon pools. *Proceedings of the National Academy of Sciences*, 109(40), 16083-16088. https://doi.org/10.1073/pnas.1211658109

Seto, Karen C. and Reenberg, A. (2014). *Rethinking Global Land Use in an Urban Era*. MIT Press.

Shao, H., Song, J. and Ma, H. (2013). Sensitivity of the East Asian Summer Monsoon Circulation and Precipitation to an Idealized Large-Scale Urban Expansion. *Journal of the Meteorological Society of Japan. Ser. II*, 91(2), 163-177. https://doi.org/10.2151/jmsj.2013-205

Shepherd, J. M., Pierce, H. and Negri, A. J. (2002). Rainfall Modification by Major Urban Areas: Observations from Spaceborne Rain Radar on the TRMM Satellite. *Journal of Applied Meteorology*, 41(7), 689-701. https://doi.org/10.1175/1520-0450(2002)041<0689:RMBMUA>2.0.CO;2

Shepherd, J. M., Carter, M., Manyin, M., Messen, D. and Burian, S. (2010). The Impact of Urbanization on Current and Future Coastal Precipitation: A Case Study for Houston. *Environment and Planning B: Planning and Design*, 37(2), 284-304. https://doi.org/10.1068/b34102t

Skinner, C. B. and Diffenbaugh, N. S. (2013). The contribution of African Easterly Waves to monsoon precipitation in the CMIP3 ensemble: AEWs and precipitation in CMIP3. *Journal of Geophysical Research: Atmospheres*, 118(9), 3590-3609. https://doi.org/10.1002/jgrd.50363

Stevens, B., Giorgetta, M., Esch, M., Mauritsen, T., Crueger, T., Rast, S., Salzmann, M., Schmidt, H., Bader, J., Block, K., Fast, I., Kinne, S., Lohmann, U., Pincus, R., Reicher, T. and Roeckner, E. (2013). Atmospheric component of the MPI-M Earth System Model: ECHAM6: ECHAM6. *Journal of Advances in Modeling Earth Systems*, *5(2),* 146-172. https://doi.org/10.1002/jame.20015

Stocker, T. F., Qin, D., Plattner, G.-K., Tignor, M. M. B., Allen, S. K., Boschung, J., Nauels, A., Xia, Y., Bex, V. and Midgley, P. M. (2013). *Working Group I Contribution to the Fifth Assessment Report of the Intergovernmental Panel on Climate Change*. 14.

Stone, B., Vargo, J. and Habeeb, D. (2012). Managing climate change in cities: Will climate action plans work? *Landscape and Urban Planning*, 107(3), 263-271. https://doi.org/10.1016/j.landurbplan.2012.05.014

Sultan, B. and Janicot, S. (2003). The West African Monsoon Dynamics. Part II: The "Preonset" and "Onset" of the Summer Monsoon. *Journal of Climate*, 16(21), 3407-3427. https://doi.org/10.1175/1520-0442(2003)016<3407:TWAMDP>2.0.CO;2

Sultan, B., Baron, C., Dingkuhn, M., Sarr, B. and Janicot, S. (2005). Agricultural impacts of large-scale variability of the West African monsoon. *Agricultural and Forest Meteorology*, 128(1-2), 93-110. https://doi.org/10.1016/j.agrformet.2004.08.005

Sun, R., Lü, Y., Yang, X. and Chen, L. (2018). Understanding the variability of urban heat islands from local background climate and urbanization. *Journal of Cleaner Production*. https://doi.org/10.1016/j.jclepro.2018.10.178

Sun, R., Lü, Y., Yang, X. and Chen, L. (2019). Understanding the variability of urban heat islands from local background climate and urbanization. *Journal of Cleaner Production*, 208, 743-752. https://doi.org/10.1016/j.jclepro.2018.10.178

Sy, S., Noblet-Ducoudré, N., Quesada, B., Sy, I., Dieye, A., Gaye, A. and Sultan, B. (2017). Land-Surface Characteristics and Climate in West Africa: Models' Biases and Impacts of Historical Anthropogenically-Induced Deforestation. *Sustainability*, 9(10), 1917. https://doi.org/10.3390/su9101917

Sylla, M. B., Gaye, A. T., Jenkins, G. S., Pal, J. S. and Giorgi, F. (2010). Consistency of projected drought over the Sahel with changes in the monsoon circulation and extremes in a regional climate model projections. *Journal of Geophysical Research*, 115(D16). https://doi.org/10.1029/2009JD012983

Sylla, M. B., Giorgi, F., Ruti, P. M., Calmanti, S. and Dell'Aquila, A. (2011). The impact of deep convection on the West African summer monsoon climate: A regional climate model sensitivity study. *Quarterly Journal of the Royal Meteorological Society*, 137(659), 1417-1430. https://doi.org/10.1002/qj.853

Sylla, M. B., Giorgi, F. and Stordal, F. (2012). Large-scale origins of rainfall and temperature bias in high-resolution simulations over southern Africa. *Climate Research*, 52, 193-211. https://doi.org/10.3354/cr01044

Sylla, M. B., Giorgi, F., Coppola, E. and Mariotti, L. (2013a). Uncertainties in daily rainfall over Africa: Assessment of gridded observation products and evaluation of a regional climate model simulation: Uncertainties in observed and simulated daily rainfall over Africa. *International Journal of Climatology*, 33(7), 1805-1817. https://doi.org/10.1002/joc.3551

Sylla, M. B., Diallo, I. and Pal, J. S. (2013b). West African Monsoon in State-of-the-Science Regional Climate Models. In A. Tarhule (Ed.), *Climate Variability Regional and Thematic Patterns*. https://doi.org/10.5772/55140

Sylla, M. B., Giorgi, F., Pal, J. S., Gibba, P., Kebe, I. and Nikiema, M. (2015). Projected Changes in the Annual Cycle of High-Intensity Precipitation Events over West Africa for the Late Twenty-First Century. *Journal of Climate*, 28(16), 6475-6488. https://doi.org/10.1175/JCLI-D-14-00854.1

Sylla, M. B., Pal, J. S., Wang, G. L. and Lawrence, P. J. (2016a). Impact of land cover characterization on regional climate modeling over West Africa. *Climate Dynamics*, *46*(1-2), 637-650. https://doi.org/10.1007/s00382-015-2603-4

Sylla, M. B, Nikiema, P. M., Gibba, P., Kebe, I. and Klutse, N. A. B. (2016b). Climate Change over West Africa: Recent Trends and Future Projections. In J. A. Yaro & J. Hesselberg (Eds.), *Adaptation to Climate Change and Variability in Rural West Africa*. 25-40. https://doi.org/10.1007/978-3-319-31499-0_3

Taylor, C. M., Lambin, E. F., Stephenne, N., Harding, R. J. and Essery, R. L. H. (2002). The Influence of Land Use Change on Climate in the Sahel. *Journal of Climate*, 15(24), 3615-3629. https://doi.org/10.1175/1520-0442(2002)015<3615:TIOLUC>2.0.CO;2

Taylor, C. M., Parker, D. J., Kalthoff, N., Gaertner, M. A., Philippon, N., Bastin, S., Harris, P. P., Boone, A., Guichard, F., Agusti-Panareda, A., Baldi, M., Cerlini, P., Descroix, L., Douville, H., Flamant, C., Grandpeix, J. Y. and Polcher, J. (2011). New perspectives on land-atmosphere feedbacks from the African Monsoon Multidisciplinary Analysis. *Atmospheric Science Letters*, 12(1), 38-44. https://doi.org/10.1002/asl.336

Taylor, C. M., Belušić, D., Guichard, F., Parker, D. J., Vischel, T., Bock, O., Harris, P. P., Janicot, S., Klein, C. and Panthou, G. (2017). Frequency of extreme Sahelian storms tripled since 1982 in satellite observations. *Nature*, 544(7651), 475-478. https://doi.org/10.1038/nature22069

Thorncroft, C. D. and Blackburn, M. (1999). Maintenance of the African easterly jet. *Quarterly Journal of the Royal Meteorological Society*, 125(555), 763-786. https://doi.org/10.1002/qj.49712555502

Thorncroft, C. D., Nguyen, H., Zhang, C. and Peyrillé, P. (2011). Annual cycle of the West African monsoon: Regional circulations and associated water vapour transport. *Quarterly Journal of the Royal Meteorological Society*, 137(654), 129-147. https://doi.org/10.1002/qj.728

Tiedtke, M. (1989). A Comprehensive Mass Flux Scheme for Cumulus Parameterization in Large-Scale Models. *Monthly Weather Review*, 117(8), 1779–-1800. https://doi.org/10.1175/1520-0493(1989)117<1779:ACMFSF>2.0.CO;2

United Nations Department of Economic and Social Affairs. (2018). *The World's Cities in 2018*. https://doi.org/10.18356/8519891f-en

Wang, G. and Eltahir, E. A. B. (2000). Ecosystem dynamics and the Sahel Drought. *Geophysical Research Letters*, 27(6), 795-798. https://doi.org/10.1029/1999GL011089

Wang, G., Yu, M. and Xue, Y. (2016). Modeling the potential contribution of land cover changes to the late twentieth century Sahel drought using a regional climate model: Impact of lateral boundary conditions. *Climate Dynamics*, 47(11), 3457-3477. https://doi.org/10.1007/s00382-015-2812-x

Wang, M., Zhang, X. and Yan, X. (2013). Modeling the climatic effects of urbanization in the Beijing–Tianjin–Hebei metropolitan area. *Theoretical and Applied Climatology*, 113(3-4), 377-385. https://doi.org/10.1007/s00704-012-0790-z

World Bank. (2016). *World Development Report 2016: Digital Dividends*. https://doi.org/10.1596/978-1-4648-0671-1

Xue, Y. (1997). Biosphere feedback on regional climate in tropical North Africa. *Quarterly Journal of the Royal Meteorological Society*, 123(542), 1483-1515. https://doi.org/10.1002/qj.49712354203

Xue, Y., Juang, H. M. H., Li, W. P., Prince, S., DeFries, R., Jiao, Y. and Vasic, R. (2004). Role of land surface processes in monsoon development: East Asia and West Africa: Land surface processes in monsoon development. *Journal of Geophysical Research: Atmospheres*, 109(D3). https://doi.org/10.1029/2003JD003556

Xue, Y., De Sales, F., Lau, W. K. M., Boone, A., Kim, K. M., Mechoso, C. R., Wang, G., KucharsKi, F., Schiro, K., Hosaka, M., Thiaw, W., Zeng, N., Comer, R.E., Ruby, L. L., Kalnay, E., Kitoh, A., Lu, C. H., Mahowald, N. M. and Zhang, Z. (2016). West African monsoon decadal variability and surface-related forcings: Second West African Monsoon Modeling and Evaluation Project Experiment (WAMME II). *Climate Dynamics*, 47(11), 3517-3545. https://doi.org/10.1007/s00382-016-3224-2

Yang, L., Tian, F., Smith, J. A. and Hu, H. (2014). Urban signatures in the spatial clustering of summer heavy rainfall events over the Beijing metropolitan region: Urban modification of heavy rainfall. *Journal of Geophysical Research: Atmospheres*, 119(3), 1203-217. https://doi.org/10.1002/2013JD020762

Yang, X., Hou, Y. and Chen, B. (2011). Observed surface warming induced by urbanization in east China. *Journal of Geophysical Research*, 116(D14). https://doi.org/10.1029/2010JD015452

Yang, X., Ruby L. L., Zhao, N., Zhao, C., Qian, Y., Hu, K., Liu, X. and Chen, B. (2017). Contribution of urbanization to the increase of extreme heat events in an urban agglomeration in east China: Urbanization and the Increase of EHEs. *Geophysical Research Letters*, 44(13), 6940-6950. https://doi.org/10.1002/2017GL074084

Yang, Z., Dominguez, F., Gupta, H., Zeng, X. and Norman, L. (2016). Urban Effects on Regional Climate: A Case Study in the Phoenix and Tucson "Sun Corridor." *Earth Interactions*, 20(20), 1-25. https://doi.org/10.1175/EI-D-15-0027.1

Yu, M., Wang, G. and Pal, J. S. (2016). Effects of vegetation feedback on future climate change over West Africa. *Climate Dynamics*, 46(11-12), 3669-3688. https://doi.org/10.1007/s00382-015-2795-7

Yuen, B. and Kumssa, A. (Eds.). (2011). *Climate Change and Sustainable Urban Development in Africa and Asia*. https://doi.org/10.1007/978-90-481-9867-2

Zhang, C. L., Chen, F., Miao, S. G., Li, Q. C., Xia, X. A. and Xuan, C. Y. (2009). Impacts of urban expansion and future green planting on summer precipitation in the Beijing metropolitan area. *Journal of Geophysical Research*, 114(D2). https://doi.org/10.1029/2008JD010328

Zhang, D. L., Shou, Y. X. and Dickerson, R. R. (2009). Upstream urbanization exacerbates urban heat island effects. *Geophysical Research Letters*, 36(24). https://doi.org/10.1029/2009GL041082

Zhang, N., Chen, Y., Gao, H. and Luo, L. (2019). Influence of urban land cover data uncertainties on the numerical simulations of urbanization effects in the 2013 high-temperature episode in Eastern China. *Theoretical and Applied Climatology*. https://doi.org/10.1007/s00704-019-02926-5

Zheng, X. and Eltahir, E. A. B. (1997). The response to deforestation and desertification in a model of West African monsoons. *Geophysical Research Letters*, *24*(2), 155–158. https://doi.org/10.1029/96GL03925

Zope, P. E., Eldho, T. I. and Jothiprakash, V. (2016). Impacts of land use–land cover change and urbanization on flooding: A case study of Oshiwara River Basin in Mumbai, India. *CATENA*, 145, 142-154. https://doi.org/10.1016/j.catena.2016.06.009